TS6-1

摩周湖 ― 鋭敏でありかつ安定である湖における環境記録の読み取り

田中敦 [1], 武内章記 [1], 五十嵐聖貴 [2], 小林拓 [3], 大八木英夫 [4], 深澤達矢 [5], 南尚嗣 [6], 藤江晋 [7]

[1] 国立環境研究所, [2] 北海道立総合研究機構, [3] 山梨大, [4] 日大, [5] 北大, [6] 北見工大, [7] 自然公園財団

キーワード:摩周湖, 透明度, 長期変動, 微量分析, 安定同位体

抄録

摩周湖は北海道東部にある複循環を示すカルデラ湖で, 流出入河川のない閉塞湖である。1931 年に 41.6m の透明度を記録し, 長く陸水における世界最大の透明度を示していた, 集水域内には農業を含む一切の人為汚染源はない。例えば, 湖水中の有害元素等の濃度は極めて低く, モニタリング対象としてチャレンジングであるとともに, 世界的にも希有な観測フィールドと言える。そのため, 摩周湖は国連環境計画 GEMS/Water において, 国内唯一のベースラインモニタリングステーションに登録されている。国立環境研究所を主体とする観測が, 唯一の科学的モニタリングである。

ここでは, 3 つの研究結果について発表する。1)厳しい自然環境における連続データの採取による高い透明度の生成機構と透明度の年間変動の推定について。2)水収支や湖水の成分の高精度・高感度測定を通じた長期的変動の検出について。3)鉛同位体の精密測定によるさらに長期の環境変動の解析について。

1. はじめに

摩周湖は北海道の東部(北緯 43 度, 東経 144 度), 阿寒摩周国立公園内に位置し, 湖面を含む集水域全域が国立公園特別保護地区に指定されている。最大水深は 212 m で, カルデラ湖の特徴として湖底面は比較的平坦である。湖面は比高 100 m を超える切り立った崖で覆われており, 流出入河川のない閉塞湖である。

観光客は展望台から湖面を望むだけで, 湖面への立入は自粛されている。加えて, 集水域内での農業・林業を含む一切の人為的活動はなく, 流入による人為汚染源は極めて乏しい。春秋の 2 回, ほぼ全層混合をする複循環で, 厳冬期には結氷することも多い。

高安・近藤は1931 年に 41.6 m の透明度を記録した[1]。これは, 長く陸水における世界最大の透明度であった。一方, 長期にわたる透明度の低下傾向があり, 地元自治体や観光業にとっての懸念事項となっている。

湖水中の栄養塩, 水銀などの有害元素や残留有機物質等の濃度は極めて低い。このことから, 摩周湖は国連環境計画が進める陸水監視プログラム(GEMS/Water)において, 国内唯一のベースラインモニタリングステーションに登録されている。国立環境研究所を主体とする機関が, 過去30 年以上, 物理的, 化学的, 生物的観測を行ってきた。これは摩周湖における唯一の水質モニタリングデータと言える。観測結果は, GEMS/Water のデータベース(GEMStat)に登録するとともに, 国立環境研究所のホームページにおいてデータ公開している[2]。

2. 方法

摩周湖での水質調査の地点等の概要を図 1 に示した。中央火口丘であるカムイシュ島により, 南北 2 つの湖盆に分かれている。我々の調査は主として北側湖盆に位置する最深部で行っている。小規模調査では, 南側湖盆や, 比較的岸に近い地点を調査地点とした。
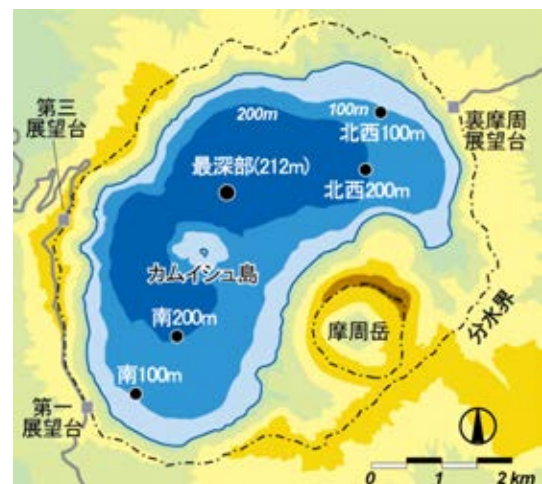
図 1 摩周湖の概観と主な調査地点

湖水中の成分分析法は, ICP 発光分光法(AES), ICP 質量分析法(MS), 吸光光度法, イオンクロマトグラフィ(IC), GC/MS をはじめ, 多岐にわたる。光学観測は, 輝度・照度・スカラー照度(TriOS 社), プロファイリング及び係留による観測は, クロロフィル・濁度・水中光量子・水温計(JFE アドバンテック)によった。水深20 m と40 m に測器群を配置し, ブイを含め全体を水中に沈めた。別途, Onset 社等の水温ロガーを複数台係留している。

特記すべき方法は，以下のとおりである。微量ニッケルは溶媒抽出後，同位体希釈 MIP-MS，鉛同位体比は精製後，多重検出器型(MC)ICP-MS によった。湖水のほかにも，湖底堆積物や湖沼周辺の湧水・河川についても採取，観測を行っている。

3. 結果・考察

図 2 に摩周湖に特徴的な項目の鉛直分布を示した。硝酸態窒素は貧栄養であることを端的に示す。0.04 mg/kg 程度の濃度であり，吸光光度法では検出困難なレベルであった。夏季には生物に利用され大きく減少する。溶存酸素飽和度は，底層直上まで 80%以上を示し，底質からの栄養塩の溶出も少ないと推定される。
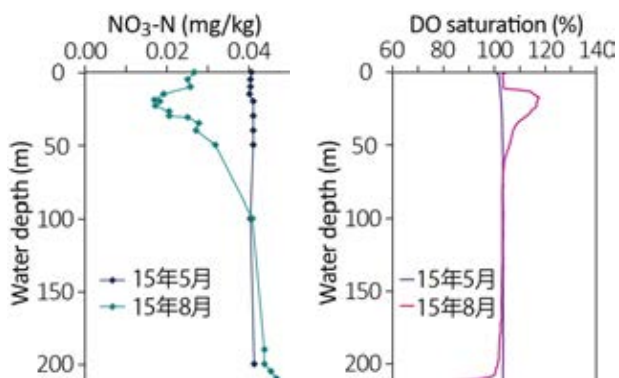
図 2 硝酸塩と溶存酸素飽和度の鉛直分布（2015 年）

1）係留観測による透明度の年間変動の推定と高い透明度の形成機構

湖面に出ることが難しい厳冬期を含む通年観測には，データロガーを用いた連続観測が必須となる。図 3 に，2015 年の 1 年間の水温の変動を示した。この年は，5 月及び 12 月末にほぼ全層循環していることがわかる。
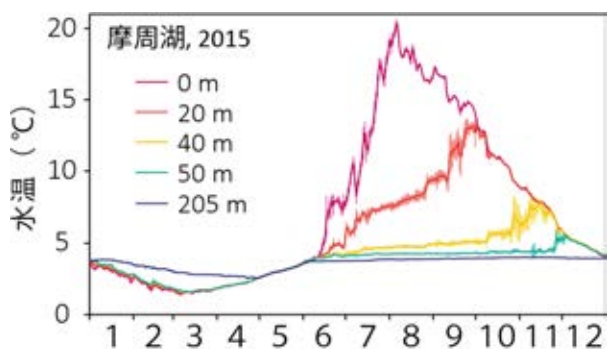
図 3 摩周湖水温の年間変動（2015 年）

また，2015 年 8 月の吸収係数の二次元分布を図 4 に示した。この時の透明度は 17.2 m であり，波長 400 nm 近傍に代表されるクロロフィルによる吸収が顕著であり，透明度はこのような植物プランクトンの極大層に大きく影響されることが示されている。図 3 と同期間の推定透明度を図 5 に掲げた。透明度は，異なる深度に係留し

た光量子ロガーの指示値から求められた下向き減衰係数を利用して推定した。夏季の植物プランクトンの増殖とともに，クロロフィル濃度が極大を示し，循環期に極小となる。栄養塩濃度が低く，生物粒子量の少ない底層水の湧昇によって，光透過性が上がり，透明度が上昇する。図に○で示した実測透明度との一致が高いことも確認できる。
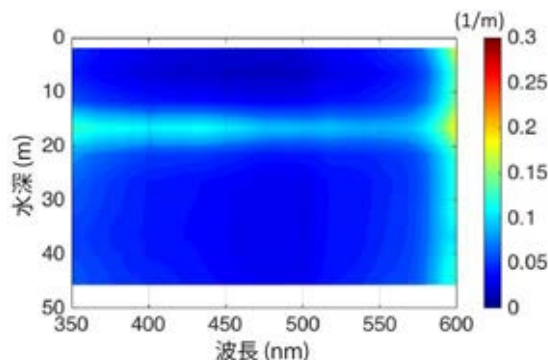
図 4 摩周湖水の吸収係数（2015 年 8 月）
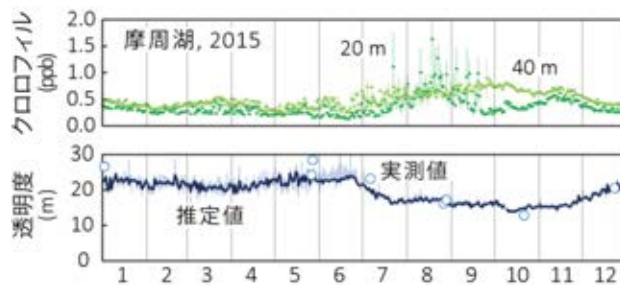
図 5 クロロフィルと透明度推測値の年間変動
（2015 年。○は実測値）

2）湖水成分の高精度・高感度測定と長期的変動

図 6 に成層期（2017 年 9 月）のマグネシウムの鉛直分布を示す。この鉛直プロファイルには 3 つの特徴がある。表層部の低濃度は，雨水による希釈効果を示す。粒子化による除去や生物による同化が起きにくいマグネシウムは，中層部では完全に一定の濃度となる。底層部の高濃度は，溶存成分に富んだ湖底湧水からの負荷を示す。

このことは，イオン成分に限らず，微量汚染成分等にもあてはまる。循環期と成層期との鉛直プロファイルの変化から，当該期間内の湖面への物質流入の有無や単位時間あたりの負荷量に関する情報を与える。

一方，図 7 に示したニッケルの鉛直分布の場合，通常の ICP-MS では検出が困難な濃度レベルであり，濃縮操作を必要とした。有機溶媒を直接導入する同位体希釈 MIP-MS 法を適用することで，高精度かつ高感度な観測が可能となった[3]。これによると，燃焼起源の指標元素であるニッケルは，水温躍層上部に濃集することが多く，大気経由の負荷物が蓄積，除去されるプロセス

を示していると考えた。
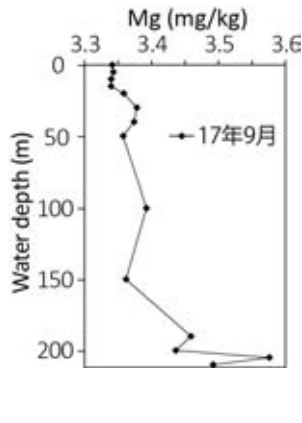
図6 マグネシウムの鉛直
分布（2017年9月）
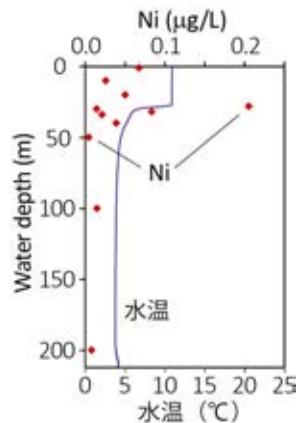
図7 ニッケルの鉛直分布
（2007年10月）

摩周湖水は外輪山外の周辺湧水へ流出しており，同位体混合モデルや水収支から 120 年程度の長い滞留時間を持つと推定されている。また，SF_6 等のガス成分の輸送モデルからも数十年かけて流出することが推測されつつある[4]。

鉛直プロファイルで例示したように，摩周湖は大陸間の長距離輸送などについて，年々の負荷情報に鋭敏に応答する特性を持っている。このためには，変化を検出する相対的な高精度分析，あるいは微量成分を定量する高感度分析法を必要とする。一方，長い滞留時間を有することは，平均濃度（観測では，中層部の濃度）の年変化は 0.1%を大きく下回ることになる。この点で，摩周湖は非常に安定な湖と言うことができる。

摩周湖においては，30 年以上にわたって観測を続けており，分析者，分析手法ともに変化している。表1にマグネシウム濃度の分析例を示した。相対精度（再現性）にくらべて，正確性を伴う絶対精度を確保することは難しい。自然の濃度変化を検出するには，それを上回る正確な分析技術を維持することが求められる。分析者や手法，標準物質の供給体制などの問題から，これを実現することは極めて困難な課題である。濃度比を用いた解析は，1 つの有効な対策であろう。

表1 摩周湖水中のマグネシウム濃度の長期観測値

観測年	中層平均濃度 （mg/kg）	n	方法
1931[1]	3.92	3	滴定法
1983	3.55	7	原子吸光法
1992	3.20	10	ICP–AES
2017	3.38	7	IC

3）鉛同位体比の精密測定による長期間の環境解析

さらに過去にさかのぼった環境解析には，湖底堆積物を利用することが一般的であろう。流入河川のない摩周湖の場合，年間 10 mg/cm² 程度の遅い堆積速度となる。柱状堆積物試料を用いることで，過去数百年までの情報が得られた。

代表的な汚染物質である鉛は，起源によって同位体比が比較的大きく変動することが知られている。図 8 に 2006 年に採取したの堆積物表層，中層，深層と底質標準物質（文献値[5]と実測値）の鉛同位体比を示した。

過去 30 年で，ICP-MS は飛躍的な進歩と普及をとげた。しかしながら，四重極型 ICP-MS による同位体測定精度では，底質の深さごとの同位体変動を正確に描けなかった。MC-ICP-MS による測定結果では，深層部は日本固有の鉛同位体比，表層部は海外由来の鉛の影響を受けて 1%程度異なる値，中層部では両者の中間的値が得られ，両成分の混合比が計算できる。
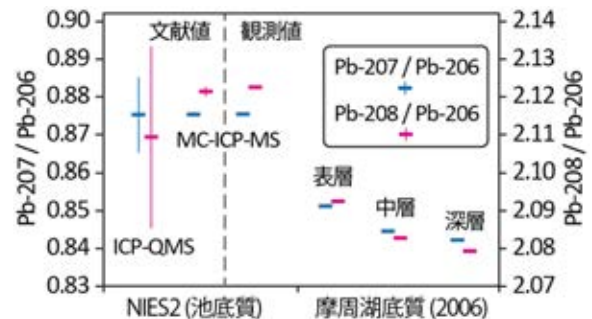
図8 摩周湖底質と底質標準物質(NIES2)の
鉛同位体比

4. 結論

世界的にも珍しい観測フィールドである摩周湖において，30 年間のモニタリング結果を概観した。

透明度については湖水循環と生物量が重要なキーとなっていた。物質負荷については，循環期と成層期との鉛直分布の差から評価できた。一方，滞留時間の長い摩周湖では，自然の微小変化を下回る正確性を持つ観測体制が必要となる。MC-ICP-MS のような高精度測定を行うことで，長期的な環境変動を底質から読み取ることも可能であった。

引用文献

[1] 高安三次・近藤賢蔵: 水産調査報告, 35, pp.1-18, 1934.

[2] 国立環境研究所: http://db.cger.nies.go.jp/gem/inter/GEMS/mashu/index_j.html.

[3] J. Bai, H. Minami, H. Sakagami, K. Mantoku, I. Atsuya, N. Takahashi, A. Tanaka, K. Jin, T., Kawai: Int. J. Environ. Anal. Chem., 91:9, pp.811-820, 2011.

[4] 大八木英夫・浅井和由・五十嵐聖貴・小林拓・武内章記・深澤達矢・藤江晋・南尚嗣・田中敦: JpGU, A-HW25-C003502, 2018.

[5] A. J. Walder, N. Furuta: Anal. Sci., 9, pp.675-680, 1993.

TS6-1

Lake Mashu – How we revealed environmental records from a sensitive and stable lake

Atsushi Tanaka[1], Akinori Takeuchi[1], Seiki Igarashi[2], Hiroshi Kobayashi[3], Hideo Oyagi[4],
Tatsuya Fukazawa[5], Hirotsugu Minami[6] and Shin Fujie[7]

[1]National Institute for Environmental Studies, [2]Hokkaido Research Organization, [3]University of Yamanashi,
[4]Nihon University, [5]Hokkaido University, [6]Kitami Institute of Technology, [7]Kawayu Branch, Natural Parks Foundation

Keywords: Lake Mashu, Secchi disk transparency, environmental changes, trace analysis, stable isotopes

ABSTRACT

Lake Mashu is a dimictic caldera lake located in the eastern part of Hokkaido, Japan. It is a typical closed lake with no inflowing nor outflowing rivers. In 1931, Lake Mashu recorded 41.6 m of Secchi disk transparency, which has been the largest transparency record exceeding that of Lake Baikal. There is no anthropogenic pollution sources including agricultural nor forestry activities inside the watershed. For example, concentrations of heavy metals and persistent organic substances in lake water are extremely low. Therefore the detection of trace components itself was a challenging monitoring objective and it can be said that Lake Mashu is a unique field for the environmental scientists. Lake Mashu is the sole lake registered as a baseline monitoring station in Japan at the UNEP GEMS/Water programme. Physical, chemical and biological observation by the National Institute for Environmental Studies and collaborating institutions is the only scientific monitoring of water qualities for the last three decades.

Three findings about the lake monitoring will be provided. 1) A mechanism of formation of large transparency, and reproduction of seasonal variation of transparency by planktonic evidences and continuous logging data in the severe environmental conditions. 2) An estimation of long term variation of lake water constituents through the isotopic and gaseous analysis of water balance and accurate and/or sensitive analytical methods for elements. 3) Examination of longer term environmental changes by a precise measurement of lead isotope ratios.

1. INTRODUCTION

Lake Mashu, located in the east part of Hokkaido (N43, E144), is a closed oligotrophic lake. It is dimictic and occasionally ice-covered in winter. The maximum depth is 212 m. The lake surface is surrounded by steep caldera walls exceeding 100 m in height.

The world largest Secchi disk transparency of 41.6 m was recorded in 1931[1]. The transparency decreased gradually. It is a concern for local governments and tourism.

There is no human activity such as agriculture and forestry in the catchment area, and anthropogenic pollution load is extremely small. Concentrations of nutrients, heavy metals, POPs in lake water are quite low. Therefore Lake Mashu has been registered as the only baseline monitoring station lake in Japan in the UNEP GEMS/Water programme. National Institute for Environmental Studies and collaborative institutions have conducted physical, chemical and biological observations for over 30 years. The monitoring data are registered to GEMStat database, and also available on the web[2].

2. METHOD

An overview of Lake Mashu is shown in Fig.1. A central volcanic cone, Kamuishu Is., divides lake bottom into two basins. Our survey is conducted mainly at the deepest part located in the northern basin. In the small scale observation, the survey site was chosen from the southern basin or the points close to the shore.
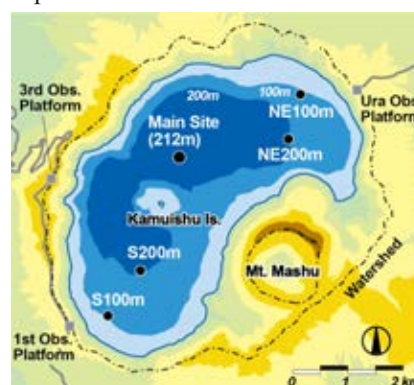
Fig. 1 Overview of Lake Mashu

Constituents were analyzed mainly by ICP-AES, ICP-MS, spectrophotometry, ion chromatography (IC), GC/MS. Optical data were recorded on TriOS instruments. Data loggers for chlorophyll, turbidity, photon flux and water temperature (JFE Advantech) were used for profiling and mooring. Instruments were moored at water depths of 20 m and 40 m, and the whole system including buoys was submerged in water. Several water temperature loggers

(Onset and JFE Advantech) were also moored.

Notable methods are as follows. Trace Ni was solvent extracted and determined by isotope dilution MIP-MS, Pb isotope ratios were analyzed by multiple collector (MC) ICP-MS. Spring and river waters around the lake, and lake sediment samples were also analyzed.

3. RESULTS AND DISCUSSION

Two vertical profiles characteristic to the oligotrophic state were depicted in Fig.2. The concentration of NO_3-N was as low as 0.04 mg/kg, which was difficult to detect by spectrophotometry. It seems to be deficient around 20 m where photosynthesis activity is dominant in summer. Dissolved oxygen was abundant down to the bottom and elution of nutrients from the sediment was limited.
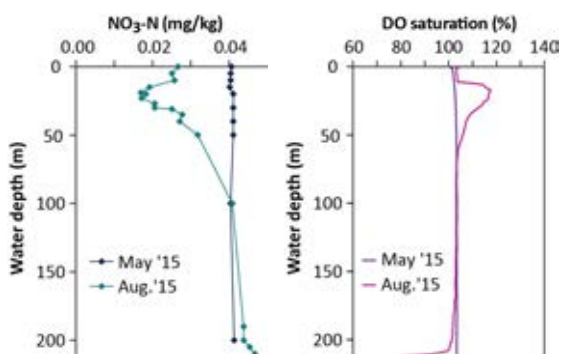
Fig. 2 Profiles of nitrate and DO saturation (2015)

1) Mechanism of formation of high transparency

Continuous data using data loggers are essential for full year observation including severe winter season when it is difficult to reach to the lake surface. Figure 3 shows a seasonal variation of water temperature in 2015. Perfect mixing occurred twice a year in May and the end of December.
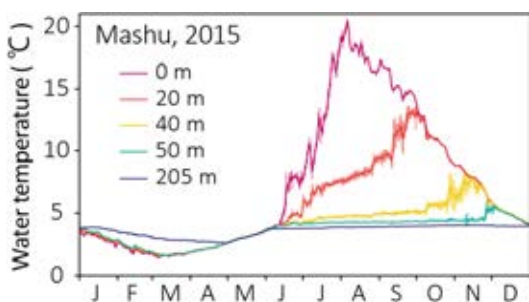
Fig. 3 Time variation of water temperature (2015)

A two-dimensional distribution of the absorption coefficient in August 2015 is shown in Fig.4. Relatively high absorption band was found near the transparency depth of 17.2 m and it corresponded to the chlorophyll maximum. Prominent absorption around 400 nm also corresponded to the absorption band for chlorophylls. Temporal variations of chlorophyll and transparency in 2015 are shown in Fig.5. Transparency was estimated using the downward attenuation coefficient obtained from the readings

of two photon flux loggers moored at different depths. The estimated transparency agreed well with the observed transparency indicated by ○ in the figure. From July to September, concentration of chlorophyll, indicating phytoplankton biomass, was maximized at the shallower depth and it becomes minima in the circulation periods. Concentrations of nutrients and biological particles are low in the bottom layer water. When it upwells, the light permeability and transparency increase.
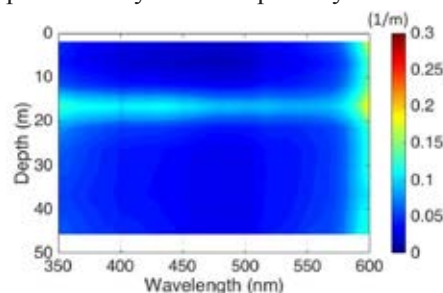
Fig. 4 Distribution of absorption coefficient (Aug. 2015)
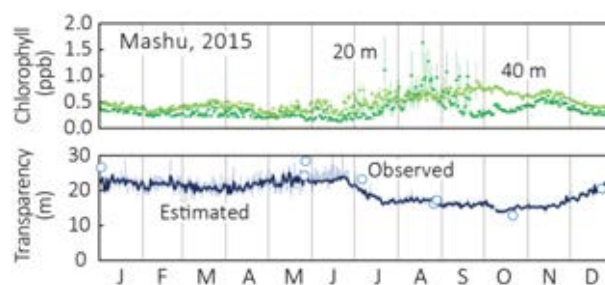
Fig. 5 Time variation of chlorophyll and estimated transparency (2015)

2) Need for accurate and/or sensitive measurement

Figure 6 shows a vertical profile of dissolved Mg in the stratification period (Sep. 2017). This vertical profile has three features. The low concentration in the surface layer is attributed to the dilution effect by rainwater less abundant than lake water. Magnesium is one of conservative elements and assimilation by organisms is low. Constant distribution in the middle layer was found. The high concentration near the bottom is attributed to the load from the bottom spring affected by volcanic activities.

This applies not only to ionic components but also to trace contaminants. From the change of vertical profiles between the circulation period and the stratification period, we can detect the event such as addition, decomposition or removal of material fallen onto the lake surface after the last circulation, and the flux can be calculated.

On the other hand, concentration of Ni is too low for conventional ICP-QMS equipping Ni interface due to an interference of molecular ion. By a combination of solvent extraction of Ni chelate and isotope dilution for the preconcentration, organic phase can be directly introduced to nitrogen plasma MIP-MS equipping Pt cone. By developing this method, precise and sensitive determina-

tion became possible[3]. Nickel, which is an indicator of combustion, often concentrated in the upper part of thermocline (Fig.7), indicating the process of atmospheric load and accumulation in the water column.
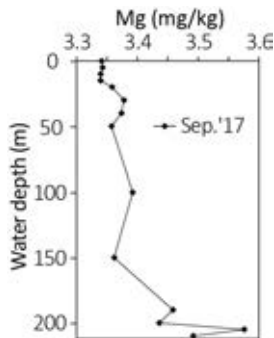
Fig. 6   Profile of Mg (Sep. 2017)   **Fig. 7   Profile of Ni (Oct. 2007)**
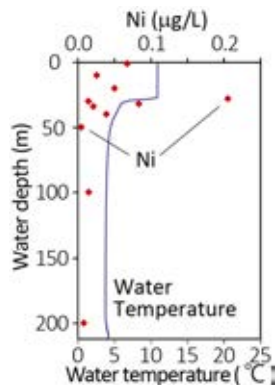
Lake water flows through the outer rim of crater and flows out as surrounding springs. A long residence time of about 120 years was obtained from the water balance and isotope mixing model. It is estimated that the age of spring water is over several decades from the transportation model of gaseous components such as SF_6 [4].

As exemplified in the vertical profile of Mg, Lake Mashu has characteristics that respond sensitively to a load of long-range transported material or supply from the bottom. To fulfil this purpose, a precise analytical method to detect the change or a highly sensitive technique to determine ultratrace components is required. On the other hand, having a long residence time implies that the annual change of the average concentration (appearing in the middle layer in the observation) is far less than 0.1%. In this respect, Lake Mashu can be said a very stable lake.

During the monitoring of Lake Mashu over 30 years, both analysts and analytical methods varied. An example of Mg results is shown in Table 1. It is difficult to ensure absolute accuracy, as compared to relative precision (repeatability). To detect natural minute changes, it is required to maintain accurate and precise analytical techniques over the years. It is an extremely difficult task to realize this because the analytical conditions (analysts, methods and even standard substances) change. Analysis using concentration ratios normalized with one component would be an effective measure to detect natural changes.

Table 1 Analytical values for Mg for a long period

Year	Mean concentration of middle layer (mg/kg)	n	Analytical method
1931[1]	3.92	3	titration
1983	3.55	7	AAS
1992	3.20	10	ICP−AES
2017	3.38	7	IC

3) Sedimentary records of lead isotopes

Sediment it often utilized for a retrospective analysis. However, because of the lack in inflowing rivers and narrow catchment area, the sedimentation rate is as low as 10 mg/cm^2/y. By using sediment core samples, information up to the past hundreds of years was obtained.

Lead, a typical pollutant, shows relatively large isotopic deviation depending on its origin. Figure 8 shows the lead isotope ratios of sediment in the surface, middle and deep layers collected in 2006, and of a sediment reference material (literature[5] and observed value).

In the past 30 years, ICP-MS has made a striking progress and become popular. However, it was almost impossible to distinguish isotopic variation precisely each other by ICP-QMS. According to the measurement by MC-ICP-MS, the deep layer has a Pb isotopic ratio inherent to Japan, the surface layer has a value different by about 1% affected by Pb overseas, and intermediate values were obtained in the middle layer. A mixing ratio of both components can be calculated.
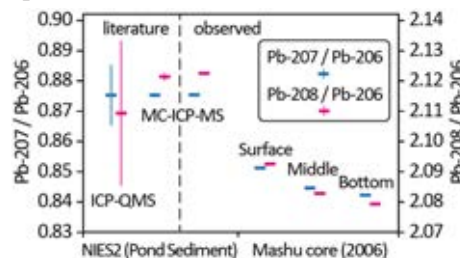
Fig. 8 Pb isotope ratios of Mashu sediment and CRM

4. CONCLUSION

Water circulation and biomass are important key factors which control transparency. It was possible to evaluate material flux from the difference in vertical distributions between the circulation and stratification periods. Due to the long residence time, it is required to maintain an accurate observation system lower than natural minute change. By conducting precise measurements by MC-ICP-MS, long-term environmental changes can be revealed from the sediment core.

REFEENCES

[1] S. Takayasu, K. Kondo: Suisan Chosa Hokoku (Fishery Investigation Report), 35, pp.1-19, 1934.

[2] National Institute for Environmental Studies: http:// db.cger. nies.go.jp/gem/inter/GEMS/mashu/index_j.html.

[3] J. Bai, H. Minami, H. Sakagami, K. Mantoku, I. Atsuya, N. Takahashi, A. Tanaka, K. Jin, T., Kawai: Int. J. Environ. Anal. Chem., 91:9, pp.811-820, 2011.

[4] H. Oyagi, K. Asai, S. Igarashi, H. Kobayashi, A. Takeuchi, T. Fukazawa, S. Fujie, H. Minami, A. Tanaka: JpGU, A-HW25-C003502, 2018.

[5] A. J. Walder, N. Furuta: Anal. Sci., 9, pp.675-680, 1993.

TS6-2

Integrated data, models and networks provide opportunities to advance lake science and predictions

David Hamilton

Australian Rivers Institute, Griffith University, Brisbane, Australia

Keywords: GLEON, networks, high frequency data, databases, professional societies

ABSTRACT

The challenge to manage lakes under global change trajectories of increasing diffuse nutrient pollution, climate change and invasive species is intensifying. Network-based science will have an increasingly important role in addressing these threats to the sustainability and service provisions of lakes. Network science can increase the number and breadth of case studies, provide greater interdisciplinary coverage, and advance the uptake of novel technologies like high-frequency sensor monitoring. The Global Lake Ecological Observatory Network (GLEON) uses network-based science to seek to understand and interpret high-frequency sensor data from lakes across the world. Complimenting networks are databases like LAGOS-NE and Takiwa, which provide geospatially and temporally resolved databases for lakes at national scale (USA and New Zealand, respectively). New sensing technologies and practices, as well as greater accessibility of this information, are leading to dissemination of best practice approaches and implementation of systems to avoid 'reinventing the wheel' in terms of data acquisition and modelling tools. Global networks of researchers are well positioned to address the challenges of increasing availability of high frequency data but the synthesis studies that are enabled by these networks need to be directed towards improved process representations as well as statistical generalizations. Moreover, societies will continue to play an important role as persistent organizations to promote the profession, provide regular meetings and maintain the standards of disciplinary journals.

1. INTRODUCTION

Affiliations of water managers, scientists and engineers to international professional societies can have important career implications and provide opportunities to engage in dialogue about research agendas and sustainable water management practices. Nowadays, with global issues of water scarcity, floods, diffuse pollution and water quality impairment, there is a wide variety of networks and societies to support exchange of research ideas and develop management plans to deal with these issues. The objective of this study is to analyze a lake research network in the context of the evolving nature of professional scientific societies and research agendas, and to consider some of the advantages and disadvantages of trends towards more network-based science.

2. RESULTS AND DISCUSSION

Figure 1 outlines some of the scientific affiliations available to water science researchers and professionals. Four main affiliation categories have been identified:

(1) limnology-related networks,
(2) research coordination networks,
(3) international societies, and
(4) groups whose objective is mostly to organize international disciplinary meetings.

The foundation of international professional engagement is international societies like the International Lake Environment Committee Foundation (ILEC; http://www.ilec.or.jp/en/) and the Association for the Sciences of Limnology and Oceanography (ASLO; https://aslo.org/), but many societies have not maintained high rates of growth that occurred in the 1960s-80s and some appear to have reached ceiling numbers of members, or may even be declining[1]. The reasons for the existence of these societies are as important today as ever; to develop collegial networks, exchange knowledge, support early career scientists, and raise issues that are important for human society (e.g., to develop sustainable management of the world's lakes and reservoirs – ILEC).
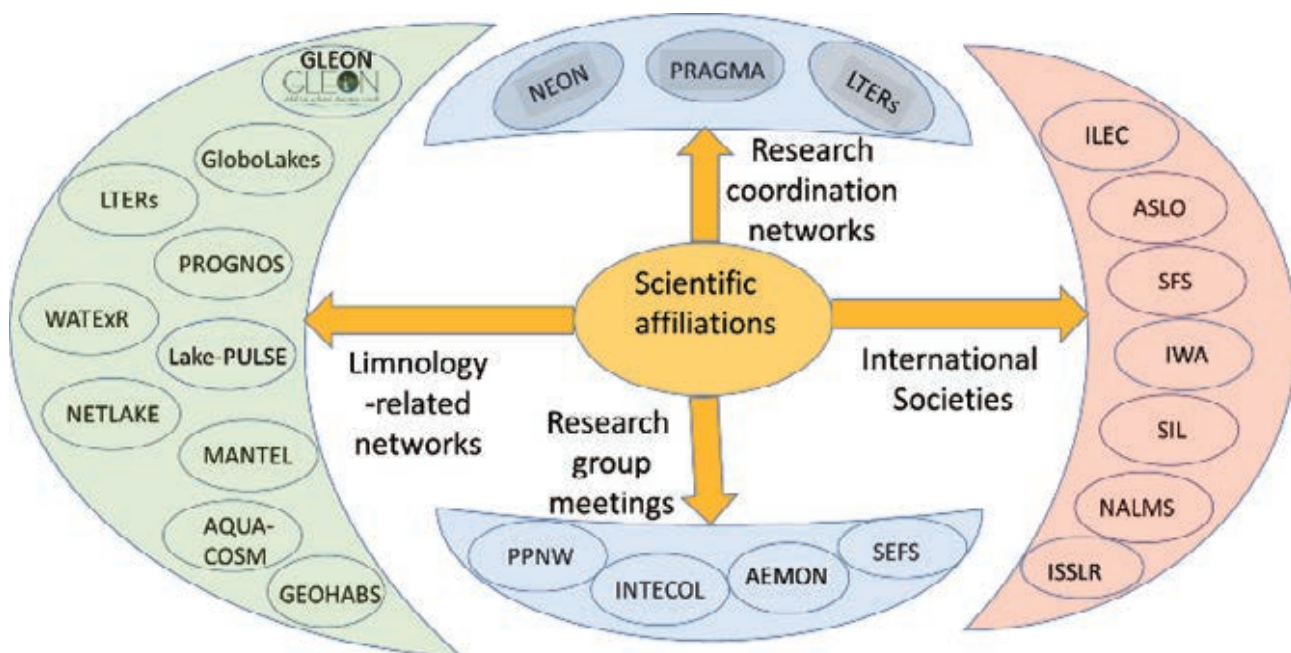
Fig. 1 Scientific affiliations that support researchers and water professionals, grouped by four categories

One of the reasons for the static nature of many societies is the advent of research networks, which are generally either dedicated to specific areas of research or to coordinating a body of research[2]. These networks have often been able to provide funding to support travel and meetings on a regular (e.g., biannual, annual) basis, and members do not generally pay a subscription – a basic tenet for membership of a society. The networks have been a means of focusing research on topical areas and bringing teams and diversity to research and management challenges. These aspects of team science, diversity and topical research issues are attractive to funding agencies[2]. However, networks tend to be temporary, often lasting the duration of a funding cycle, and for this reason they do not necessarily provide persistence and stability that are required to support careers in research and industry. For example, many international societies support scientific journal publications which are not the domain of networks. Even in this area, however, international societies have increased competition from independent publishers whose motivation is primarily profit-driven and who may be more responsive to the changing modes of publication (e.g., Open Access publication)[3].

The Global Lake Ecological Observatory Network (GLEON; www.gleon.org) is an example of a network that has been stable and persistent since its inception in 2005. It has grown to have over 800 members across the globe and it has well developed operating principles and procedures. GLEON is a grassroots organization that relies on locally supported high-frequency monitoring platforms in lakes and provides a coordinating network to synthesize and analyze the data arising from these platforms[4]. Some features of GLEON have been its ability to develop software to assist with analysis and interpretation of high-frequency lake data, and new insights into lake processes generated from the high-frequency data across a diversity of latitudinal, size and trophic state gradients.

Tools to analyze high-frequency lake data have evolved quickly in the GLEON environment. They include:

- VEGA, a program that allows storage of time series in an environment where lake sensor deployments and configurations may need to be highly flexible, and its component software VADER (VegA Data EditoR) – see www.gleon.org;

- B3 (Buoys 3) and dbBadger, software to carry out quality analysis/quality assurance of data – see www.gleon.org;

- A collaboration of GLEON with the Data Observation Network for Earth (DataONE – https://www.dataone.org/) to provide a data repository and archiving system;

- Analytical tools to examine specific lake processes using high frequency data, including rLakeAnalyzer[5] to quantitatively evaluate lake mixing zones and stratification; LakeMetabolizer[6] to carry out lake metabolism calculations (see www.gleon.org); and Lake Heat Flux Analyzer[7] to evaluate the constituents of lake heat fluxes with user flexibility in the equations that are used to parameterize the heat flux.

- Numerical modelling tools that are being used to simulate lake hydrodynamics and water quality, including the General Lake Model (GLM; www.gleon.org) and can link to other model developments like the Framework for Aquatic Biogeochemical Models (FABM)[8] to link
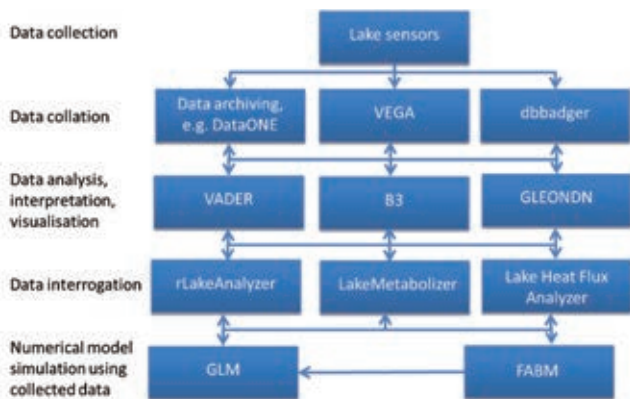
Fig. 2 Software tools developed and utilized in GLEON (Global Lake Ecological Observatory Network) to facilitate understanding of lake processes from lake sensor data. See text for descriptions of the tools and acronyms.

ecological models to a number of different hydrodynamic models including GLM.

Increasingly, geospatial platforms are being associated with sensor and other lake data, as well as model outputs, to visualize data. Examples of these platforms include LAGOS-NE[9] and Takiwa (lakes.takiwa.co), which provide multi-scale geospatial and temporal resolution for lakes across the United States and New Zealand, respectively.

3. CONCLUSION

GLEON is an example of a lake research network that has been successful in terms of its longevity, engagement of early career scientists, and contributions to new understanding of lake processes using high frequency sensor data. It is more 'organic' in form than a professional society, which primarily promotes scholarly publications and disciplinary meetings. Through GLEON, many software tools have been developed to assist with processing, archiving, visualizing and modelling data. Efficiency gains have been made and cross-continental-scale studies have become possible through the network. At the same time, however, there is a need to encourage process-based understanding of lake systems and not solely statistical inference derived from the growing volume of lake data. A wider dialogue is required about how the acquired information can be used to contribute to some of the goals of ILEC based on

promoting integrated lake basin management and contributing to some of the Sustainable Development Goals.

REFERENCES

[1] J. Willinsky: Scholarly associations and the economic viability of open access publishing, Journal of Digital Information 4(2), 2004.

[2] A.L. Porter, J. Garner, T. Crowl: Research Coordination Networks: Evidence of the relationship between funded interdisciplinary networking and scholarly impact, BioScience, Vol. 62, pp. 282–288, 2012.

[3] A. Smith: Alternative open access publishing models, European Commission Directorate-General for Communications Networks, Content and Technology Report, https://ec.europa.eu/futurium/en/system/files/ged/oa_report.pdf, 2015.

[4] K.C. Weathers, P.C. Hanson, P.W. Arzberger et al.: The Global Lake Ecological Observatory Network (GLEON): the evolution of grassroots network science. Limnology and Oceanography Bulletin, 22, pp. 71-73, 2013.

[5] J.S. Read, D.P. Hamilton, I.D. Jones, K. Muraoka, L.A. Winslow, R. Kroiss, C.H. Wu, E. Gaiser: Derivation of lake mixing and stratification indices from high-resolution lake buoy data. Environment Modelling and Software, 26, pp. 1325-1336, 2011.

[6] L.A. Winslow, J.A. Zwart, R.D. Batt et al.: LakeMetabolizer: An R package for estimating lake metabolism from free-water oxygen using diverse statistical models, Inland Waters, Vol 6, pp. 622-636, 2016.

[7] R.I. Woolway, I.D. Jones, D.P. Hamilton, S.C. Maberly, K. Muraoka, J.S. Read, R.L. Smyth, L.A. Winslow: Automated calculation of surface energy fluxes with high-frequency lake buoy data, Environmental Modelling & Software, 70, pp. 191-198, 2015.

[8] F. Hu, K. Bolding, J. Bruggeman: FABM-PCLake – linking aquatic ecology with hydrodynamics, Geoscientific Model Development, 9, 2271-2278, 2016.

[9] P.A. Soranno, L.C. Bacon, M. Beauchene et al.: LAGOS-NE: a multi-scaled geospatial and temporal database of lake

ecological context and water quality for thousands of US lakes, GigaScience, Vol. 6, 2017.

O6-1

Web Application for Examining Hydroclimate Information of Global Lake Basins: CGLB Using a latest world lake database

Tosiyuki Nakaegawa[1]

[1]Meteorological Research Institute, Japan

Keywords: lake database, climate variabilities and disaster preventions and reductions, modeling, ILBM

ABSTRACT

More than 1 million of lakes are listed in the upgraded version of Web application, Climates of Global Lake Basins (CGLB). CGLB combines existing datasets and interactively displays geographical, hydrological, and climatological information for hundreds of lakes around the world. CGLB also provides landscape photographs provided by Global Confluence Project as well as quasi-real time monitoring of lake water levels using satellite altimetry provided by U.S. Department of Agriculture. CGLB can interactively create and animate time series of climatological data in a one-dimensional or two-dimensional (geographical) form. The listed lakes in the new version is based on the HydroLAKES provided. Other new features of the CGLB are: interactive drawing lake shapes, topography, land cover type, lake surface temperature, submonthly climatology in ClimatView developed by Japan Meteorological Agency. SQLite is embedded into the end program, allowing more than 1 million entry and search by key word. These functions are useful for education, expedition planning, and scientific research.

1. INTRODUCTION

Lakes has roughly 0.5% of the global land area[1] and hold more than 90% of the world's liquid freshwater in readily accessible bodies. Lakes are also one of the important components of hydrological cycles and at the same time have biogeochemical and ecological processes. In a changing climate under greenhouse gas emissions, these aspects will be affected by the global warming and will impact on human societies as well as on readily accessible water bodies.

Future projections of climates require the biogeo-chemical and ecological processes in lakes since they are embedded in the Earth system and interact with each other. Future projections of lakes require the lake information about their hydrological properties of distribution, volume and residence time. Therefore, global lake databases have been developed. Such databases are usually based on only the lake information because of their objectives. Public may want to know a climate in a target lake.

Then, we developed web application, Climates of Global Lake Basins (CGLB; http://hydro.iis.u-tokyo.ac.jp/CGLB/), combines existing datasets and interactively displays geographical, hydrological, and climatological information for hundreds of lakes around the world in 2015[2]. The lake information in CGLB is based on the World Lake database (WLDB) [3]. Unique features of WLDB is comprehensive information about lakes from geographical information to biogeochemical one but lists only about 650 lakes. The number of the lakes in WLDB for each country is distinctly biased since they are selected as important order for people.

Recently, a new lake database, HydroLAKES has been developed with more than 1 million entry[4]. We upgraded CGLB based on HydroLAKES.

2. WEB APPLICATION

We designed CGLB as provision of climatological information for a target lake basin so that one who want to look into the lake basin can obtain the information interactively for each own purpose.

SQLite is employed to deal with more than 1 million entry. SQLite is a relational database management system and often embedded into the end program but not client-server database engine.

New features of the CGLB are summarized below:

- replace of base lake geo-spatial information: HydroLAKES; more than 1 million lakes are listed in CGLB and other components such pouring points are newly included in CGLB,

- figures of lake shapes with either elevation or land cover type can be drawn interactively,

- Lake surface temperature can be drawn in one- or two-dimensional time series,

- link to submonthly climatology in ClimatView developed by Japan Meteorological Agency: daily data can be seen but the number of the stations are small, and
- SQLite is embedded into the end program, allowing more than 1 million entry and search by keywords.

3. CASE STUDY

We demonstrate what CGLB can provide the data for the Caspian Lake as a target. Fig. 1 shows a screenshot of CGLB for the Caspian Lake. Geographical area of the Caspian Lake are shown on the Google Maps on the left-hand side and lake information based on WLDB and HydroLAKES are displayed on the right-hand side. Left-bottom below the Google Maps provides interactive draw of figures: 1-dimensional time series and 2-dimensional geographical distribution of land surface meteorological variables.

Observation stations operated by National Meteorological and Hydrological Services appear on this Google Map by one click and climatological monthly mean surface air temperature and precipitation can be seen on ClimatView developed by Japan Meteorological Agency (Fig. 2). These data are called as CLMAT and provided through World Meteorological Organization (WMO)[5]. CLIMAT is the names of the codes for reporting monthly values of meteorological parameters from weather stations and for reporting monthly aerological means from weather stations.

4. DISCUSSION AND CONCLUSION

We upgraded a web application of CGLB by introducing a new lake database, HydroLAKES with more than 1 million entry of lakes by combining existing datasets and interactively displays geographical, hydrological, and climatological information around the world. These functions are useful for education, expedition planning, and scientific research.

Global Framework for Climate Service (GFCS) led by WMO is a global partnership of governments and organizations that produce and use climate information and services. It seeks to enable researchers and the producers and users of information to join forces to improve the quality and quantity of climate services worldwide, particularly in developing countries. CGLB may contribute to GFCS by bridging dialogues between lake-relevant communities and climate ones. Since CGLB is developed by climatologists and/or producers, more ideas by limnologists and/or lake-relevant users must be
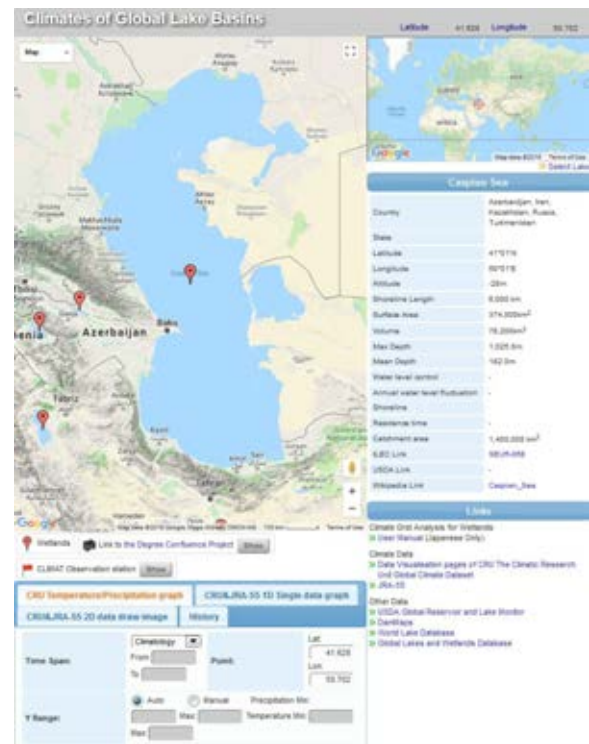
Fig. 1 Screenshot of CGLB for the Caspian Lake.

Fig. 2 Screenshot of climatological monthly mean surface air temperature and precipitation at Fort Shevchenko on the shore of the Caspian Lake for the Caspian Lake. http://ds.data.jma.go.jp/gmd/tcc/tcc/products/climate/climatview/
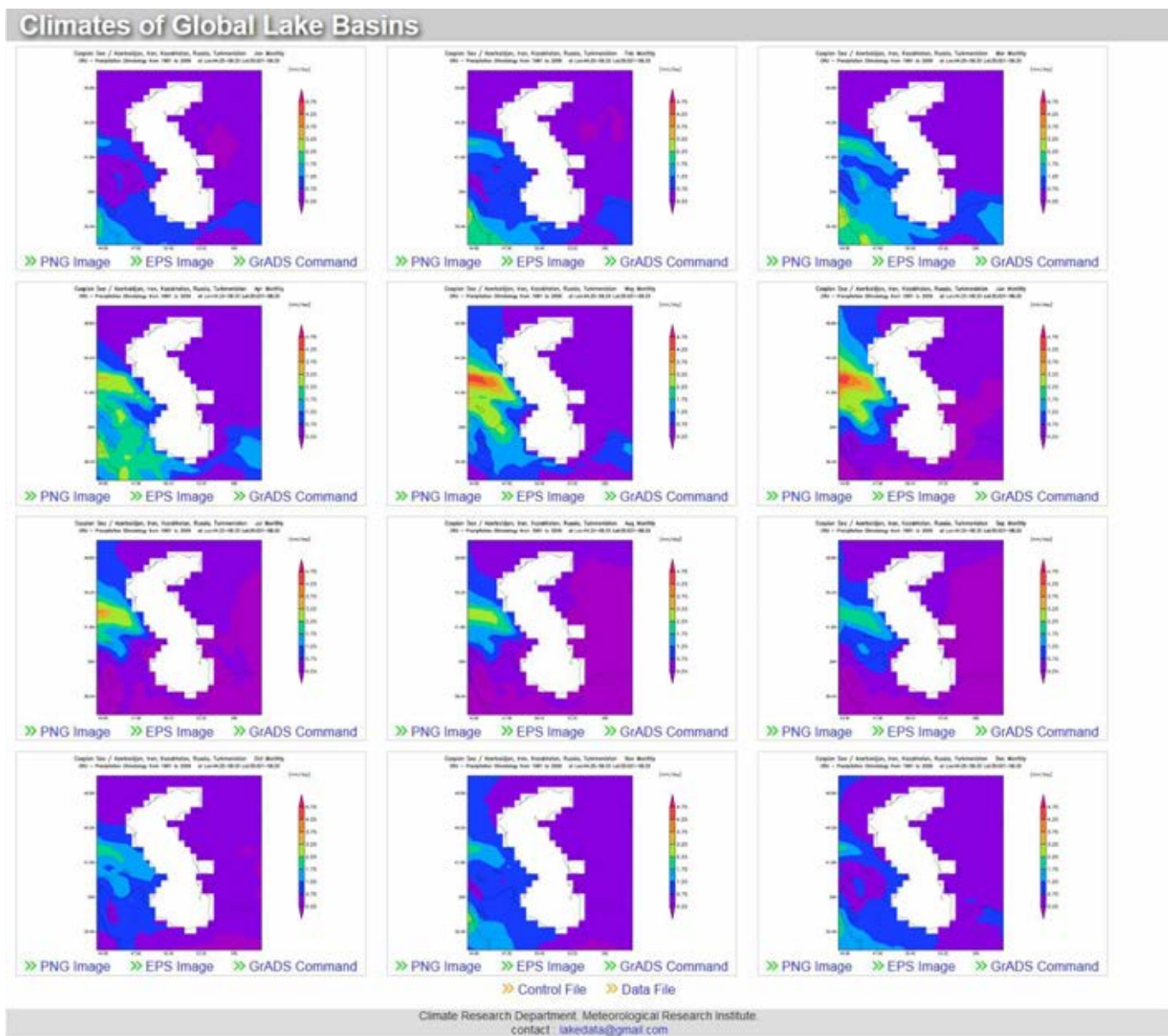
Fig.3 Climatological mean monthly precipitation around the Caspian Lake for each month in two-dimensional form or geographical one. The area drawn in each panel is completely same area as in Fig.1. This figure is drawn interactively on CGLB.

required for further developments.

Although CGLB provides figures on demand, but not even simple analysis. This implementation may depend on users' request. CGLB contains comprehensive information, and therefore would provide an opportunities in a variety of unique research on global lakes.

AKNOWLEDGEMENTS

REFERENCES

[1] Nakaegawa T: Comparison of water-related land cover types in six 1-km global land cover datasets, Journal of Hydrometeorology, Vol. 13, pp. 649–664, 2012. DOI: 10.1175/JHM-D-10-05036.1.

[2] International Lake Environmental Committee: World Lake Database, 1999. http://wldb.ilec.or.jp. Last access April 11, 2018.

[3] Nakaegawa T, S. Horiuchi, and H. Kim: Development of a web application for examining climate data of global lake basins: CGLB, Vol. 9, pp.125-132, 2015. DOI: 10.3178/hrl.9.125

[4] Messager M.L., Lehner B., Grill G., Nedeva I., Schmitt O: Estimating the volume and age of water stored in global lakes using a geo-statistical approach. Nature Communications: pp.13603. 2016. DOI: 10.1038/ncomms13603

[5] World Meteorological Organization: Handbook on CLIMAT and CLIMAT TEMP Reporting, WMO Technical Document, No.1188, pp.115, 2009.

O6-2

Environmetric techniques for spatiotemporal hydrochemical characterization and Pollution source identification of the Dal lake, Kashmir Himalaya, India

Shakil Ahmad Romshoo and Shabir Ahmad Khanday

Department of Earth Sciences University of Kashmir, Srinagar, India

Keywords: Environmetric, Water Quality Index, GIS, Aquatic Vegetation, Himalaya

ABSTRACT

The paper explains the background processes responsible for the spatial distribution of hydrochemistry of the picturesque Himalayan Lake, Dal, in Kashmir, India. Statistical analyses were used to understand the spatiotemporal variability of 18 hydrochemical parameters collected from 30 sampling sites well distributed within the lake (grid spacing of 1 km^2) from Mar 2014-Feb 2016. Hierarchical Cluster Analysis (HCA) grouped all the data into 3 clusters based on the hydrochemical similarities, Discriminant analysis (DA) also revealed the same clusters and patterns, validating the results of HCA. Wilk's λ distribution revealed the contribution of ions, nutrients, secchi disk transparency, dissolved oxygen and pH in the formation of clusters in the lake. The results are in consonance the Principal Component Analysis (PCA) of the whole lake data and individual clusters, which showed that the variance is maximally explained by the ions (46.82%), DO and pH (9.36%), nitrates and phosphates (7.33%) and SDH (5.98%). Overall, the WQ of the lake is unfit for drinking due to the presence of coliform bacteria.

1. INTRODUCTION

Anthropogenic and natural causes contribute towards the deterioration of surface water quality of a lake and seriously impair its use for drinking, recreation, aquatic life, agricultural and industrial purposes [1]. Understanding the lake processes and functions to deduce its ecological significance is dependent on our ability to determine the patterns of variation in physical, chemical and biological characteristics at relevant ecological spatiotemporal scales. Dal lake, spread over an area of about 24 km^2 with a catchment of 337 km^2 and average water depth of 2.32 m, is known for its scenic, environmental, cultural and socio-economic importance in Kashmir valley, India (Fig. 1). However, due to the rapid unplanned urbanization, land use/land cover changes in the catchment, and inflow of nutrients, the lake WQ has severely degraded over time [2]. Since a large population in the region is dependent on the lake for varied services and products, the lake degradation besides hindering sustainable development of the lake, exposes the human and aquatic life within and in the vicinity of the lake to various risks. Regular monitoring of lake WQ on scientific basis is a challenging task and requires human resources and equipment to sustain the program. The present research, to the best of our knowledge, is first of its kind in terms of the scientifically adequate time series of WQ data well represented in time and space for understanding the spatial variability of hydrochemical characterization of the Dal waters using rigorous statistical methods in GIS environment. The main objectives of this work are to; a) assess the overall Dal lake hydrochemistry; b) evaluate the spatial variability and distribution pattern of WQ parameters and; c) to identify the underlying ecological processes that cause this pattern.
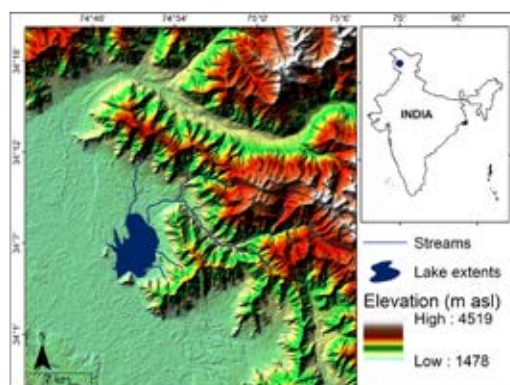
Figure1: The Dal lake, Kashmir Himalaya

2. METHODS

18 WQ parameters, analysed as per the standard methods[3] for 2 years at 30 locations of 1 km^2 grid each (12960 observations) are; Temperature, SDT, pH, EC, DO, TA, TH, Ca^{+2}, Mg^{+2}, Na$^+$, K$^+$, Cl$^-$, SO$_4^{2-}$, NH$_3$-N, NO$_2$-N, NO$_3$-N, PO$_4^{2-}$-P and TP. Environmetric analysis of the WQ data was conducted using HCA, DA and PCA. Suitability of the data for PCA was determined using Kaiser-Meyer-Olkin (KMO) and Bartlett's Sphericity test (BST). DA was applied on the original data, whereas HCA and PCA were used on the standardized data by z-scale transformation to avoid any errors due to the differences in data dimensions. HCA was done using Ward's method and squared Euclidean distance. DA was used to verify the accuracy of clusters delineated by HCA using the equation (1).

$$f(G_i) = k_i + \sum_{j=1}^{n} w_{ij} p_{ij} \quad \cdots\cdots (1)$$

where i is the number of groups (G), k$_i$ is the constant inherent to each group, n is the number of parameters used to classify a set of data in a given group, w$_j$ is the weight coefficient assigned by DA to a given parameter (p$_j$). After

the verification of the clusters, the influence of every WQ parameter in the formation of a cluster was determined using Wilk's λ distribution given below.

$$\lambda = \frac{\sum_i \sum_j (x_{ij} - \overline{x}_i)^2}{\sum_i \sum_j (x_{ij} - \overline{x})^2} \qquad (2)$$

where x_{ij} is the jth element of the ith cluster, $\overline{x}i$ the ith cluster's mean and $\overline{x}$ the total mean.

PCA works with a correlation matrix and thus reflects the stochastic interdependencies. The correlation coefficients obtained between the original parameters and PCs are the factor loadings which describes the weights of the PCs in the original variables. The PC is expressed as:

$$z_{ij} = a_{i1}x_{1j} + a_{i2}x_{2j} + \cdots + a_{im}x_{mj} \qquad (3)$$

where z is the component score, a the component loading, x the measured value of parameter, i the component number, j the sample number and m the total parameters. The WQ maps were prepared in GIS using natural neighbour (NN) interpolation method. To determine the value of an attribute at location x, values of the points which are the natural neighbours of x and their relative weights are used. If we assume that each data point in a set has a scalar attribute *ai*, then the NN is represented by:

$$f(x) = \sum_{i=1}^{n} w_i(x)a_i \qquad (4)$$

where f (x) is the interpolated function value at location x. WQI is a very useful method for assessing water quality. Each of the lake WQ parameter was assigned different weights ranging from 1 to 5 based on critical health effects. WQI is computed using the following equations:

$$Rw_i = \frac{w_i}{\sum_{i=1}^{n} w_i} \qquad (5)$$

where Rwi is the relative weight, wi is weight of each WQ parameter and n is the number of WQ parameters.
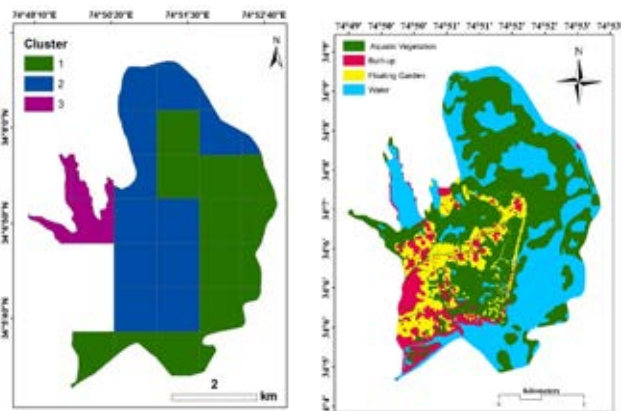
Figure2: Showing the 3 cluster(a) and land use and land cover

3. RESULTS

The analysis of the WQ shows that water temperature varied from 2.5 °-30.3° C. SDT, that represents not only the inorganic suspended solids but also the phyto-planktons, showed a mean value of 1.31m. The average values for pH and EC of all the sites were in the range of 7-10 and 110-680 μS/cm respectively. DO varied greatly from 0.8 to 14 mg/l with a mean value of 7.17. The Dal waters are well buffered and hard with an average value of 101.8mg/l and 112.8mg/l for TA and TH respectively. Among the ions, Ca^{+2} was found to be the dominant ion with an average value of 31.7(mg/l), followed by Cl^-, calcium chloride (10.3), Mg^{+2}(8.1), SO_4^2(7.1), Na^+(4.6) and K^+(1.7). NO_3-N among other forms showed dominance with the value ranging from 0.01 to 2.03 mg/l. Similarly, presence of TP varied between 0.02 to 1.21 mg/l.

Spatiotemporal variability of the WQ of Dal lake is aptly represented by the cluster analysis which identified 3 distinctive and homogenous clusters (Fig. 2a**).** DA showed that the original clusters were correctly recognized in 78.3% of the cases. Wilk's λ quotient was determined for all the WQ parameters at each point to assess the influence of each parameter on the cluster pattern. The lower values are depicted by Cl^-(0.570), Na^+(0.599), K^+(0.621), SDT(0.641), NO_3-N(0.753) and EC(0.781). It is clear from the Wilk's λ distribution that there is a mixed role of most of the parameters; both nutrients and ions in the cluster formation. This is due to the fact that the Dal, besides being hard and well buffered has a significant anthropogenic influence and allochthonous organic matter, mostly in the form of sewage and aquatic vegetation respectively.

A similar kind of pattern and behavior is exhibited by ions, total alkalinity, total hardness and conductivity. Therefore, to keep the discussion succinct and avoid the repetition, we chose chloride as the representative WQ parameter for discussion here, as it scores highest value in discrimination of clusters. In Cluster 3, the chloride shows the higher median value and the lowest value of the parameter is observed towards eastern (crescent shaped) part of the lake (Cluster1). The 3 clusters cover variable number of sites based on the WQ of the Dal lake. The eastern crescent shaped basin (Cluster 1) of the lake comprises of the maximum number of sites (14). The cluster encompasses the lake area from the northern side stretching through the eastern shore and ends up at the southern tail of the lake, which is also its outlet. The cluster is having higher values of pH, DO and SDT compared to other clusters. Aquatic vegetation is also significant in this cluster as can be seen in the land use land cover map of the lake (Fig. 2b). Cluster 2 mostly comprises of lake areas located towards the inner portion of the lake and is spread over 12 grid samples. The Cluster 2 is complex in terms of the heterogeneity of LULC (Fig. 2b) comprising of built-up (permanent structures), floating gardens and aquatic vegetation.

To understand underlying ecological and hydrochemical processes responsible for the observed distribution and clusters of WQ patterns, PCA was performed on the entire WQ dataset and on the clusters as well. PCA yielded four Principal Components (PCs) accounting for 69.5% of the data variance. Isoline maps of PCs were generated in GIS describing spatial changes of the component scores for each sampling site. Since cluster analysis showed that there are three distinguishable areas in the lake, hence, PCA was applied on the WQ data cluster-wise. The 1st PC of the clusters explains 51-55% of the cumulative variance of the data, 2nd PC of the cluster data accounts 10-14% and 3rd PC accounts only 9-10% of the variance.

The WQI was computed cluster-wise which were identified using HCA and DA analysis, and have distinct WQ characteristics. The data pertaining to coliform bacterial count was taken from the published and unpublished work. The seasonal WQI values of the 3 clusters indicated that the highest WQI values are observed in summers and the lowest in winters in all the 3 clusters. Moreover, the seasonal WQI values were registered higher in cluster 3 (~2011) followed by cluster 2 (~1977) and then cluster 1 (~710), which further substantiates the fact that the most polluted part of the lake lies within the cluster 3.
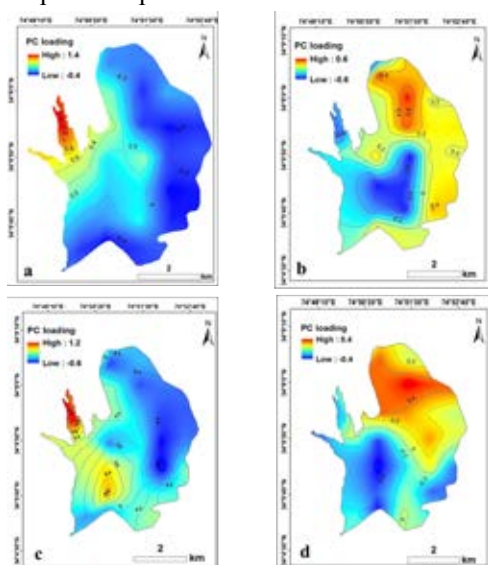
Figure 3: Spatial distribution of PC loading scores (a-d) 1st-4th PC

4. DISCUSSION

The environmetric analysis indicates the dominant role of inorganic variables, which could be attributed to the weathering, dissolution and erosion of the geological formations in the catchment. The high concentration of WQ parameters during winter is due to the low vegetation metabolism; as a result of which the decomposed organic matter remains unutilized. The determining character of pH and DO is due to the presence of luxuriant aquatic vegetation which during the photosynthetic process releases oxygen and utilizes dissolved CO_2 and its

associated hydrogen ions. The higher score of pH and DO are observed in the eastern part of the lake as compared to the central and western parts, which have less macrophytes. The sources of nitrate and phosphate nutrients are domestic sewage from the settlements in the vicinity, agricultural run-off, stream effluents, fertilizers and manures used in croplands in the catchment. The high PC scores are observed in Nigeen and central portion of the lake due to the high anthropogenic pressures. A positive loading of moderate nature was exhibited by SDT due to the presence of macrophytes which provides a refuge to zooplanktons, thus effectively checking the population of phytoplankton, leading to the less turbidity. Also, the presence of the aquatic plant slows down the flow of the lake waters, resulting in a decrease in the concentration of suspended sediments in the water. The PC scores (Fig. 3d) are in conformity with this reasoning as high scores are found in the eastern basin compared to the central and western basins having less vegetation. The striking observation of this assessment is that the highest effective weights are contributed by the coliform bacteria in all the 3 clusters and ranged from 95.874% to 99.497%. This clearly indicates that the coliform bacterial count is the primary parameter responsible for making the waters of the lake unfit for drinking.

5. CONCLUSION

The environmetric and GIS techniques are appropriate for inferring the intricate spatiotemporal variability of water quality and pollution sources in the lake. These methods recognize the lake spatial heterogeneity in terms of the water quality with much robustness and would therefore help planning any future spatial sampling strategy in an optimal manner by reducing time and costs. Moreover, the approach is helpful in understanding the consequence of lake water interventions and the underlying processes in both space and time. Therefore, the environmetric techniques, used in this study for assessing the spatiotemporal variability and pattern recognition of the lake water quality, should act as a pre-requisite for lake managers across the globe to effectively initiate and implement any lake conservation and restoration strategies.

REFERENCES

[1] Rashid I, Romshoo SA, Amin M, Khanday SA, Chauhan P. Linking Human-Biophysical Interactions with the trophic status of Dal lake. Limnologica- Ecology and Management of Inland Waters, Vol. 62, pp. 84–96, 2017

[2] Badar B, Romshoo SA, Khan MA. Modeling the catchment hydrological response in a Himalayan lake as a function of changing land system. Earth System Science, Vol. 112(2), pp. 433-449, 2013

[3] APHA. Standard methods for the examination of water and waste water. 21st Edition. Washington, USA, 2005.

[4] Mei K, Liao L, Zhu Y, Lu P, Wang Z, Dahlgren RA, Zhang M. Evaluation of spatial-temporal variations and trends in surface water quality across a rural suburban-urban interface. Environmental Science and Pollution Research 21:8036–8051, 2014

O6-3

Using Multimetric Benthic Macroinvertebrate Index for the Assessment of River Health in Thailand

Chotiwut Techakijvej[1] and Chitchol Phalaraksh[1,2]

[1]Environmental Science Program, Faculty of Science, Chiang Mai University, Chiang Mai, Thailand

[2]Department of Biology, Faculty of Science, Chiang Mai University, Chiang Mai, Thailand

Keywords: bioassessment, biotic index, multimetric index, Loei river, water quality

ABSTRACT

Today, the health of streams and rivers has been dramatically changed by anthropogenic disturbances. The Loei River in Loei province, Thailand is one of the Mekong River tributary which affected by many anthropogenic disturbances such as agricultural activities, urbanization and industry. In Thailand, standard water quality is based on chemical measurements, which are not reflect cumulative stressors. Use of multimetric benthic macroinvertebrate index can reflect overall streams and rivers ecological. The aim of this research is to evaluate rivers health by using multimetric benthic macroinvertebrate index. Ten sampling sites were selected to evaluate rivers health. The result showed that Loei river has been threating by many anthropogenic activity. Thus, river and land use management are urgent need in this catchment.

1. INTRODUCTION

Today, rapid population growth, industrialization and urbanization are the main threats to river basins especially developing countries. Many bioassessment approaches are used for evaluating the conditions of streams and rivers. Use of macroinvertebrate species as indicator are one of aquatic bioassessment approaches in the United States, Europe, Australia, Thailand and other countries [1-3]. However, the indicator species concept is an insufficient to measure of overall streams and rivers ecological [4-5]. Thus, other bioassessment approaches, such as multimetric indices, have been developed to reflect overall streams and rivers ecological. The first multimetric method which was developed for use with fish communities [6]. Now various types of multimetric indices have been subsequently proposed in other aquatic habitats and benthic macroinvertebrates [7,8,9].

The Loei River in Loei province, Thailand is one of the Mekong River tributary which affected by many anthropogenic disturbances such as agricultural activities, urbanization and industry. In Thailand, the national standard assessment of water quality is based on chemical measurements [10], which are not reflect cumulative stressors. However, the official national standard method on using macroinvertebrates as key biological indicators has not been established. The multimetric benthic macroinvertebrate index for the assessment of The Loei River was developed by Boonsoong et. al. in 2009 [11].

The aim of this research is to evaluate rivers health by using multimetric benthic macroinvertebrate index.

2. METHOD

Study area and site selection

The study area was in The Loei River catchments, Loei province, Northeastern Thailand. The study area was at latitude 16°58′–17°52′ N, longitude 101°28′–101°47′ E. Sampling periods were chosen to follow seasonal patterns in Thailand (hot, wet, and cold seasons).
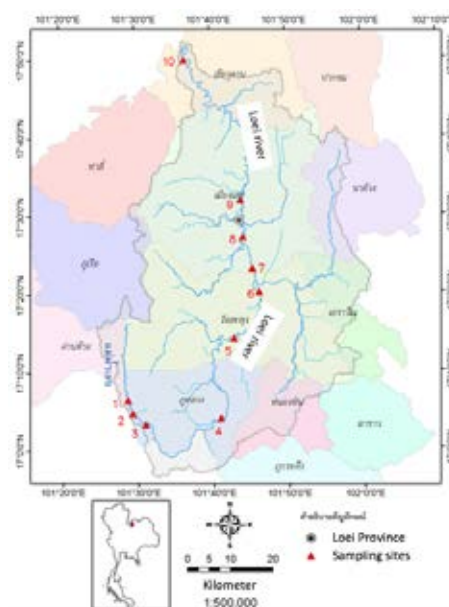
Fig.1 Map of Loei river catchment and sampling sites

Water quality and macroinvertebrate samples were collected seasonally for a period of 2 years, which included cold season (January 2016 and late of February 2017) and hot season (March 2016 and May 2017). No samples were collected in wet season because flooding and other seasonal disturbance. Sampling sites were divided in 3

groups, upstream (site 1-3), midstream (site 4-7) and downstream (site 8-10) (fig.1).

Field and laboratory methods

Ten water quality parameters (table 1) were measured along with the collection of macroinvertebrate at each of the sampling sites.

Table 1 Mean ± SD of physico-chemical parameters of The Loei river

Parameters	Cold 2016	Cold 2017	Hot 2016	Hot 2017
Temperature (◦C)	25.5 ±1.5	28.5 ±1.5	28.7 ±2.0	26.0 ±1.7
pH	7.25 ±0.31	8.18 ±0.29	7.42 ±0.43	6.38 ±0.29
conductivity (μS cm^{-1})	247.6 ±110.4	314.2 ±155.2	357.2 ±178.9	97.2 ±44.3
TDS (mg l^{-1})	124.2 ±54.7	167.2 ±81.2	178.5 ±90.3	49.8 ±22.9
Turbidity (NTU)	11.5 ±8.3	25.1 ±57.7	6.9 ±4.0	281.4 ±290.8
Dissolved Oxygen(mg l^{-1})	7.1 ±1.1	7.5 ±0.7	7.4 ±2.4	5.9 ±1.4
BOD (mg l^{-1})	2.2 ±2.7	2.8 ±2.1	2.8 ±0.9	1.9 ±1.4
NH^{4+} (mg l^{-1})	0.07 ±0.08	0.49 ±0.21	0.22 ±0.15	0.43 ±0.23
NO^{3-} (mg l^{-1})	1.2 ±0.7	1.5 ±0.7	1.3 ±0.6	3.9 ±1.9
PO$_4$$^{3-}$ (mg l^{-1})	0.22 ±0.15	0.41 ±0.46	0.48 ±0.37	0.14 ±0.12

At each site, both river banks were divided into 3 transects (total 6 transects for each site). Macroinvertebrates were collected using a D-frame (0.3 m. wide, 500 μm. mesh) 5 sweeps for each transects. All samples were preserved in the field with 80% ethanol. In the laboratory, specimens were rinsed in 500 μm. mesh sieves and large organic materials were removed. All organisms from the sorted sample were identified to the lowest possible taxonomic.

Data analysis

Benthic macroinvertebrate assemblage data were analyzed for 9 metrics follow Boonsoong et. al [11] and categorized into 3 scoring range (table 2). The multimetric index was calculated by aggregating the scores of each of the 9 metrics. The possible index values ranged from 9 to 43; this was derived by summing the minimum and maximum scores for each metric. The range of the multimetric index was divided define five classes of biological integrity, excellent condition (scores of 37-43) equivalent good (30-36), fair (23–29), poor (16–22) and very poor (9–15).

3. RESULTS AND DISCUSSION

Mean of 10 water quality parameters were showed in table 1. The macroinvertebrates multimetric index of ten sites were showed in table 3. The index showed good-fair water quality for upstream site (1-3) of cold 2017 and hot 2016. The upstream of Loei river was disturbed by some agricultural activities such as farming. Agricultural activities can be a non-point source pollution that polluted the river by runoff water [12]. Most sampling site of the midstream and downstream of Loei river were categorized into fair and poor water quality because most of the area are urban area, industrial and mining.

4. CONCLUSION

The multimetric benthic macroinvertebrate index can be used to evaluate rivers health. From the results, the Loei river was treated by many human activities. Thus, river and land use management are urgent need in this catchment.

5. ACKNOWLEDGEMENT

REFERENCES

[1] Barbour, M. T., Stribling, J. B., & Karr, J. R.: Multimetric approach for establishing biocriteria and measuring biological condition, Biological assessment and criteria: Tools for water resource planning and decision making, Vol. 3, pp. 63-77, 1995.

[2] Thorne R. S. T., Williams W. P.: The response of benthic macroinvertebrates to pollution in developing countries: a multimetric system of bioassessment, Freshwater Biology, Vol. 37, pp. 671-686, 1997.

[3] Mustow, S. E.: Biological monitoring of rivers in Thailand: Use and adaptation of the BMWP score, Hydrobiologia, *Vol. 479*, pp. 191–229, 2002.

[4] Metcalfe, J.L.: Biological water quality assessment of running waters based on macroinvertebrate communities: History and present status in Europe, Environ. Pollut., Vol. 60, pp. 101-139, 1989.

[5] Barbour, M.T., Stribling, J.B., Karr, J.R.: The multimetric approach for establishing biocriteria and measuring biological condition. in biological assessment and criteria: tools for water resource planning and decision making, pp. 63-77, 1995.

[6] Karr, J.R.: Assessment of biotic integrity using fish communities, Fisheries, Vol. 6, pp. 21-27, 1981.

[7] Barbour M. T., Gerritsen J., Snyder B. D., Stribling J. B.: Rapid bioassessment protocols for use in streams and wadeable rivers: periphyton, benthic macroinvertebrates and fish. 2nd edition, U.S. EPA 841-B-99-002, Environmental Protection Agency, 339 pp., 1999.

[8] Blocksom K. A., Johnson B. R.: Development of a regional macroinvertebrate index for large river bioassessment,

Ecological Indicators, Vol. 9, pp. 313-328, 2009

[9] Cuadrado V., Neira X. X., Cuesta T. S.: A multimetric model to assess the biological quality of the Cabe River, NW Spain, Ecohydrology, Vol. 7, pp. 1196-1207, 2014.

[10] Pollution Control Department: Water quality criteria & standard in Thailand. Bangkok: Pollution Control Department, Ministry of Science Technology and Environment, 1997.

[11] Boonsoong B., Sangpradub N., Barbour M. T.: Development of rapid bioassessment approaches using benthic macroinvertebrates for Thai streams, Environmental Monitoring and Assessment Vol. 155, pp. 129-147, 2009.

[12] Javier, M., Sara, M. Z., Hugh, T.: Water pollution from agriculture: a global review, The food and agriculture organization of the united nations rome and the International Water Management Institute on behalf of the Water Land and Ecosystems research program Colombo, 2017.

Table 2 Score for the core metrics for the cold season and hot season.

Metric	Categorical scoring range for cold season			Categorical scoring range for hot season		
	5	3	1	5	3	1
No. of total taxa	≥ 32	31-16	< 16	≥ 35	34-18	< 18
No. of Diptera taxa	≥ 5	4-3	< 3	≥ 5	4-3	< 3
No. of EPTC taxa	≥ 19	18-10	< 10	≥ 21	20-11	< 11
(%) Plecoptera	≥ 3.0	2.9-1.5	< 1.5	≥ 3.1	3.0-1.5	< 1.5
(%) Tolerant organisms	≤ 22.4	22.3-33.6	> 33.6	≤ 33.7	33.8-50.6	> 50.6
Beck's Biotic Index	≥ 14	13-7	< 7	≥ 13	12-7	< 7
(%) Intolerant organisms	≥ 9.9	9.8-5.0	< 5.0	≥ 16.8	16.7-8.4	< 58.4
No. of shredders taxa	–a	≥ 3	< 3	–a	≥ 2	< 2
No. of clingers taxa	≥ 16	15-8	< 8	≥ 15	14-8	< 8

a Considered a weak metric for discrimination and given only two scoring criteria

Table 3 Class of water quality of 10 sampling sites and index score.

Site	Multimetric			
	Cold 2016	Cold 2017	Hot 2016	Hot 2017
1	fair 29	good 33	good 31	fair 27
2	v-poor 11	good 35	good 31	fair 25
3	fair 25	fair 29	good 27	poor 15
4	fair 25	fair 27	poor 17	poor 19
5	fair 25	fair 25	fair 29	fair 23
6	poor 17	good 31	poor 21	poor 17
7	fair 25	fair 25	poor 21	v-poor 15
8	poor 21	fair 23	poor 19	poor 17
9	fair 25	good 33	poor 21	poor 17
10	poor 21	fair 29	fair 27	poor 15

O6-4

Environmental monitoring and Ecotoxicology for Tropical Environment: Standard and Application in Mekong River Countries

Chuleemas Boonthai Iwai[1,2]*, Naksayfong Khounnavongsa[1], Lyly Soeung[1] and Tham C. Hoang[3]

[1] Department of Soil Sciences and Environment, Faculty of Agriculture, Khon Kaen University, Khon Kaen, Thailand, 40002, [2] Integrated Water Resource Management Research and Development Center in Northeast Thailand, Khon Kaen, Thailand, 40002, [3] Institute of Environmental Sustainability, Loyola University Chicago 25 1032 W. Sheridan Road, Chicago, Illinois, USA

* Corresponding author. E-mail: chulee_b@kku.ac.th, chuleemas1@gmail.com
Keywords: water quality guideline, Environmental Risk Assessment, water pollution, sustainable development

ABSTRACT

The aquatic resources of the Mekong River are importance to supporting the livelihoods of a large percentage of 60 million who live along the Lower Mekong Basin. The protection of aquatic habitat from damage and understanding of both sensitivity of aquatic organisms to contaminant and ecological effects are needed. Mekong River quality criteria of aquatic life for metals are largely driven by the extremely sensitive small organism's toxicity which should be the Mekong native species. Environmental monitoring and Ecotoxicology of heavy metal (copper) on several tropical freshwater biota was studied using field-collected water from local sites along Lower Mekong Basin in Thailand, Laos and Cambodia, which had different water quality parameters under tropical environment in the range of total hardness, alkalinity, pH and dissolved organic carbon. The result showed the mortality rate of organisms increased with increasing of copper concentrations and exposure time. The results found that copper toxicity of fish, invertebrates and other aquatic organisms are influenced by water quality parameters such as hardness, alkalinity, pH and DOC. Copper (Cu) is a big concern for environment, human and aquatic organisms because it can accumulate in to plant and animals via food web. The outcoming of this series of laboratory experiment will provides a worst-case scenario and useful for determine the risk assessment of copper on local freshwater organisms in Mekong River Basin in order to help and protect the Mekong River in the future and to set a water quality standard for heavy metal in the Mekong River Basin countries.

1. INTRODUCTION

The Mekong River is one of the world's greatest river systems and sustains human life and ecosystems. The livelihoods of 60 million people who live along the Lower Mekong Basin (LMB) rely on both the economic resource and the ecological health of the river [1]. However, the development activities during the past decade and up to now, including mining, industries, agriculture, deforestation, and household wastes have caused of extensive soil erosion and contributed increasingly to environmental levels of heavy metals especially copper (Cu) into water body [2]. Although the water quality of the Mekong River is considered to be remarkably good, some areas of the Mekong Delta, which are adversely inflicted by high population density, irregular mining activities, and increasing agricultural activities, have experienced worsening water quality [1].

Copper is known as the important that all living organisms require its small amounts (5-20 µg/g) to survive. However, too much copper concentration more than (20µg/g) become toxic [3]. Copper has been documented as one of the most toxic metals to aquatic organism and ecosystem [4].

Impacts of copper on an aquatic atmosphere are complex and depend on the physicochemical characteristics of water [5]. Copper toxicity of fish, invertebrates and other aquatic organisms are influenced by water quality parameters such as hardness, alkalinity, pH and DOC (dissolved organic carbon) [6].

The United States Environmental Protection Agency (US.EPA) has issued a guideline for conducting

early-life-stage toxicity test suitable for acute and chronic toxicity tests used for measuring the aggregate toxic chemicals in an effluent or receiving water to freshwater and marine organisms [4]. Moreover, many research papers were designed and conducted on ecotoxicology of copper worldwide, but most of them focused on temperature aquatic species. In Mekong River Basin Countries, the information on the impact of toxicity effects of soluble

copper on the tropical aquatic biota is limited. Therefore, the ecotoxicology of copper on local species with Mekong River will be a good representative for tropical aquatic

species. In the present study, the ecotoxicology of copper on several local aquatic biota under different water parameters were investigated in order to help and protect the Mekong River in the future and to set a water quality standard for heavy metal in the Mekong River in the Mekong River Basin.

2. METHOD
Water sampling

Water samples were collected from several sites along the Mekong River in Thailand, Laos and Cambodia during wet and dry season in Year 2016 which focused on different water quality parameters.

Surface water for physical-chemical analysis and toxicity tests was sample at the middle of the River. All water samples were transferred back to the Ecotoxicology laboratory in Khon Kaen University.

Water quality Analysis

Water quality parameters including heavy metal, pesticide and nutrient concentrations were measured using standard techniques [8]. Concentrations of metals were estimated by the analysis by inductively-coupled plasma mass spectrometry (ICPMS). Measurements were made of pH, electrical conductivity (EC), temperature, dissolved oxygen (DO) concentration in river water using field equipment. Active sampling was employed to collect water samples (1L) for total dissolved solids (TDS), total alkalinity (mg/L $CaCO_3$), hardness (mg/L $CaCO_3$), nutrients (total N and P, nitrate (NO_3^-) and ortho-phosphorus [P]) and dissolved organic carbon (DOC). All measurements on the active water samples were undertaken in the field or at the Division of Land Resources and Environment, Department of Plant Sciences and Agricultural Resources, Faculty of Agriculture Khon Kaen University.

Ecotoxicology Test

In this study, US EPA method (2002) was used for the acute toxicity with different water quality parameter on tropical aquatic biota.

RESULTS

The result of chemical characteristics and water quality parameters of field-collected samples are given in Table 1 and Table 2. In general, the waters are considered as not being contaminated. In table was shown concentration of toxic metal (e.g., Cu, Cr, Pb, Ca, As, Fe, Zn and Mn) were below detection limit or less than the

maximum acceptable limited for aquatic life in Thailand. And also, pesticides (Organochlorine group, Organophosphate group, Chlrorinated Baenzenes, Chloronitirile Pesticides, Cholordane-related Compounds and Cholorinated Herbicides) were not detected in the collected water were shown in (Table 3)

Table 1. water quality parameters of Mekong River in Thailand, Laos and Cambodia

Parameters	Results		
	Thailand	Laos	Cambodia
pH	6.39	6.67	7.2
EC (µS/cm)	86	94	84
Total alkalinity (mg/LasCaCO₃)	81	94	83
Total hardness (mg/LasCaCO₃)	95	120	92
TDS (mg/L)	93	96	91
Total N (mg/L)	10	23	10
NO₃⁻ (mg/L)	1.0	1.8	1.2
Ortho-P /Total P (mg/L)	0.002/0.26	0.05/0.36	0.04/0.34
BOD (mg/L)	3.7	18.1	9.3
DOC (mg/L)	1.9	6.83	2.3
Calcium (mg/L)	30	41	33
Magnesium (mg/L)	3.91	8.34	3.93
Mn (µg/L)	1.19	9.17	2.08
Zn (µg/L)	2.98	3.86	2.75
Fe (µg/L)	0.68	4.80	2.43
Arsenic (µg/L)	0.028	0.053	0.022
Cadmium (µg/L)	0.01	0.021	0.00
Lead (µg/L)	0.042	0.081	0.047
Cr (µg/L)	0.048	0.059	0.050
Copper (µg/L)	0.35	0.39	0.32

Table 2. LC_{50} with 95 percent confidence interval of formalin on chironomus javanus *(C. javanus)* and fish Nile tilapia *(Oreochromis niloticus)* of two different DOC of Mekong River

Species	DOC (mg/L)	LC_{50} with 95% Cl (µg/L)			
		24h	48h	72h	96h
Nile tilapia	5.74	1228 (1138-1340)	1052 (890-1296)	939 (771-1185)	742 (562-981)
	1.12	1236 (1128-1371)	806 (494-1334)	561 (129-1177)	397 (123-761)
C. javanus	5.74	8237 (5471-32105)	5033 (3035-88359)	2206 (-)	853 (-)
	1.12	2864 (-)	2443 (-)	983 (-)	707 (-)

CL= Confidence limit, $LC_{50=}$ Median lethal concentrations, (-) = 95% Confidence limit (lower-upper value) exposure at 96 hours

Table 3. Pesticide in Mekong River in Thailand, Laos and Cambodia

Parameters	Results		
	Thailand	Laos	Cambodia
Organochlorine Group			
Alpha HCH	nd	nd	nd
Gamma HCH	nd	nd	nd
Delta HCH	nd	nd	nd
Beta HCH	nd	nd	nd
Mirex	nd	nd	nd
Aldrin	nd	nd	nd
Dieldrin	nd	nd	nd
Endrin	nd	nd	nd
Heptachlor Epoxide/OCS	nd	nd	nd
Gamma Chlordane	nd	nd	nd
Alpha Chlordane	nd	nd	nd
2,4' DDE/ENDOSULFAN I	nd	nd	nd
4,4' DDD	nd	nd	nd
4,4' DDT	nd	nd	nd
2,4' DDT	nd	nd	nd
2,4' DDD	nd	nd	nd
Endosulfan sulfate	nd	nd	nd
Endosulfan II	nd	nd	nd
Organophosphate Group			
Chlorpyrifos	nd	nd	nd
Chlrorinated Benzenes			
Tetrachlorobenzene 1,2,4,5	nd	nd	nd
Tetrachlorobenzene 1,2,3,4	nd	nd	nd
Pentachlorobenzene	nd	nd	nd
Hexachlorobenzene	nd	nd	nd
Chloronitrile Pesticides			
Chlorthalonil	nd	nd	nd
Chlordane-related Compounds			
Heptachlor	nd	nd	nd
cis-Nonachlor	nd	nd	nd
trans-Nonachlor	nd	nd	nd
Methoxychlor	nd	nd	nd
Oxychlordane	nd	nd	nd
Chlorinated Herbicides			
Pentachloroanisole	nd	nd	nd

Note: Organochlorine Group: LOD=0.001 mg/L, LOQ=0.01 mg/L
Organophosphate Group: LOD=0.001 mg/L, LOQ=0.01 mg/L
Pyrethroid Group: LOD=0.001 mg/L, LOQ=0.01 mg/L
Cabamate Group: LOD=0.01 mg/L, LOQ=0.01 mg/L

3.   DISCUSSION

Generally, water quality of Mekong River in Thailand is good, but some areas of the Mekong Delta, which are harmfully inflicted by high population density, irregular mining activities, and increasing agricultural activities, have experienced worsening water quality. Present study indicated that water chemistry parameters can influence on copper toxicity to tropical freshwaters biota. Increasing hardness ions, and DOC all resulted in some reduction of copper neurotoxicity to individual sensory neurons in

Moina (*Moinama crocopa*), Chironomidae (*Chironomus javanus*), Grass Carp (*Ctenopharyn godon* Idella) Nile tilapia (*Oreochromis niloticus*) and Greater bony-lipped barb (*Osteochilus melanopleurus)*

4.   CONCLUSION

Present study indicated that water chemistry parameters can influence on copper toxicity to tropical freshwaters biota. DOC, pH and hardness might provide protection against Cu toxicity in the freshwater. This series of laboratory experiment provide a worst-case scenario and useful for determine the risk assessment of copper on Mekong tropical freshwater animals. Other acute toxicity studies of copper under the different water quality parameters with more tropical organism's species should be encouraged and help and protect the Mekong River in the future and to set a water quality standard for heavy metal in the Mekong River Basin countries.

REFERENCES

[1]   MRC. (2013). 2011 Annual Water Quality Data Assessment Report (pp. 59). Vientiane, Lao PDR.

[2] Coates, D., O. Poeu, U. Suntornratnana, T. Nguyen & S. Viravong (2006) Biodiversity and fisheries in the Mekong River Basin. *Mekong development series*.

[3] Bradl, H. (2005) Heavy Metals in the Environment: Origin. *Interaction and Remediation, Elsevier/Academic Press, London*

[4] Kamunde, C. & R. MacPhail (2011) Effect of humic acid during concurrent chronic waterborne exposure of rainbow trout (Oncorhynchus mykiss) to copper, cadmium and zinc. *Ecotoxicology and Environmental Safety,* 74**,** 259-269.

[5] U.S.EPA. 2002. *Methods for measuring the acute toxicity of effluents and receiving waters to freshwater and marine organisms*. Environmental Monitoring Systems Laboratory, Office of Research and Development, US Environmental Protection Agency.

[6] APHA (American Public health Association), EPA (United State Environmental Protection Agency and AOAC (Association of Official Chemists).

O6-5

汽水湖涸沼における水質の周期変動について

松本 俊一[1], 中川 圭太[1], 福島 武彦[1]

[1]茨城県霞ケ浦環境科学センター

キーワード：データ解析とモニタリング，ウェーブレット解析，周期変動，汽水湖

抄録

　茨城県中央部に位置する涸沼は，那珂川を介して太平洋に接続する汽水湖である。茨城県では 1970 年代から湖内3地点で毎月1回の定期観測を継続してきた。水質の代表的な指標である化学的酸素要求量(COD)は，湖内において長期的には横ばいに推移し，基本的には1年周期で変動しているが，他に数年周期の変動も見られるなど複雑な水質変動が認められる。そこで湖内並びに流入河川，流出河川の水質変動についてウェーブレット解析を行い，その変動周期と各種水質項目の関係を検討した。その結果，COD は全期間中で，1 年周期のピークが確認され，1年周期のピークは 7〜8 年の期間で途切れ，その期間中の季節変化が小さくなること，3 年周期が検出される期間は COD が増加することが分かった。また，湖内 COD の1年周期の出現パターンは上流側河川のそれに似ており，湖内変動は上流側からの影響をより強く受けることが示唆された。

1. はじめに

　茨城県中央部に位置する涸沼は，湖面積 9.35km^2，平均水深 2.1m，那珂川を介して太平洋に接続する汽水湖である(図1)。そのため，上流河川のみならず，那珂川の影響を受けた海水が湖内に遡上流入し，それぞれが相互に作用するという複雑な水域であり，湖内水質の変動について未解明な部分がある。これまでは汽水湖であることから潮汐の影響を把握する調査研究を行われ，湖内の塩分成層の状況やそれに伴う貧酸素水塊発生状況，そして湖内の流況など短期間の水理的考察[1]が行われてきた。

　一方，長期的な水質変動については，茨城県が1970 年代から涸沼湖内及びその流域において定期観測を継続しており 40 年以上に観測データが蓄積されているが十分な解析は行われておらず，長期的観点からの水質の変動要因が明らかにされていない。涸沼湖心(宮前)の湖内水質(COD)は，図 2 の上段で示すように長期的には低下傾向にあるが，現在においても 6mg/L程度と環境基準(湖沼 B 類型)を達成できない状況にある[2]。水質は，基本的には年周期で変動しているが，他に数年周期のうねりも見られ，また，近年は年間の最大値と最小値の差が，小さくなる傾向にあるなど複雑な水質変動が認められる。

　水質は，様々な要因が重なり合い一つの値を形作っているものであることから，成分に分け解析することは要因を明らかにするため重要である。汽水域である本水域は周期性の強い潮汐の影響を受ける特徴があり，その他の様々要因の変動周期により水質が変動している。そのため，本研究では水質変動の周期性に着目し，ウェーブレット解析により周期解析を行った。

　周期解析には代表的なものとしてフーリエ変換があるが，これは継続する波動の周期を分離するものであり，含まれる波動の周期を示すのみである。一方，ウェーブレット解析は波動周期だけでなく，分離した波動の存在期間を示すことが可能であることから[3]，変動要因が時期により異なり周期の存在が不均一な湖水などの解析により効果的である。[4]

　ウェーブレット解析により長期間の湖内水質の周期解析を行い，地点間や項目間の比較などから，長期的な視点から湖内水質の変動要因について検討を行った。
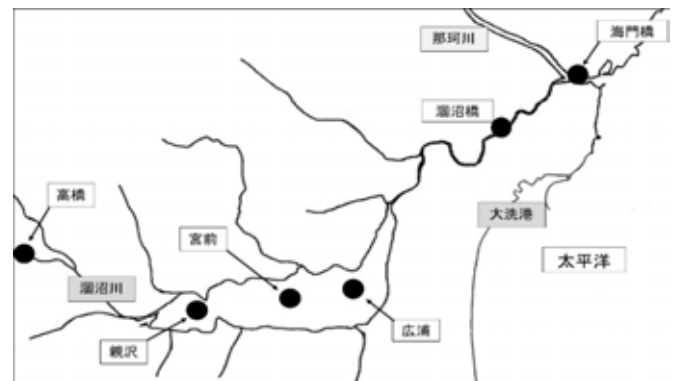
図1　涸沼流域図

2. 方法

　解析対象には，茨城県が公表している公共用水域の水質測定結果（1974年度〜2016年度）の測定データを用い，そのうち当初から測定を継続している水温，pH，DO，COD，BOD及びSSについてウェーブレット解析（R言語 morlet関数を使用）による周期解析を実施した。

　なお，周期解析により，「主要周期とその出現傾向」，「地点毎の周期傾向から上下流域からの寄与」及び「水質項目の周期傾向から項目間の関係」を検討した。

3. 結果及び考察
3.1 主要周期とその出現傾向

　涸沼湖心（宮前）の COD ウェーブを対象としたウェーブレット解析の結果を図2の下段に示す。周期分布上方の網掛部分は棄却域であり，有意水準は1%とした。

　ウェーブレット解析の結果は，縦軸は周期としての月数，横軸を測定年とするコンター図として表現され，時間ごとの周期(周波数)をピークとして示し，そのピークが継続する場合は帯として表現される。ピークの強度は灰色の明るさよって示され，明るい灰色が最も強度が強い。

　湖内 COD のウェーブレット解析の結果は全期間中で1年（12ヶ月）周期のピークが認められ，1年周期のピークが 7〜8 年の間隔で途切れる。期間中のピークの途切れは，1983年，1994年，2007年及び2014年の4か所で確認されるが，それに対応する年では COD の季節変化も著しく小さくなる。また，1 年周期の以外にも3年（36ヶ月）周期と7年（84ヶ月）周期もあり，3年周期は，1978年と1998年の2度出現し，4年ほど継続し，その時期はCOD が上昇していた。
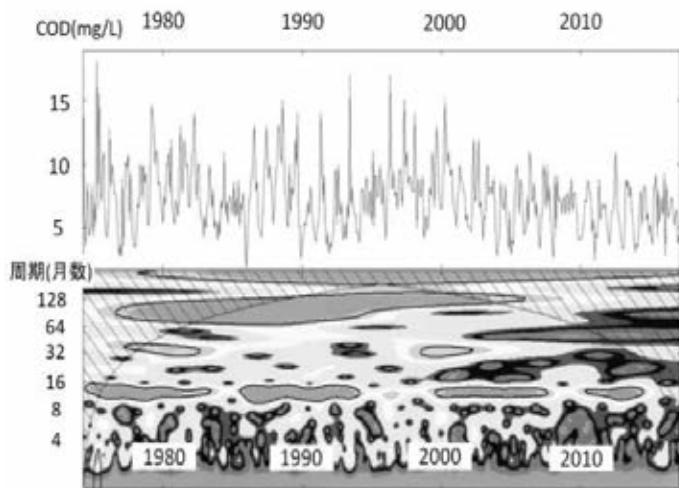
図2 COD 経年図（上段） 周期分布図（下段）

3.2 地点毎の周期傾向と上下流域からの寄与

　次に涸沼湖内の水質に対する上・下流域の影響を検討するため，涸沼川の流下方向 6 地点の COD についてウェーブレット解析を行い，1 年周期のみを切り出し，その出現パターンを比較した。ピークは明灰色の帯状として示される（図 3）。なお，1 年周期を選択した理由は，最も強いピークであること，対象期間全域でピークが出現することから，周期の比較がしやすいためである。

　湖内 3 地点（親沢，宮前，広浦）とその上流に位置する高橋は1年周期の出現パターンが似ており，涸沼の下流域に位置する涸沼橋，海門橋でも 1 年周期は出現するが，湖内より断続することが多く，より下流に位置する海門橋のほうがその傾向が強い。下流域の涸沼橋，海門橋は出現パターンが異なる。下流域での出現位置は，湖内で隙間が生じる箇所に見られる。このことから遡上水が湖内に影響を及ぼし，1年周期を断絶させている可能性が示唆される。一方，海水が及ばない上流側（高橋）においても湖内同様の1年周期のパターンが見られることから，湖内変動は上流側からの影響をより強く受けることが示唆された。
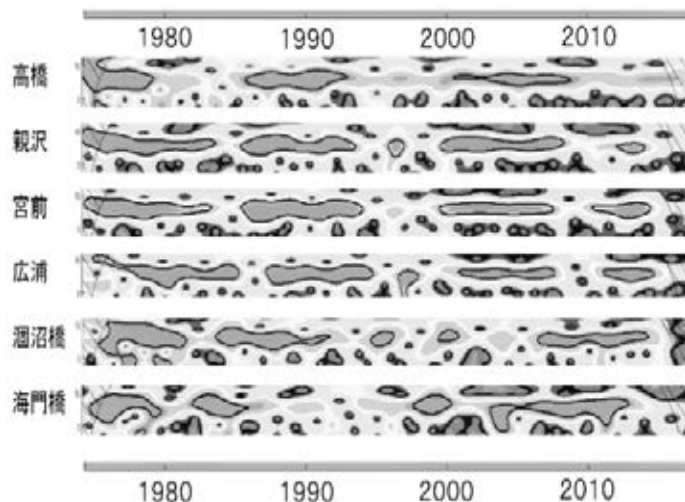
図3 地点別 COD の1年周期分布図

　なお，湖内3地点の1年周期の出現パターンおいて，下流側の地点ほど出現と消滅の時期に遅れが生じているが，出現パターンは3地点とも同じような継続時間，消失時間を有していることから似ていると判断した。下流側ほどずれが大きいのは海の影響と考えられる。

　また，公共用水域の観測は表層のみのため河川の影響が強く出すぎている可能性ある。しかし，塩分が底層で高い場合は，表層でもその影響を受け塩分は多少上昇することから，底層と表層の塩分は連動する。さらに遡上水に関する周期は数日単位と月単位比べ短いことか

ら，長期間の変動を見ているかぎり，短期的な塩分躍層など影響は相殺され周期解析への影響は少ないと思慮される。

3.3 水質項目の周期傾向と項目間の関係

　涸沼湖心（宮前）において水温，pH，DO，COD，BOD 及び SS についてウェーブレット解析を行いにより1年周期のみを切り出しの出現パターンを比較した。1年周期のピークは濃灰色で示される（図4）。水温は全期間中で 1 年周期が途絶えることなく出現し，安定した周期性が認められる。その他項目については，1980 年代半ばまでは同じような周期パターンであったが，その後は，SS は断続的に短期間のピークが出現しており，pH，DO，COD は比較的出現パターンが似ていた。BOD は COD と 1990 年代まで同パターンであったが，2000 年以降ほとんど出現されなくなっている。

　これらのことから，1年周期の出現パターンが似ており，湖内の COD，pH，DO に関連があることが示唆された。これらの項目は，一次生産に関わる項目であるが，湖内の栄養源は河川を通じて流入してくることから，湖内での一次生産の増減は河川の挙動が影響する。そのため，湖内でのこれらの項目の挙動は，上流域からの影響を反映したものであり，3.3 で示したように上流側からの影響をより強く受けることと合致する。

図4　項目別の1年周期分布図（宮前）

4．結論

　ウェーブレット解析の結果，涸沼湖内 COD 変動の主要周期は1年であり，その他に3年及び7年周期が確認された。1年周期は7〜8年間継続し，断絶した区間は

COD の年間変動が小さかった。また，3年周期が出現した時期は COD が上昇していた。

　涸沼湖内 COD の1年周期の出現パターンは上流側のそれに似ており，湖内変動は上流側からの影響をより強く受けることが示唆された。また，湖内では pH，DO，COD の一年周期の出現パターンから，COD と pH，DO との密接な関係が示唆された。

引用文献

[1]　松本俊一他：汽水湖涸沼の水質変動要因の検討，茨城県公害技術センター研究報告,11,pp.15-20,2001.

[2]　茨城県：平成 29 年度版環境白書,pp.36,2017.

[3]　山田道夫他，日本応用数理学会監修：応用のためのウェーブレット解析,pp.31-34,2016.

[4]　T.Subba rao,北源四郎訳：時系列分析ハンドブック,pp.651-652, 2016.

O6-6

Mixing processes associated with hypoxia in Lake Kasumigaura

Eiji Masunaga[1] and Tomoko Ozawa[2]

[1]Center for Water Environment Studies, Ibaraki University, [2]Collage of Engineering, Ibaraki University.

Keywords: Hypoxia, Shallow lake, Vertical mixing, Stratification, Heat flux.

ABSTRACT

This study reports hypoxia events associated with suppressed vertical mixing during the summer season, Kitaura, Lake Kasumigaura, Japan. Mooring data obtained at the Kamaya monitoring station were used to investigate physical processes causing hypoxia events. Hypoxia appears under conditions of strong stratification due to strong incoming heat flux into the lake. The square of buoyancy frequency (indicator of the stratification strength), N^2, reaches 2.4×10^{-3} in July, 2016. On the other hand, hypoxia water disappears under weak stratified or mixing conditions when moderate winds (~ 5 m s^{-1}) and weak incoming heat flux. The bottom oxygen concentration is highly related with the buoyancy frequency, thus, the bottom oxygen concentration can be explained by the vertical physical mixing processes. In order to evaluate forcing conditions controlling mixing processes in the lake, we propose a non-dimensional number, the ratio of two forcing into the lake, (1) time-integrated incoming heat flux and (2) horizontally-integrated surface wind stress. The non-dimensional number is in a good correlation with the buoyancy frequency. This study found that suppressed vertical mixing causing hypoxia can be simply explained by the balance of the two surface forcings (heat flux and wind stress). In addition, the heat budget analysis shows a contribution of the sediment hear flux to mixing processes in the lake.

1. INTRODUCTION

Mixing processes are essential to understand oceanic and lake's physical processes and ecosystems [1, 2]. It is well known that vertical heat and mass transports are suppressed by vertical stratifications. In stratified oceans and lakes, vertical transports are dominated by diffusive processes by mixing, rather than advections due to currents. Mixing mechanisms have to be revealed to understand and maintain lake environments [2].

Hypoxia is one of crucial problems that have to be solved for worldwide lakes [3]. Oxygen supplies into water is mainly from surface gas exchanges and photosynthesis by phytoplanktons. In bottom boundary layers with limited solar radiation, oxygen supplies are only from upper layers through vertical mixing. This study investigates mixing processes associated with hypoxia in Lake Kasumigaura (Kitaura) located in the middle of Japan main land (Fig. 1). The depth of the lake is quite shallow with a maxumium depth of approximately 6 m, however, the solar radiation is limited in the bottom boundary layer due to highly concentrated turbidity. This condition leads to serious hypoxia issues in the lake.

2. METHOD

Observed data from the Kamaya monitoring station
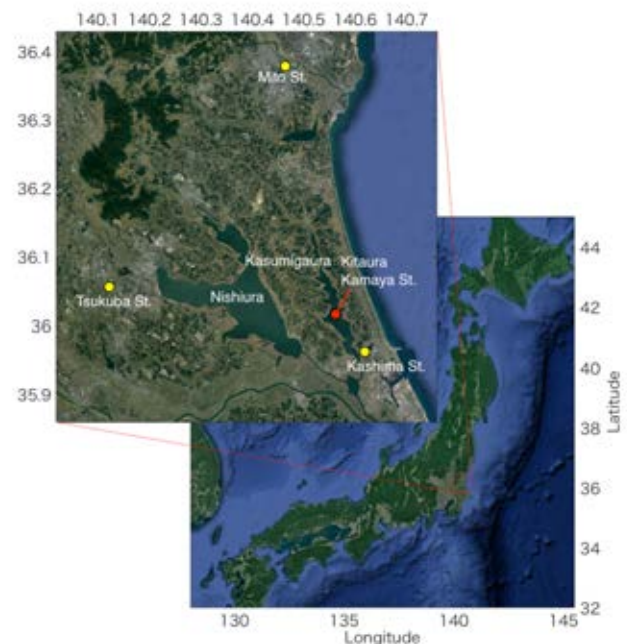
Fig. 1 Map of the study site. Red circle and yellow circle show locations of the Kamaya monitoring station and JMA weather stations.

(Japan Water Agency) in Kitaura Lake and weather stations (Japan Meteorological Agency, JMA) nearby the study site were sued to investigate physical processes associate with mixing processes and hypoxia. The Kamaya monitoring station is located at the middle of the Lake Kitaura (Fig. 1) and obtains data of water temperature, pH, chlorophyll *a* concentration, dissolved oxygen (DO) concentration, turbidity, conductivity every one hour with

a vertical interval of roughly 1 m. This study used temperature and oxygen concentration data from the Kamaya mooring station. Three JMA weather stations (Kashima, Tsukuba, Mito stations, Figure1) were selected to obtain data used for the heat flux analysis: Air temperature, wind data are from the Kashima station; Relative humidity (RH), pressure and shortwave radiation data are from the Tsukuba station; Data of the cloud cover ratio are from Mito station. The incoming heat flux into the lake was computed by using data from the mooring station and weather stations. The total heat flux is assumed as the sum of the long wave radiation (L_w), shortwave radiation (S_w), sensible heat flux (H_s) and latent heat flux (H_l), and these flux are estimated by conventional methods. We analyzed six years data set from 2011 to 2016, results from 2016 are shown in this paper.

3. RESULTS

Data from Kamaya monitoring station show that hypoxia water intermittently appears on the bottom during the summer season in every year (2011–2016). An example of temperature and DO in July, 2016 are plotted in Fig1. ab. Low oxygen concentration waters appear two periods July 10–15 and 17–23. In these two periods, the surface DO is approximately 10 mg L^{-1} (close to saturation) and the vertical temperature gradient is high, reaching 2.5 ^{o}C between the surface and bottom. Meanwhile, hypoxia waters disappear coinciding with vertical mixing after the hypoxia events (July, 16 and 23). According to long term mooring data, the time scale of hypoxia events is roughly one day–several days.

To evaluate the strength of the stratification, the buoyancy (Brunt-Väisälä) frequency, N, is computed, which is given by

$$N^2 = -\frac{g}{\rho_0}\frac{\partial \rho}{\partial z} \tag{1}$$

where g is the gravitational acceleration, ρ is the density and ρ_0 is the reference density (1000 kg m^{-3}). Fig. 2bc clearly shows that hypoxia events coincide with strong stratifications events ($N^2 \sim 10^{-4} - 10^{-3}$ s^{-2}). The stratification decreases on July, 16 and 23 with a high wind stress and weak incoming heat flux event. The 48 hourly time averaged N^2 in 2016 is plotted as a function of the 48 hourly averaged bottom DO in Fig 3a. The bottom DO concentration is clearly related with N^2 and hypoxia events (DO < 3 mg L^{-1}) only appear N^2 higher than 3.1×10^{-4} s^{-2}.

4. DISCUSSION

4.1 Physical forcing controlling mixing

According to results described above, hypoxia events in Lake Kitaura are highly related with the strength of the stratification, and the vertical mixing (stratification) is supposed to be controlled by two surface physical forcings: (1) surface heat flux and (2) surface wind stress. In global scale fluid dynamics (in large lakes and oceans), the earth's rotation and tides need to be considered [4, 5]. However, the scale of our study filed is much smaller than the global scale, thus we don't have to pay attention to the earth's rotation, tides. In order to explain vertical mixing

Fig. 2 Time series data of temperature, DO, buoyancy frequency (N^2), surface heat flux in the lake, surface wind stress in July 10–25, 2016.
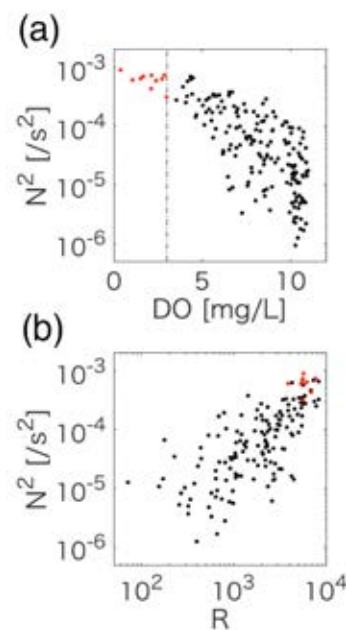
Fig. 3 Scatter plots of (a) the time-averaged bottom DO against N^2 and (b) the surface flux mixing number, R, against N^2. Red dots indicate DO less than 3 mg L^{-1}.

in the lake, we developed a non-dimensional number, the ratio of the time-integrated surface heat flux and horizontally-integrated wind stress, given by

$$R = \frac{\tau_w L}{H_F T}$$

where τ_w is the surface wind stress, L is the fetch length of the wind over the lake (10 km), H_F is the incoming heat flux into the lake, T is the scale for the heat flux integration (3600 s). Fig.3b shows the time-averaged R and time-averaged N^2 with an averaging scale of two days, which indicates a clear relationship between the ratio of the two forcings and stratification (correlation coefficient = 0.73). Therefore, mixing/stratification can be explained by the surface heat flux and surface wind stress for Lake Kitaura. This paper only presents results for 2016, but data from other years (2011–2015) also show similar results to that of 2016.

4.2 Contribution of the sediment heat flux

Annual averaged short wave radiation (S_w), long wave radiation(L_w), sensible heat flux (H_s) and latent heat flux (H_l) in 2016 are listed in Table1. Excepting the short wave radiation, L_w, H_s and H_l are negative values, namely heat transports toward the atmosphere. If the annual heat budget is only controlled by the surface heat flux, the sum of these four averaged heat fluxes has to be close to zero. However, our heat budget analysis show that the sum of the heat fluxes is 61 W m^{-2}, far from zero, which implies that only the surface heat flux cannot explain the total heat budget in Lake Kitaura.

In addition to the surface heat flux, the bottom heat flux into bottom sediments play a significant role in heat budgets in shallow lakes [6]. Although the monitoring station did not observe the bottom sediment heat flux, we hypothesized that the sediment heat flux largely contributes to the lake heat budget. Assuming the sediment heat flux is 61 W m^{-2}, 42% of the incoming short wave heat flux radiates into the bottom of the lake. Although we don't have enough observed results to prove the sediment heat processes, the sediment heat radiation might enhance the stratification leading to hypoxia in the bottom boundary layer.

Table1. The annual averaged surface heat flux into the lake in 2016 with a unit of W m^{-2}.

	S_w	L_w	H_S	H_l
Heat flux	145	-54	-6	-24

5. CONCLUSION

This study investigated hypoxia events in the bottom boundary layer in Lake Kasumigaura (Kitaura) with long term observed data and found following mixing mechanisms associate with hypoxia:

(1) The strong stratification condition ($N^2 > 3.1 \times 10^{-4}$ s^{-2}) leads to hypoxia (DO < 3 mg L^{-1}).

(2) The stratification is controlled by two forcings, the surface heat flux and surface wind stress. The ratio of these two forcings can explain the stratification is the lake.

(3) The heat flux from the lake water toward the sediment might lead to decreasing in the bottom temperature resulting in increasing in the stratification. The sediment heat flux is desire to understand heat budget in the lake.

REFERENCES

[1] Munk, W. and Wunsch, C., 1998. Abyssal recipes II: Energetics of tidal and wind mixing. *Deep Sea Research Part I: Oceanographic Research Papers*, *45*(12), pp.1977-2010.

[2] Yamazaki, H., Honma, H., Nagai, T., Doubell, M.J., Amakasu, K. and Kumagai, M., 2010. Multilayer biological structure and mixing in the upper water column of Lake Biwa during summer 2008. *Limnology*, *11*(1), pp.63-70.

[3] Jenny, J.P., Francus, P., Normandeau, A., Lapointe, F., Perga, M.E., Ojala, A., Schimmelmann, A. and Zolitschka, B., 2016. Global spread of hypoxia in freshwater ecosystems during the last three centuries is caused by rising local human pressure. *Global change biology*, *22*(4), pp.1481-1489.

[4] Rao, Y.R., Hawley, N., Charlton, M.N. and Schertzer, W.M., 2008. Physical processes and hypoxia in the central basin of Lake Erie. *Limnology and oceanography*, *53*(5), pp.2007-2020.

[5] Auger, G., Yamazaki, H., Nagai, T., Jiao, C. and Kumagai, M., 2013. Hypolimnetic turbulence generation associated with superposition of large-scale internal waves in a strongly stratified lake: Lake Biwa, Japan. *Limnology*, *14*(3), pp.229-238.

[6] Likens, G.E. and Johnson, N.M., 1969. Measurement and analysis of the annual heat budget for the sediments in two Wisconsin lakes. *Limnology and Oceanography*, *14*(1), pp.115-135.

O6-7

無試薬光反応を利用した水質分析法のメンテナンス低減化・高感度化

中里哲也

国立研究開発法人 産業技術総合研究所 環境管理研究部門

キーワード：水質、分析、モニタリング、全有機炭素、重金属

抄録

溶存有機炭素および有機態ヒ素を分解試薬を使用せず、1分以内に迅速に無機化できるLamp-pass-through (LPT)光反応器を開発した。LPT 光反応器は水銀ランプに反応管を貫通させることにより、ランプから発する真空紫外光の反応管内の試料水への照射効率を高めることで、試料水に含まれる水分子からの OH ラジカル発生および溶存有機物の分解を高効率化した。この無試薬無機化法と非分散赤外分光法を組み合わせた溶存有機物(DOM)の分解試薬フリー・オンライン全有機炭素(TOC)分析法を開発した。本法は酸化剤や触媒など分解試薬を使わずに河川水中溶存有機物のオンライン TOC 分析を実現した。また、この無試薬無機化法はヒ素化学形態分析法の高感度化にも有用であった。液体クロマトグラフにより分離したヒ素化合物を無試薬無機化することで、全てのヒ素化合物を水素化物発生法により還元気化し、誘導結合プラズマ質量分析(ICP-MS)装置に大量導入することで、ヒ素化学形態分析の高感度化を実現した。

1. はじめに

水中の溶存有機物(Dissolved Organic matter。以下 DOM と略称)は水環境の炭素循環の鍵物質の1つであり、また、水質管理において、過剰量の DOM は水質汚染の主要因の一つである。このような水環境の炭素循環の解明や適切な水質管理や処理を行うためには DOM の全有機炭素(TOC)量を安価、簡便、迅速、そしてメンテナンス負担が少なく測定できる手法が必要とされている。

水中の全有機炭素量を測定するためには、試料水中の有機炭素を分解して二酸化炭素などの無機炭素に変換して非分散赤外分光分析法などで検出する。この有機炭素の無機化については、従来法は試薬を用いて行うものがほとんどであり、例えば、高温燃焼酸化(High Temperature Combustion Oxidation。HTCO と略称)による分解は、600 度を超える高温条件下で白金触媒を用いて酸化分解を行う。また、紫外光照射条件下でペルオキソ二硫酸塩を用いた酸化分解法もある。いずれの方法も有害・高価な試薬を要し、加えて、水現場での TOC 監視を想定した場合、試薬の交換、補充、廃水管理といった保守の負担が大きいと考える。

本研究では、水銀ランプから発する真空紫外光を試料水に高効率に照射できる Lamp-pass-through(LPT)光反応器を開発した。この光反応器を利用して、酸化剤や触媒などの分解試薬を必要としないオンライン TOC分析法を確立した。また、この方法の実用性を明らかにするため、河川水および水道水試料中 DOM に適用できるかを検証した。

また、この LPT 光反応器は無試薬光反応による高効率な有機物分解が可能であることから、別の元素分析への応用も検討した。具体的には、ヒ素の化学形態分析法の高感度化である。ヒ素の高感度化学形態分析法の代表的分析法としては液体クロマトグラフ−誘導結合プラズマ質量分析法(LC-ICP-MS)がある。例えば、イオン排除クロマトグラフを分離部とした LC-ICP-MS は、人尿中の陽・陰イオン・中性化合物といった広範囲のヒ素化合物を対象とした化学形態分析が可能であるが[1]、検出したヒ素化合物濃度の総和は、人尿中のヒ素総濃度よりも低値となった[2]。このことは、LC-ICP-MS であっても、一部のヒ素化合物が LC による分離や ICP-MS の感度が十分でないためと考えられる。

本研究では後者の ICP-MS の感度を改善するため、LPT 光反応器を用いて LC 分離後のヒ素化合物を無試薬条件下で迅速に無機化してひ酸に変換し、水素化物発生法によってアルシンに気化することで ICP-MS 装置への大量導入を可能とすることで高感度化した。また、この方法の実用性を検証するため、人尿試料への適用性を検証した。

2. 方法

有機炭素化合物、河川水試料中 DOM、ヒ素化合物の無試薬光反応処理は、LPT 光反応器を用いた。LPT

光反応器は水銀ランプに反応管を貫通させる構造とした[2]。LPT 光反応器の概略図を図 1 に示す。有機炭素および有機態ひ素の無機化率は、光反応後の残留有機炭素濃度を HTCO 式 TOC 計および LC-ICP-MS により定量することで決定した。

LPT 光反応器を用いた TOC 測定装置の概略図を図 1 に示す。TOC 測定装置[3]は、総炭素(Total carbon。以下、TC)測定と無機炭素(Inorganic carbon。以下、IC)測定との差分である TC-IC 測定モード、および不揮発性有機炭素 (Non-purgeable organic carbon。以下、NPOC) 測定モードに対応可能である。本報告では TC-IC 測定モードについて述べる。TC 測定は、試料水にリン酸緩衝液をオンラインで添加して pH2 に調整した後に、LPT 光反応器に送液し、有機炭素を無機化した。得られた無機炭素は二酸化炭素として気液分離器で分離後、高純度空気をキャリアガスとして用いて非分散赤外分光計に導入し検出した。IC 測定は、試料水を酸性化後、上記の LPT 光反応器を通過させずに測定した。

LPT 光反応器を用いたヒ素の化学形態分析装置の概略図を図 2 に示す。試料水中のヒ素化合物は東ソー社の分離カラム TSKgel OApak-A および硫酸塩酸性溶液を溶離液として用いたイオン排除クロマトグラフィーにより分離し、その溶離液を LPT 光反応器に通液し、ヒ素化合物をヒ酸に変換した。この処理液に硝酸を添加して酸性化した後に、水素化ホウ素ナトリウム水溶液と混合することでアルシンを発生させ、これを気液分離器で分離して、アルゴンガスをキャリアガスとして ICP-MS 装置 (Agilent 社 7500cx)に導入しひ素を m/z75 で検出した。

TOC 測定で使用した河川水、および湖水試料は涸沼川および霞ケ浦(共に茨城県)で採取し、$0.45\,\mu$m のフィルターでろ過し、測定まで 4℃で保存した。人尿試料は採取後直ちに $0.45\,\mu$m のフィルターでろ過し分析に供した。
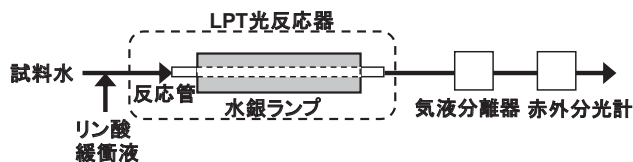
図 1 LPT 光反応器および分解試薬フリーTOC 測定装置の概略図
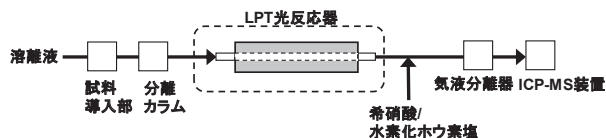
図 2 ヒ素の高感度化学形態分析装置の概略図

3. 結果と考察

LPT 光反応器は水銀ランプに反応管を貫通させることにより、ランプから発する真空紫外光の反応管内の試料水への照射効率を高めることが可能となり、試料水に含まれる水分子からの OH ラジカル発生と、そのラジカルによる溶存有機物質の分解を高効率化させることが可能となった。例えば、自然水由来の有機炭素物質の中で難分解性物質として知られる腐植物質の無機化については、International Humic Substances Society の標準物質であるフルボ酸(Nordic Aquatic Fulvic Acid, 1R105F) およびフミン酸(Nordic Aquatic Humic Acid, 1R105H)、各々2 ppm(mg of Carbon/L)を 6W 出力の水銀ランプを用いた LPT 光反応器を用いて分解したところ、わずか1 分で各々90%以上の無機化率を示した[2]。この無機化性能を検証するため、従来のバッチ式光反応器法として、試料溶液が入った試験管に同出力の 6W ペン型水銀ランプを挿入し無試薬分解を行う方法と比較した。比較のため反応時間を短くして 15 秒としたときの 2ppm のフミン酸標準物質の無機化率を表 1 に示す。

表 1 フミン酸標準物質の無機化

(フミン酸炭素濃度、2ppm; 水銀ランプ 6W)

	無機化率
LPT 光反応器	62%
バッチ式光反応器 (ペン型ランプ+試験管容器)	～0%

LPT 光反応器は約 62%の高い無機化率が得られたのに対して、バッチ式光反応器は無機化が観測されなかった(無機化率～0%)。他の低分子有機酸、アルコール、糖類についても同様に LPT 光反応器の方が無機化率は高かった。これは、LPT 光反応器の構造によって差が生じると考えている。水銀ランプの真空紫外光 (185nm)は試料水中の水による光吸収による減衰が極めて大きいため、内径がミリメートルレベルの狭い反応管を有し、全方向から光照射が行われる LPT 光反応器は、高い光照射率および無機化率が得られると考えられる。次に、この LPT 光反応器の実用性について検証した。多種の無機物質が含まれる実際の河川水および湖水(涸沼川よおび霞ケ浦)中 DOM も、1 分以内で90%以上の迅速な無機化が得られた。さらにこの LPT 光反

応器を組み込んだ 図 1 に示す分解試薬を使わない TOC 測定装置を開発した。分析性能を従来の金属触媒を用いる HTCO 式 TOC 分析法と比較すると、検出下限は1/8倍程度の 6ppb である一方、分析時間は TC-IC 測定モードで 10 分とほぼ変わらなった[2]。また、実際の河川水試料(涸沼川)中の DOM の TOC 測定では、本法の分析値は HTCO 法の 98±5%と測定誤差内で一致した。

　LC-ICP-MS によるヒ素の化学形態分析法の高感度化については、水素化物発生法(HG)によりヒ素化合物を気化して ICP-MS 装置に大量導入して高感度化を図る LC-HG-ICP-MS は、有機態ヒ素はメチルヒ素など一部の化合物しか気化せず高感度化範囲は限定的であった。そこで 110W 出力のランプを用いた LPT 光反応器を用いることで、HG 法で気化しないアルセノベタインやテトラメチルヒ素など含む全てのヒ素化合物をわずか約 3.5 秒で気化可能なヒ酸に変換することが可能となった[1]。この機構を取り入れた図 2 の装置によりひ素の化学形態分析法の高感度化が行われ、アルセノベタインの検出下限は、LC-ICP-MS の約 1/10 倍の 3ppt (ng of As /L)に低減された。この高感度化は、LPT 光反応器による迅速な無試薬無機化が要因と考えている。一方、酸化剤など試薬を用いる無機化処理は酸化剤溶液の添加による希釈および後段の水素化還元反応への残留酸化剤による高感度化への抑制効果が生じない点にあると考える。また、本研究法は人尿試料や食事由来のヒ素の有害性評価を行うための食事試料の模擬胃液抽出液(塩酸、ヘパリン混合液)のヒ素の高感度化学形態別分析に適用可能であった[1][4]。例えば、人尿試料の分析では、LC-ICP-MS では 7 種類のヒ素化学種を検出したのに対して、本分析法は 20 種類のヒ素化合物を検出することができた。

4. 結論

　溶存有機炭素および有機態ヒ素を分解試薬を使用せず、1 分以内に迅速に無機化できる LPT 光反応器を開発した。この光反応器を用いることで、分解試薬由来のコストやメンテナンスを低減しつつ、河川水に適用できる TOC オンライン測定法を確立した。また、この光反応器による無試薬無機化法と、LC-ICP-MS および水素化物発生法を組み合わせることで、ヒ素の化学形態分析を高感度化した。この LPT 光反応器を用いた無機化処理はこの他にもセレンの還元気化原子吸光分析の高感度化にも有用であった[5]。このように試薬を使用しな

いため広範囲の元素分析への適用が期待される。

引用文献

[1] Nakazato, T.; Taniguchi, T.; Tao, H.; Tominaga, M.; Miyazaki, A., Ion-exclusion chromatography combined with ICP-MS and hydride generation-ICP-MS for the determination of arsenic species in biological matrices. Journal of Analytical Atomic Spectrometry 2000, 15 (12), 1546-1552.

[2] Nakazato, T.; Tao, H., A high-efficiency photooxidation reactor for speciation of organic arsenicals by liquid chromatography - Hydride generation - ICPMS. Analytical Chemistry 2006, 78 (5), 1665-1672.

[3] Satou, T.; Nakazato, T.; Tao, H., Online TOC Analysis Based on Reagent-free Oxidation of Dissolved Organic Matter Using a Mercury Lamp-Pass-Through Photoreactor. Anal. Sci. 2013, 29 (2), 233-238.

[4] Oguri, T.; Yoshinaga, J.; Tao, H.; Nakazato, T., Inorganic Arsenic in the Japanese Diet: Daily Intake and Source. Arch Environ Contam Toxicol 2014, 66 (1), 100-112.

[5] Suzuki, T.; Sturgeon, R.E.; ZHENG, C.; Hioki, A.; Nakazato, T.; Tao, H., Influence of Speciation on the Response from Selenium to UV-Photochemical Vapor Generation, Anal. Sci. 2012, 28(8), 807-811.

O6-8

Graphene-based electrochemical sensor as a microcystin-LR detection tool in water

Wei Zhang[1,2] and Hiroaki Furumai[1,3]

[1]Research Centre for water Environment Technology, Department of Urban Engineering, The University of Tokyo, Tokyo 113-0033, Japan, [2]School of Natural and Built Environments, University of South Australian, Mawson lakes, SA 5095, Australia, [3]Collaborative Research Institute for Innovative Microbiology, The University of Tokyo

Keywords: Graphene film, MC-LR, biosensor, electrochemical detection, nanomaterials

ABSTRACT

In this work, we showcased a novel graphene film composite biosensor for microcystin-LR detection as an alternative to time-consuming, expensive, non-portable and often skills-demanding conventional methods of analysis involved in water quality monitoring and assessment. Excellent linear correlation (R^2=0.99) of the electron-transfer resistance was achieved over a wide range of MC-LR concentration, i.e. 0.05-100 μg/L. As-prepared graphene film composite biosensors can specifically detect MC-LR with remarkable sensitivity and detection limit much lower than the World Health Organization (WHO) provisional guideline limit of microcystin-LR concentration (i.e. 1 μg/L) in different water sources. Their great potential can be attributed to large active surface area of graphene film and efficient charge transfer process enabled by their high conductivity. Developed graphene film composite biosensors were also successfully applied to determination of MC-LR in several environmental water samples with high detection recovery. The developed technique offers a promising solution to quick in-situ detection of MC-LR in the contamination point of water source.

1. INTRODUCTION

Access to safe drinking water is of paramount importance to people's health and quality of life in any community around the world. Ever increasing episodes of harmful algal blooms (HAB) resulted from intensified anthropogenic activities such as agricultural run-off, urban waste discharge, and manufacturing of detergents has exerted a significant strain in drinking water access worldwide, especially where drinking water treatment plants receive from surface water sources. Since they contain harmful cyanobacteria, which are also known as blue-green algae and can produce and release highly potent cyanotoxins to the surrounding environment, their occurrence has become serious hazards to local public health. For example, residents in the city of Toledo, USA could not use and drink tap water in the summers of 2013 and 2014 due to the presence of cyanotoxins in drinking water supplies. Estimated 50 to 70% of intracellular metabolite released during a cyanobacterial HAB are harmful toxins (i.e. cyanotoxins) [1]. Microcystins is one of most frequently detected cyanotoxin throughout the world and some variants of MCs have been claimed to be bioaccumulative through the biological chain. To date, 80 variants of MCs have been isolated and identified from freshwater cyanobacteria genera, among which microcystin-LR (MC-LR) is the most toxic variant. Due to

its severe toxicity, the provisional guideline concentration limit of 1 μg/L MC-LR in drinking water was assigned by the World Health Organization (WHO) in 1998 [2]. Following a significant HAB event, there is an urgent need to establish when a water source is safe to use or to evaluate the level of treatment required to make a source safe using a cost-effective generic analysis platform. These platforms should be easily tailored to provide early warnings of contamination episodes and allow reliable screening in water quality from catchment to consumer. Well-established methods to detect MC-LR in water include high-performance liquid chromatography/mass spectrometry (LC/MS), bioassays, biochemical assays, and immunoassays, which often require long processing times, sophisticated instruments, complex procedures, or high processing cost and are in general used in the laboratory, not in situ.

Recent advances in graphene synthesis and understanding of properties have led to enormous applications in a variety of areas. Graphene and its unique electrical properties can favour electrochemical biosensor applications for aqueous toxin monitoring. Graphene-based biosensors can be used as an alternative to time-consuming, expensive and non-portable conventional methods of analysis involved in water quality monitoring and assessment. In this work, we showcased a novel graphene-based biosensor for microcystin-LR (MC-LR) detection and quantification.

We report the efficient functionalization and immobilization of microcystin-LR and its antibodies on the facile synthesized CVD graphene/PET composite electrode.

2. METHOD

Cu foils (25 μm thick, 99.8%, Alfa) as graphene growth substrate was cut into pieces of 10×10 mm² and cleaned by acetone, methanol, and deionized water. During CVD process, Cu foils were first heated up to 950 °C in a horizontal quartz tube furnace under Ar (100 s.c.c.m.) and H_2 (200 s.c.c.m.) and annealed for 15 min to clean their surfaces and increase the Cu grain size. Graphene growth was then carried out at 1050 °C by introducing CH_4 of different concentrations balanced in Ar and H_2 with a total flow rate of 1500 sccm (1.3% H_2) for growth time between 5 and 60 min. After growth, samples were rapidly cooled to room temperature at a rate of ~100 °C/min in the protection of Ar (500 s.c.c.m) and H_2 (200 s.c.c.m.). In next step, GF grown on the Cu foil was attached to a thermal release tape (Nitto Denko Co.) by applying soft pressure (~0.2 MPa) between two rollers. After etching the Cu foil in a plastic bath filled with etching solution of iron nitrate (0.05 g/mL) for around 12 h, the transferred GF on the tape was rinsed with deionized water to remove residual etchant. Subsequently, the GF on the thermal release tape was inserted to the rolls together with 130 μm thick polyethylene terephthalate (PET) substrates and exposed to mild heat of 90~120°C for 3~5 min, resulting in the transfer of GF from the tape to the target substrate.

To fabricate the GF biosensor, a pre-cut GF sheet was attached to a copper wire tip using conductive silver epoxy (M. G. Chemicals, Ontario, Canada) and dried for 24 h at room temperature. This was followed by electrochemical functionalization, where a potential of 1.2 V vs. Ag/AgCl was applied to of GF biosensor tips for 1 min, in 1.0 M NaOH/0.5 M NaCl aqueous solutions. The functionalization potential (i.e. 1.2 V) was determined by choosing highest generated current on the surface of GF biosensor in linear sweep voltammetry without observations of water hydrolysis.

Specifically in this work, the GF biosensors were first incubated in a solution of 5 mM sulfo-NHS and 2 mM EDC in 0.1 M MES buffer, which was followed by 4 h incubation in 500 μg/L MC-LR solution (5 mL) made with PBS buffer. 1% (v/v) ethanol amine was used to washed them thoroughly after. As a result, amine group of MC-LR was conjugated to the oxygen containing functional groups (i.e. carboxyl group) on the surface of the electrochemically functionalized GF electrode through a stable covalent link. Next, MC-LR solutions of a range of concentrations from 0.05 to 100 μg/L were added into a

fixed concentration of antibodies (i.e. 2.2 μg/mL) and incubated for 30 min to prepare a series of incubation standard solutions (i.e. 0.05, 0.5, 5, 20 and 100μg/L) using PBS buffer. The GF biosensors saturated with 500 μg/L MC-LR solution in the previous step were then dipped into these incubation standard solutions, where remaining free antibodies in the solutions would bind to the MC-LR on the GF biosensors.

The electrochemical properties of the GF electrodes were first evaluated using cyclic voltammetry (CV) in a typical three-electrode cell (i.e. a working, an auxiliary and a reference electrodes) at ambient temperature on a potentiostat analyzer (Autolab PGSTAT128N plus an FRA32M module). The GF electrodes was characterized by CV in 2 mM potassium ferricyanide ($K_3[Fe(CN)_6]$) solution using 0.5 M KNO_3 as the supporting electrolyte, with a Pt wire (1mm diameter, 99.95%) as auxiliary electrode and a saturated Ag/AgCl electrode as the reference. Faradaic electrochemical impedance spectroscopy (EIS) analysis was carried out with an open-circuit potential from 0.1 to 1×10^4 Hz with the amplitude of 0.01 V in the same three-electrode cell configuration but in a solution of 5.0 mM potassium ferricyanide ($K_3[Fe(CN)_6]$)/potassium ferrocyanide ($K_4[Fe(CN)_6]$) solution using 0.5 M KNO_3 as the supporting electrolyte (see Figure 1).
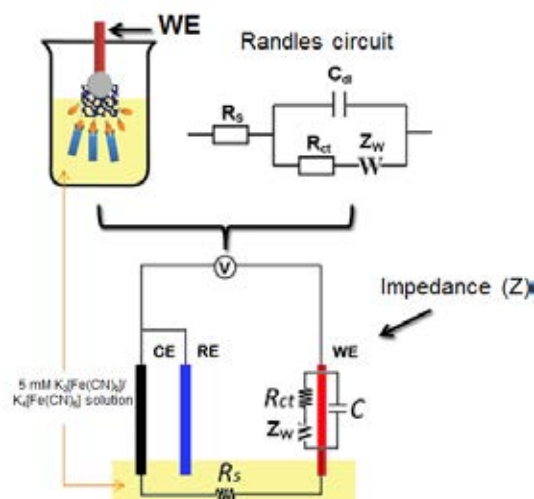
Figure 1 A illustration of Randles circuit and EIS experimental set-up

3. RESULTS AND DISCUSSION

Quantitation calibration curve of the GF biosensor response (i.e. the electron-transfer resistance) for different concentrations of MC-LR detection in the incubation solutions was shown in Figure 2. A Randles model equivalent circuit were used during the EIS measurements to interpret the behaviour of the GF biosensors, which consisted the solution resistance (R_s) in series with a parallel arrangement of the double layer capacitance (C_{dl})

and the electron-transfer resistance (R_{ct}) in series with Warbur impedance (Z_w). The determined values of the R_{ct} were then plotted as a function of the MC-LR concentration using a logarithmic scale. A great linear sensing response (R^2=0.99) of the electron-transfer resistance (R_{ct}) over a wide MC-LR concentration (C_{MC-LR}) range between 0.05 and 100 µg/L was thus achieved, which allowed the toxin detection well below the WHO provisional guideline limit of 1 µg/L for MC-LR in drinking water.
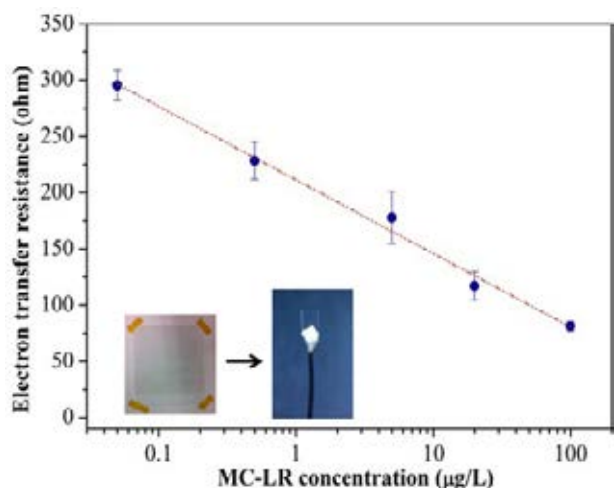
Figure 2 Linear response of MC-LR concentration to electron transfer resistance, where the inset is graphene-PET biosensor fabrication.

Table 1 Validation results of MC-LR detection using GF electrochemical biosensor

	GF biosensor value (µg /L)	Recovery (%)
Tokyo tap water	0.965±0.031	96.5
Inba lake water	0.958±0.029	95.8
Sanshiro pond water	0.949±0.037	94.9
Shinobazu pond water	0.961±0.026	96.1

GF biosensor detection results of MC-LR in four different environmental water samples are listed in Table 1, where it can be seen that potential interference (i.e. metal ions and dissolved organic compounds) has insignificant effects on the detection results. Obtained high MC-LR detection recovery (> 90 %) were also very comparable to most of recent literature studies using nanomaterial biosensor based on different electrochemical detection principle [3,4,5].

4. CONCLUSION

A fit-for-purpose biosensor for MC-LR detection as alternatives to the time-consuming, expensive, non-portable and often skills-demanding conventional methods of analysis involved in water quality assessment has been developed using GF/PET composite grown by a modified CVD method. A two-step linking procedure that enabled the immobilization of MC-LR onto the GF electrodes and conjugation of monoclonal antibodies specific to MC-LR in the incubation solutions has been employed to provide the required specificity for detecting MC-LR toxin. CV analysis revealed well-defined redox peaks in the presence of redox species, which can indicate efficient interface charge-transfer. After conjugation of MC-LR and antibodies to graphene, the increase of EIS measurements was used to detect the change of MC-LR concentration. A great linear sensing response (R^2=0.99) of EIS change was established over a wide MC-LR concentration range of 0.05 to 100 µg/L with good repeatability. Environmental water samples from different local sources, i.e. Tokyo metropolitan tap, Sanshiro pond (Tokyo, Japan), Shinobazu pond (Tokyo, Japan) and Inba lake water (Chiba prefecture, Japan), has been used to validate the sensing results of developed GF biosensors and investigate potential interfering effects of factors, such as metal ions and dissolved organic compounds. With insignificant interference effects on the detection results and high MC-LR detection recovery, developed GF biosensor technique in this work offers a promising solution to quick in-situ detection of MC-LR in the contamination point of water source with very low detection limits.

REFERENCES

[1] W. W. Carmichaeal, Cyanobacteria secondary metabolites-the cyanotoxins, *J. Appl. Bacteriol.*, 1992, 72, 445-459.

[2] World Health Organization, Guidelines for Drinking-Water Quality, 2nd ed. Addendum to Vol. *1*. Recommendations, Geneva, World Health Organization 1998, p. 13.

[3] H. Zhao, J. Tian, X. Quan, A graphene and multienzyme functionalized carbon nanosphere-based electrochemical immunosensor for microcystin-LR detection, Coll. Surf. B: Biointerf., 103 (2013), pp. 38–44.

[4] S. Eissa, A. Ng, M. Siaj, M. Zourob, Label-free voltammetric aptasensor for the sensitive detection of microcystin-LR using graphene-modified electrodes, *Anal. Chem.*, 86 (2014), pp. 7551–7557.

[5] C. Gan, L. Ling, Z. He, H. Lei, Y. Liu, In-situ assembly of biocompatible core-shell hierarchical nanostructures sensitized immunosensor for microcystin-LR detection, *Biosens. Bioelectron.*, 78 (2016), pp. 381–389.

O6-9

題名：危機管理型水位計による河川水位モニタリング技術

筒井 和雄 [1]，井出康一郎 [1]，長谷川 勉 [1]，古島 広明 [2]

[1] 株式会社日立製作所，[2] 株式会社オサシ・テクノス

キーワード：危機管理型水位計，河川，水位計測，洪水，クラウド

抄録

　日本全国には河川が約 20,000 ある。この大多数を占める中小河川において、水位計が未設置の個所が数多く存在し、洪水時の河川水位の把握が困難な状況にある。従来型の水位計は、河川管理を主体とするため、初期投資が大きく、普及を拡大するには制約がある。このため、国土交通省では従来の技術的枠組みにとらわれない新しい河川管理を目指した「革新的河川管理プロジェクト」を立ち上げ、2017 年度に実証試験を実施した。本発表では、このプロジェクトに参画し開発した危機管理型水位計の仕様概要、計測データの処理、メンテナンスフリーの対応、実証試験結果の評価について述べる。出水期の 5 回計測した洪水時観測結果は洪水波形特性を再現した安定した計測ができた。その中で 8 月 19 日は 2 時間で約 1,000 発の落雷があったにもかかわらず、データ欠測のない安定した計測が確認できた。また、水位計測データの利活用はどのようにすべきかについて、いくつかの提言をする。

1. はじめに

　平成 27 年関東・東北豪雨災害[1]、平成 28 年北海道・東北豪雨災害、平成 29 年九州北部豪雨災害等[2]、水害の頻発化・激甚化が顕著である。日本全国の河川約 20,000 の多くは中小河川である。中小河川における水害が多発しており、洪水時に河川水位の情報をもとに的確に避難の判断をすることが要求されている。このため、水害危険性の周知方法の一つとして危機管理型水位計の設置が検討[3]され、低コストの水位計を実用化し、普及を促進することとなった。

2. 革新的河川管理プロジェクトにおける実証試験

2.1 革新的河川管理プロジェクト

　「革新的河川管理プロジェクト」[4]は、国土交通省が最新の技術・ノウハウを持ち寄りスピーディーに実装化を図る技術開発の取り組みの一環として、オープンイノベーションを採用し、従来の技術的枠組みにとらわれない新しい河川管理を目指したものである。12 チーム 21 者がクラウド型メンテナンスフリー水位計として危機管理型水位計を開発し、平成 29 年夏より鶴見川水系の鳥山川に据え付け、水位観測を実施した。

2.2 危機管理型水位計の仕様概要

　従来の初期投資、維持管理コストがかかるといった課題を解決するため、国土交通省から提示された要求仕様は下記である。目標は IoT 技術を応用し、短期間で実装化し、普及することである。

(1)メンテナンスフリー

(2)省スペース

(3)通信コストの縮減

(4)クラウド化でシステム経費の縮減

(5)低コスト（1 台 100 万円以下を目標）

　要求仕様に対して開発した水位計仕様は、表 1 の通りである。要求仕様ごとに水位計の設置環境を考慮して、仕様を決定した。

表 1 危機管理型水位計の仕様

No	仕様項目	仕様
1	共通部　温度・湿度条件	-20℃～55℃
	耐用年数	5 年間
2	水位計測部　計測方法	水圧式,超音波式
	計測範囲	0～10m
	最小読取範囲	1cm
	観測精度	±0.1%以内
3	計測制御部	測定時刻,水位,電池電圧,温度をメモリ記録し、クラウド伝送
	データロガー機能	
	時刻補正機能	基地局からの電波による時刻補正
4	電源部　バッテリー仕様	12V24Ah
	太陽光パネル容量	30W
	無日照保証日数	9 日間
5	観測周期（自動切替）平常	10 分
	設定水位変動以上	1～5 分の可変

2.3 計測データの処理

　図 1 に示すように危機管理型水位計は、水位観測データと水位計環境情報を閉域無線回線経由でクラウドに伝送する。クラウドでは観測データを時系列にデータベース化すると共に水位計環境情報を記録する。水位情報は、インターネットによりスマートフォンで水位計の位置、河川断面表示と重畳した水位グラフ、過去時系列等の検索閲覧ができる。また、基準設定以上に水位が超過した場合は警報が鳴る。水位観測周期は、水位の上昇速度が設定値を超過すると自動的に平常時 10 分周期から 5 分周期に早まる。これは中小河川の水位上昇速度が速いため、観測周期を可変とし、かつ機器の電池消耗を最小限とするための方法である。

図 1　水位計測とクラウド構成

2.4 メンテナンスフリーの対応

　水位計は従来、1 回/年の定期点検等維持管理コストがかかっている。危機管理型水位計は、5 年間のメンテナンスフリーを要求されており、水位計環境情報を同時に収集し、遠隔診断処理により早期の異常検知をし、予防保全につなげる。環境情報は、センサ・通信機電源電圧、電波状態、温度等であり、通信安定性、電源状態、機器環境を判断する。

3. 実証試験結果

3.1 洪水時試験計測結果

　図 2 は 9 月～10 月の洪水時の試験計測結果である。グラフは既設の烏山水位観測所の計測データと本チーム(チーム No.9)の計測データを比較している。河床勾配より約 0.255m 水位を低く表示しているため、全体に低く表示されている。計測結果は公表[5]され、本チームを含めた 6 チームが「洪水波形特性を再現しており、良好な結果」と評価された。観測周期は、水位が急上昇したときの平常時 10 分から 5 分に自動切替されている。これにより、水位計測は急峻な水位変化に追従できた。特に 9 月 22 日の水位ピーク値は 5 分周期の場合、的確に捉えている。

　図 3 は、本チームが先行して 8 月に設置したこと

により計測できた試験結果である。8 月 19 日は、水位計設置場所近傍で 2 時間に約 1,000 発の落雷があり[6]、豪雨となった。その結果、最大水位は堤防天端から 2.41m に達し、最大水位上昇速度は 0.86m／5 分と急激であった。このような厳しい環境下でも水位計とクラウド間のデータ欠測処理機能によりデータ欠測は全くなく、安定して観測できた。

(1)平成 29 年 9 月 18 日
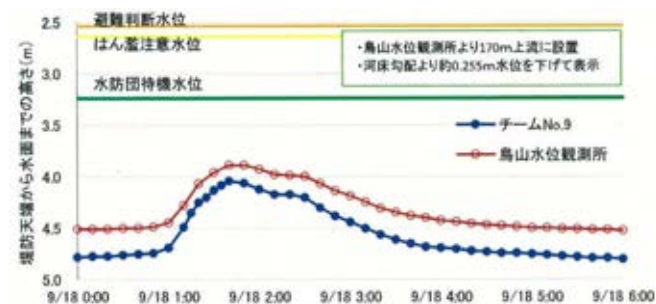
(2)平成 29 年 9 月 22 日
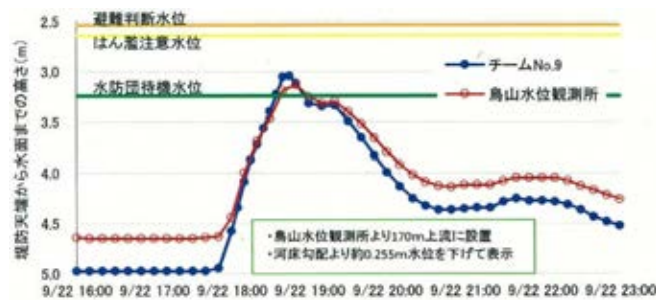
(3)平成 29 年 9 月 28 日
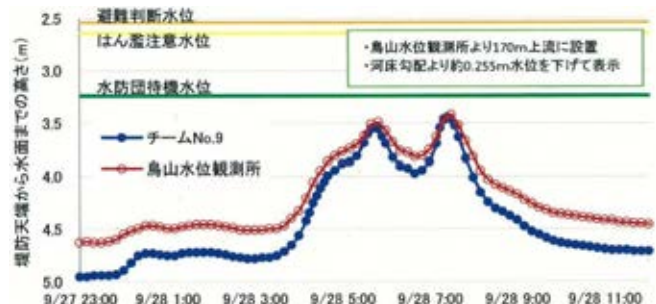
(4)平成 29 年 10 月 29 日(台風 21 号)
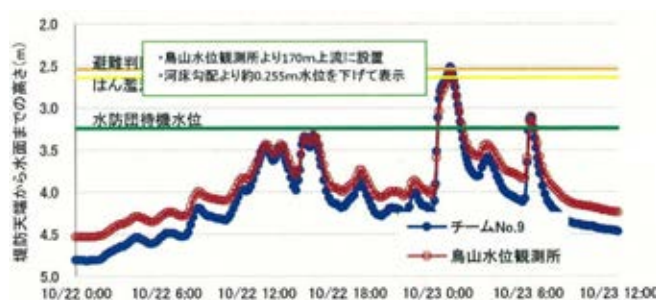
図 2　洪水時試験計測結果
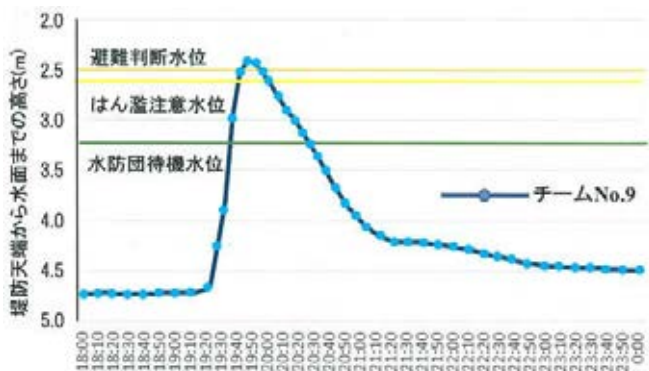
図 3 雷雨時の洪水試験計測結果(8 月 19 日)

3.2 水位計の電源電圧監視結果

　図 4 は、通信機電源電圧の気象条件による変動を示したものである。1 ヶ月間に 10 数日の降雨日があったが、天候悪化の影響を受けず基準電圧 12V の安定した電源供給を実現している。通信機電源電圧の日間変動は太陽光パネルからの充電の変化による。
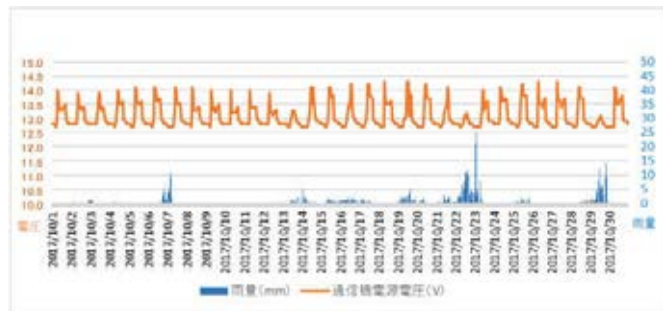
図 4　電源電圧変化と気象状況(観測地点雨量)

4. 考察

4.1 メンテナンスフリー

　5 年間無給電で運用ができるように、バッテリーと太陽光パネルを組み合せた。電源容量は 9 日間の無日照を保証する。水位計の稼働状況がリアルタイムで監視できるように電源状況、通信状況、装置環境情報を水位情報と同時にクラウドへ伝送・解析することにより、遠隔で機器の予防保全ができる環境とした。

4.2 省スペース

　水位計装置は、計測部、計測制御部、通信部、電源部を組み合せて 1 本のポールに設置できるようにコンパクト化した。

4.3 通信コストの低減

　通信は携帯無線回線を利用する。伝送項目は最適化して伝送量を極力減らし、平常時と降雨時を合わせた通信コストを低減した。また伝送時間の短縮により、災害時の通信輻輳時にも安定した通信が確保できるように配慮した。

4.4 クラウド化でシステム経費の縮減

　水位データはクラウドで処理することにより、ハードウェアの初期投資の低減、ソフトウェア開発の共有化等により重複開発を縮減した。また、実証試験の実績を生かして、早期のシステム立ち上げを可能とした。

4.5 低コスト

　水位計装置は、装置のコンパクト化、汎用部品の採用等により目標コストを実現した。通信は伝送時以外を休止モードとして低消費電力化を図り、電源部容量の小型化により、コストを低減できた。

4.6 今後の展開

　河川水位の情報は、的確な避難の判断に重要な情報である。中小河川への設置が今年度から実施され、水位計のデータはクラウドに集中して収集される[7]。これらの水位情報はオープンデータとして公開される予定であり、その利活用が今後本格化する。管理者、住民に対してわかり易く情報提供することが重要である。応用例として、避難に有用な避難所情報の提供、スマートフォンの GPS 機能を活用した位置表示、過去のアーカイブ情報との比較、地理情報との連携などが挙げられる。

5. 結論

　中小河川への設置が実現できる危機管理型水位計を開発し、実証試験により洪水時の安定した計測ができることを実証できた。危機管理型水位計はこれから本格的な設置が進められる。水害危険性の周知方法として、河川水位のモニタリングが的確な避難の判断情報として活用されるように、安定した情報提供ができる環境づくりに寄与したい。

引用文献

[1] Yasuhara, K., Murakami, S., Koarai, M., Ito, T. and Tsutsui, K.: Lesson learned from flood damage in Kinu River during the Kanto-Tohoku localized torrential downpour in 2015, Proc. International Symp. Hanoi Geoengineering 2016, pp. 16-23, Hanoi, Vietnam, 2016.

[2] 国土交通省水管理 国土保全局:水害レポート 2017,2017.

[3] 国土交通省:国土交通省の取組みと検討状況,pp.3-6,2017.

[4] 国土交通省水管理 国土保全局:報道発表資料,新しい水位計・ドローンの開発のため、32 者が 17 チームを結成し、新年度より開発に着手,2017.

[5] 国土交通省水管理 国土保全局:革新的河川管理プロジェクト(第 1 弾)における「洪水時に特化した低コストな水位計」の試験計測結果,2017.

[6] ウェザーニュース:【関東大雷雨】都心で 2 時間 1,000 発の落雷観測,2017.

[7] 国土交通省,経済産業省:ICT,データ活用等による戦略的なインフラメンテナンス等,pp.24-26,2018.

O6-10

Estimation of Secchi Disk Depth in Lake Kasumigaura from MERIS

Dalin Jiang[1*], Bunkei Matsushita[2], Takehiko Fukushima[3]

[1] Graduate School of Life and Environmental Sciences, University of Tsukuba, Tsukuba, Ibaraki, 305-8572, Japan

[2]Faculty of Life and Environmental Sciences, University of Tsukuba, Tsukuba, Ibaraki, 305-8572, Japan

[3]Ibaraki Kasumigaura Environmental Science Center, Tsuchiura, Ibaraki, 300-0023, Japan

Keywords: Secchi disk depth, remote sensing, Lake Kasumigaura

ABSTRACT

Secchi Disk Depth (Z_{SD}), also called transparency, is an important indicator of water quality. The manual and point-based measurement of Z_{SD} has a long history with more than 200 years. With the development of remote sensing, satellite image can provide the potential for large spatial and long time-series monitoring of Z_{SD}, which is also developing to an important way for lake environment management. In this study, MERIS images from 2003 to 2012 were employed to retrieve Z_{SD} in the Japanese turbid Lake Kasumigaura. The absorption and backscattering coefficients were firstly retrieved using two versions of quasi-analytical algorithm: QAA_V6 and QAA_turbid, and then Z_{SD} were estimated based on the new method proposed by Lee in 2015. Results were validated using in-situ Z_{SD}, the RMSE and MAPE of Z_{SD} estimated using QAA_turbid were 0.10m and 14.96% respectively, the estimated Z_{SD} using QAA_V6 showed overestimation with RMSE and MAPE of 0.65m and 97.83%. This indicated that Z_{SD} estimation using absorption and backscattering coefficients from QAA_turbid was more accurate than that from QAA_V6. Long time-series results of Z_{SD} estimated from MERIS using QAA_turbid matched the in-situ Z_{SD} well, all of them showed an increase trend from 2003 to 2012 in Lake Kasumigaura. Results in this study implied that estimation of Z_{SD} from MERIS images is a potential way for long time-series Z_{SD} monitoring in lakes.

1. INTRODUCTION

Secchi Disk Depth (Z_{SD}), also termed transparency, has been recorded for more than 200 years in natural waters. Measuring Z_{SD} is a direct and efficient way for water condition evaluation[1][2]. The general way to measure Z_{SD} is by lowering down a 25 or 30 cm white disk or white-and-black disk into the water, and Z_{SD} is recorded as the depth when the disk can no longer be seen[1][3]. Lee et al.[3] developed a mechanistic model to estimate Z_{SD} in different types of waters from remote sensing, which can be applied to satellite images to produce large coverage and high frequency Z_{SD} observations. In this method, absorption and backscattering coefficients are key parameters for Z_{SD} estimation, which is a big challenge for turbid waters. At present, quasi-analytical algorithm is a solution for absorption and backscattering coefficients retrieval, QAA_V6[4] and QAA_turbid[5] are two typical algorithms which can be used for absorption and backscattering coefficients retrieval in turbid waters. But the performance of those two algorithms still need more tests in turbid inland lakes, because usually the inland turbid waters are more complicated than ocean waters.

Knowing the importance and challenges of Z_{SD} retrieval in inland turbid waters, the objectives of this study were to: (1) evaluate the performance of Lee's Z_{SD} model combined with two quasi-analytical algorithms, QAA_V6 and QAA_turbid, in the turbid Lake Kasumigaura, and (2) produce the long time series of Z_{SD} from MERIS satellite image in Lake Kasumigaura.

2. METHOD

In this study, totally 507 MERIS images covering Lake Kasumigaura were downloaded from ESA, those images were further pre-processed in BEAM software following the steps as: research area subset, radiometric correction, case-2 atmospheric correction. Absorption and backscattering coefficients were then estimated from the pre-processed images using QAA_V6 and QAA_turbid respectively, and then the diffuse attenuation coefficients were estimated[6], at last, Z_{SD} were estimated using Lee's Z_{SD} model[3]. The in-situ Z_{SD} data covering 2003-2012 from the National Institute for Environmental Studies (NIES) were used for result validation, it is noted that the

in-situ data were collected every month in 10 monitoring sites in Lake Kasumigaura.

3. RESULTS

By searching the in-situ database, 19 matched in-situ Z_{SD} were found, Fig.1 shows the results of validation using in-situ Z_{SD} data which collected on the same day with satellite image. It is clear that Z_{SD} estimated using QAA_V6 shows overestimation, with RMSE and MAPE of 0.65 m and 97.83% respectively. Z_{SD} estimated using QAA_turbid shows good correlation with in-situ data, the RMSE and MAPE are 0.10 m and 14.96%, which are significant better than the results using QAA_V6.
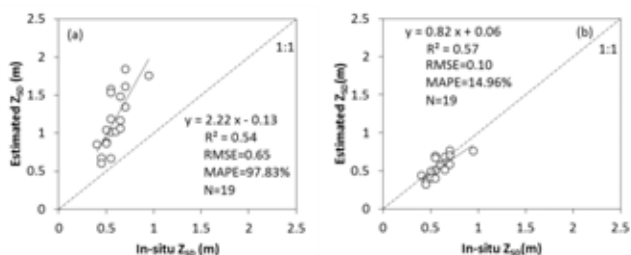
Fig1. Validation results of retrieved Z_{SD}. (a) Z_{SD} retrieved using QAA_V6, (b) Z_{SD} retrieved using QAA_turbid.

All estimated Z_{SD} were averaged to monthly mean Z_{SD} to compare with in-situ data, Fig2. shows the results of monthly mean Z_{SD} changes from 2003 to 2012 in the center of the lake. We can see that the retrieved Z_{SD} using QAA_V6 is apparently higher than the in-situ Z_{SD}, while QAA_turbid matches well with the in-situ data. Furthermore, both of the retrieved Z_{SD} and in-situ Z_{SD} show an increase trend during the 10 years.
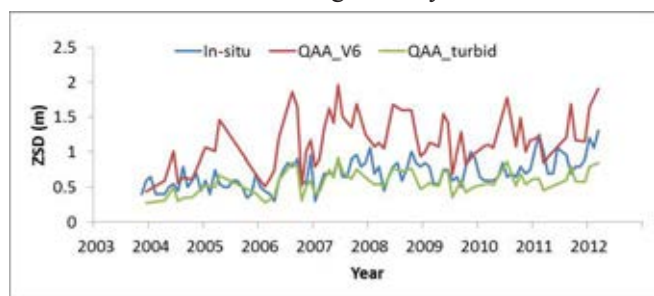
Fig.2 Z_{SD} changes in the center of Lake Kasumigaura from 2003 to 2012

4. DISCUSSION

Absorption and backscattering coefficients describe the inherent optical properties of the water, they are key parameters in Z_{SD} retrieval when using Lee's Z_{SD} model. The QAA_V6 from IOCCG can be generally used for both turbid and clear waters according to previous studies, but for extreme turbid inland waters, such as Lake Kasumigaura in this study, QAA_V6 gave an overestimation of Z_{SD}, the potential reason is that QAA_V6 is mainly used for ocean waters, therefore the retrieved absorption and backscattering coefficients are lower than the true values when using it for turbid inland waters, this leads to the overestimation of Z_{SD}. QAA_turbid was developed for turbid waters, it gives the accurate absorption and backscattering coefficients, so the estimated Z_{SD} is reasonable. Moreover, the estimated long time series Z_{SD} using QAA_turbid in this study showed the same change trend with in-situ data, that means combining Lee's Z_{SD} model with QAA_turbid can be used for Z_{SD} monitoring from satellite images in turbid inland lakes.

5. CONCLUSION

This study used MERIS images to evaluate Lee's Z_{SD} model combined with QAA_V6 and QAA_turbid in the turbid Lake Kasumigaura, results revealed that Lee's Z_{SD} model with QAA_V6 lead to overestimation of Z_{SD} in extreme turbid waters, but QAA_turbid performed well. Results in this study also indicated that long time Z_{SD} monitoring using Lee's Z_{SD} model based on QAA_turbid is reasonable in Lake Kasumigaura, retrieved results agreed with in-situ data and showed increase Z_{SD} from 2003 to 2012.

REFERENCES

[1] M.R.Wernand: On the history of the Secchi disc, Journal of the European Optical Society Rapid Publications, Vol. 5, 1013s, 2010.

[2] E. Aas, J. Høkedal, and K. Sørensen: Secchi depth in the Oslofjord-Skagerrak area: theory, experiments and relationships to other quantities, Ocean Science, Vol. 10, pp.177-199, 2014.

[3] Z. Lee, S. Shang, C. Hu et al.: Secchi disk depth: A new theory and mechanistic model for underwater visibility, Remote Sensing of Environment, Vol. 169, pp.139-149, 2015.

[4] IOCCG: Update of the Quasi-Analytical Algorithm (QAA_V6), http://www.ioccg.org/groups/software.html.

[5] W. Yang, B Matsushita, J. Chen et al.: Retrieval of Inherent Optical Properties for Turbid Inland Waters from Remote-Sensing Reflectance. IEEE Transactions on Geoscience & Remote Sensing, Vol. 51, pp.3761-3773, 2013.

[6] Z. Lee, C. Hu, S. Shang et al.: Penetration of UV‐visible solar radiation in the global oceans: Insights from ocean color remote sensing, Journal of Geophysical Research Oceans, Vol. 118, pp.4241-4255, 2013.

O6-11

気候変動観測衛星「しきさい」による湖沼観測

村上 浩[1]

[1] 宇宙航空研究開発機構（JAXA）

キーワード：気候変動観測衛星，GCOM-C，多波長光学放射計，SGLI，リモートセンシング，水色，水温

抄録

2017 年 12 月に打ち上げられた気候変動観測衛星「しきさい」には， 250m 空間解像度，1150〜1400 km 観測幅で近紫外〜熱赤外波長を 19 チャンネルで観測する多波長光学放射計（SGLI）が搭載されている。2018 年 12 月から一般配布の開始が計画されているクロロフィル a 濃度や海面水温等のプロダクトは外洋や沿岸域を想定したものではあるが，導出原理としては湖沼でも導出が可能であると考えられる。衛星打ち上げ後実際に取得されている観測画像からは，霞ヶ浦のような大規模な湖だけでなく，数 10km^2 スケールの湖沼でも水色や水温推定値の空間パターンが識別できている。湖沼の水中特性の現場観測研究との連携を通じ，「しきさい」の 250m 解像度と広い観測幅による高頻度観測を生かした湖沼の環境変動監視への貢献が期待できる。

1. はじめに

　気候変動観測衛星「しきさい」は 2017 年 12 月 23 日に種子島から打ち上げられ，2018 年 4 月から定常運用を開始している。「しきさい」には， 250m 空間解像度・1150 km〜1400 km 観測幅で近紫外〜熱赤外波長の 19 チャンネル（表1）で観測する多波長光学放射計（SGLI）を搭載している。

　この観測データから 250m 解像度の海色や海面水温プロダクトを作成・配布予定である（表 2）。これらのデータや推定手法は湖沼への応用が可能であるため，250m 解像度が生かせる比較的大きな湖沼については、2 日に 1 度（曇天でなければ）の高頻度観測データの取得が期待できる。

表 1　多波長光学放射計（SGLI）チャンネル[1]

CH	λ nm	$\Delta\lambda$	L_{std} $W/m^2/sr/\mu m$ TI: Kelvin	L_{max}	SNR TI: NEΔT	IFOV m
VN01	380	11	60	210	675	**250**/1000
VN02	412	10	75	250	800	**250**/1000
VN03	443	10	64	400	517	**250**/1000
VN04	490	10	53	120	865	**250**/1000
VN05	530	20	41	350	482	**250**/1000
VN06	566	20	33	90	1040	**250**/1000
VN07	672	22	23	62	1002	**250**/1000
VN08	672	22	25	210	549	**250**/1000
VN09	763	11	40	350	1646	250/**1000**
VN10	867	21	8	30	491	**250**/1000
VN11	867	21	30	300	498	**250**/1000
PL01	672	21	25	250	655	**1000**
PL02	866	20	30	300	723	**1000**
SW01	1050	21	57	248	951	**1000**
SW02	1390	20	8	103	346	**1000**
SW03	1630	196	3	50	100	**250**/1000
SW04	2210	51	1.9	20	379	**1000**
TI01	10800	760	300K	340K	0.039K	250/**500**/1000
TI02	12000	780	300K	340K	0.069K	250/**500**/1000

SNR is defined at L_{std} and IFOV shown by bold characters

表 2　GCOM-C 海洋分野プロダクト

カテゴリ		プロダクト名
海色	標準プロダクト	正規化海水射出放射輝度
		大気補正パラメータ
		光合成有効放射
		クロロフィル a 濃度
		懸濁物質濃度
		有色溶存有機物吸光係数
	研究プロダクト	海水固有の光学特性
		有光層深度
		植物プランクトン機能別分類
		赤潮
		海洋純基礎生産力
		多センサ複合海色
温度	標準プロダクト	海面水温
	研究プロダクト	多センサ複合海面水温

2. 方法

　衛星光学観測値から海色（水色）を導出するためには、大気の散乱や吸収を補正する必要がある。波長毎の衛星観測光を水平面に入射する太陽入射光で割った大気上端反射率ρ_tは以下のように近似できる。

$$\rho_t / t_g = \rho_r + \rho_a + t_d\, \rho_w / (1 - s_a\, \rho_w) + t_b\, \rho_g \qquad (1)$$

ここで，t_g 大気分子の吸収，ρ_r 大気分子の散乱，ρ_a エアロゾルの散乱，t_d 大気の直達+散乱透過率，t_b 直達透過率，s_a 球面アルベード，ρ_w サングリント反射率，ρ_w 水面反射率である。実際の計算では，大気放射伝達コード（例えばPstar-4[2]）を用い、観測量であるρ_tとρ_w以外の変数について，様々な観測幾何条件やエアロゾル等の条件における各波長の値を計算したルックアップテーブル LUT を作っておく（水面での反射光成分をρ_rに含めて計算し，ρ_wを水中からの射出光成分だけにすることが多い）。この LUT と複数の波長で観測したρ_t が整合するような(1)式中の変数を探すことにより，ρ_w（水色）を推定する[3]。

　クロロフィル a 濃度（Chl-*a*）等の水中の物質量については，衛星で観測された複数の波長におけるρ_w から，現場観測等による物質量と光学特性（吸収や散乱特性）の関係の知見（回帰式[4]や水中光学モデル[5]）を用いて推定する。

　海面（水面）温度については、熱赤外波長の複数のチャンネル（しきさいでは 10.8μm と 12μm）での観測値から大気の放射・吸収を分離し，水面からの熱放射を抽出することによって推定する[6]。

3. 結果
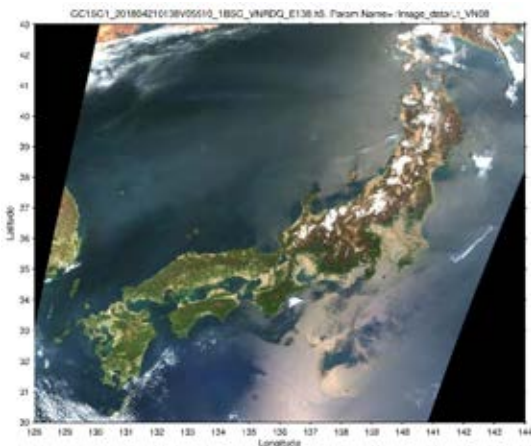
図 1 「しきさい」の観測例（RGB 合成画像 2018/04/21）

　図 1 の左上と右下の黒い部分を除いた範囲が SGLI 可視波長チャンネルの観測幅（約 1150km）である。「しきさい」は日本列島を一度に観測できるこの広い観測幅で地球を 1 日に約 14 周回（485 周/34 日）することにより，中緯度帯では 2 日に 1 度程度観測することができる（晴天の場合）。
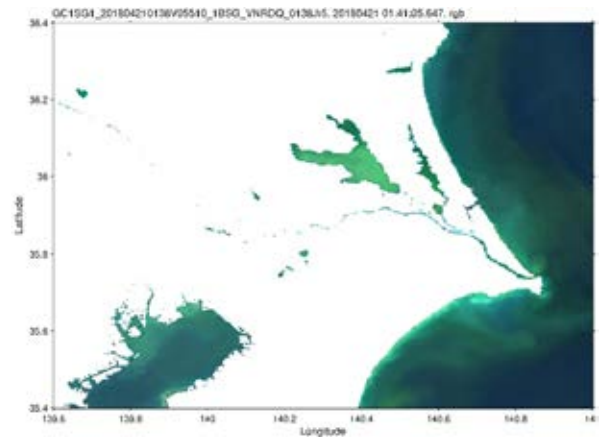
図 2 ρ_w の RGB 画像の関東東部拡大図（2018/04/21）
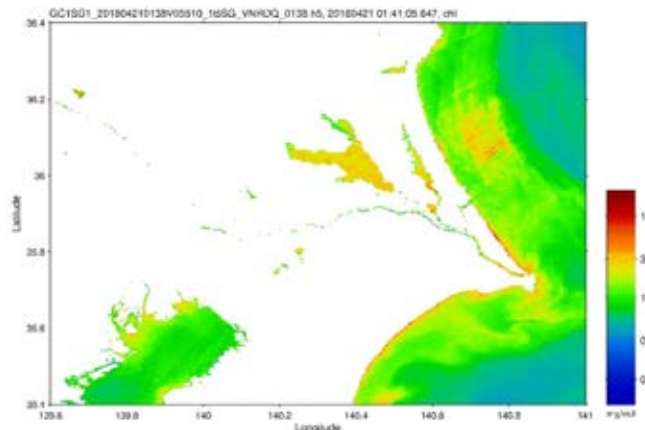
図 3 Chl-*a* の関東東部拡大図（2018/04/21）
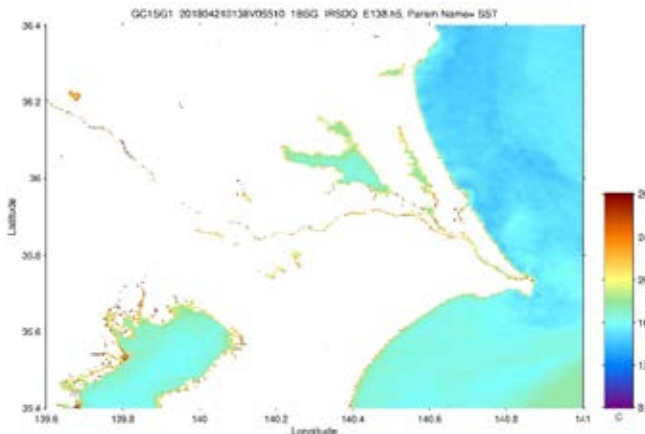
図 4　水面温度の関東東部拡大図（2018/04/21）

　図 2, 3, 4 は，大気補正後の水中射出反射率, Chl-*a*, 水面温度プロダクトを試作したものである。霞ヶ浦のような大きな湖沼だけでなく，印旛沼や谷中湖，涸沼などのサイズの湖沼（〜数 10km^2）についてもその中の空間パターンをある程度識別できている。

4. 結論

　「しきさい」の海洋分野の標準プロダクトとして Chl-*a* や水温等のプロダクトの作成が計画されており，2018 年

12 月から一般提供を開始する計画である。元々は外洋や沿岸域を想定したプロダクトであるが，実際に取得されている観測画像からは，霞ヶ浦のような大規模な湖だけでなく，数 $10km^2$ スケールの湖沼でも水色や水温推定値の空間パターンが識別できており，ある程度のサイズ以上の湖沼であれば水色や表面水温等の推定が可能であると思われる。

　もちろん，Chl-*a* 等の水中の物質量の推定に必要な水中光学特性は，湖沼では地域性が大きいと考えられるため、個々の湖沼における現場観測等による水中光学特性の知見の蓄積が重要である。今後この知見の蓄積が進めば，より定量的な物理量推定が可能となり，「しきさい」の広い観測幅による高頻度観測を生かした湖沼の環境変動監視への貢献が期待できる。

引用文献

[1]　JAXA/EORC/GCOM-C homepage: http://suzaku.eorc.jaxa.jp/GCOM_C/data/prelaunch/index.html

[2]　Y. Ota, A. Higurashi, T. Nakajima, and T. Yokota, "Matrix formulations of radiative transfer including the polarization effect in a coupled atmosphere-ocean system," J. Quantitative Spectroscopy and Radiative Transfer, **111**, 878-894, 2010.

[3]　M. Toratani, H. Fukushima, H. Murakami, and A. Tanaka, "Atmospheric correction scheme for GLI with absorptive aerosol correction", J. Oceanography, 63, 525-532, 2007.

[4]　JE. O'Reilly, S. Maritorena, D. Siegel, MO. O'Brien, D. Toole, BG. Mitchell, M. Kahru, F. Chavez, PG. Strutton, GF. Cota, SB. Hooker, C. McClain, K. Carder, F. Muller-Karger, L. Harding, A. Magnuson, D. Phinney, G. Moore, J. Aiken, KR. Arrigo, RM. Letelier, M. Culver, Ocean color chlorophyll a algorithms for SeaWiFS, OC2, and OC4: Version 4. SeaWiFS Postlaunch Calibration and Validation Analyses. 11 (CR. McClain, Ed.).:9-23., Greenbelt, Md.: GSFC, 2000.

[5]　IOCCG (2006). Remote Sensing of Inherent Optical Properties: Fundamentals, Tests of Algorithms, and Applications. Lee, Z.-P. (ed.), Reports of the International Ocean-Colour Coordinating Group, No. 5, IOCCG, Dartmouth, Canada, 2006.

[6]　Y. Kurihara, H. Murakami, and M. Kachi, "Sea surface temperature from the new Japanese geostationary meteorological Himawari-8 satellite", *Geophys. Res. Lett.*, 43, 1234–1240, doi:10.1002/2015GL067159, 2016.

O6-12

In-Situ Hyperspectral Remote Sensing as An Aid in Wetlands Condition Assessment – A Case Study of Indian Man-Made Wetland

J.K. Garg[1], Ridhi Saluja[1], Satish Prasad[1]

[1]University School of Environment Management, Guru Gobind Singh Indraprastha University, New Delhi-110078, India

Keywords: Wetland, hyperspectral, remote sensing, spectroradiometer, data analysis technologies and modeling.

ABSTRACT

Worldwide, wetland ecosystems are facing natural and anthropogenic pressures resulting in deterioration of their health and resilience. Conventional methods commonly use point physico-chemical measurements to characterize and monitor the health of lakes and aquatic ecosystems. Moreover, such methods fail to provide information in spatial domain. Hyperspectral remote sensing is fast emerging as a potential standalone tool for assessment of health of aquatic ecosystems. In the present study, *in-situ* hyperspectral remote sensing was employed to test its potential for condition assessment of Bhindawas lake, largest man-made wetland in the state of Haryana, India. Spectral reflectance data for wetland water column and representative macrophyte species was collected at different sampling sites within the wetland using a SVC GER Spectroradiometer (350-1050 nm) during the year 2014 and 2015. Water samples were collected for the analysis of bio-optical water quality parameters (Chl-a, TSS and Turbidity). Various spectroscopic methods (smoothing and derivative analysis) and linear regression were used to analyze the spectral data. Results have revealed that spectral reflectance data allows identification of various macrophyte species. Linear regression models were developed for estimation of bio-optical parameters in the wetland water column that can successfully replace the conventional field-based methods for wetland condition assessment.

1. INTRODUCTION

Globally, conservation and management of wetlands has become a cause of concern for researchers, conservation agencies and people. Multispectral Remote Sensing has been used to assess and monitor wetland condition for several decades. Inspite of its wide use, it is associated with inherent limitations associated with sensor technology, measurement methods and resolutions. According to Ustin et al., (2004) [1] imaging spectroscopy or hyperspectral remote sensing provides a prospect to overcome the shortcomings of multispectral satellite data for wetland related studies. Data dimensionality of hyperspectral sensors allows detailed analysis of ecosystem properties and processes surpassing other remote sensing modalities.

In the context of wetland science, hyperspectral data has been used to achieve a variety of objectives including delineation of wetlands and characterization of hydrophytes [2]. Monitoring of water quality conditions and parameters of freshwater ecosystems is one of the major advantages of hyperspectral data. It has been used for classifying trophic levels of lakes [3] and estuaries [4], characterizing algal bloom [5] and assessment of ammonia dynamics for wetland treatments [6]. In-situ spectroradiometer data has proved useful in estimating total suspended matter, chlorophyll content and total phosphorus [7]. With respect to wetland vegetation, hyperspectral data has been successfully used for spectral discrimination of wetland species in comparison to the general classification achieved using multispectral data [8]. In spite of the increase in application of hyperspectral remote sensing for wetland studies there exists a paucity in its application for assessment of inland wetlands of India.

The main aim of the study is (i) to develop models for estimation of bio-optical parameters which effect wetland condition functioning using *in-situ* hyperspectral data and (ii) to test the potential of *in-situ* hyperspectral data for identification of macrophyte species.

2. METHOD

Study area

Bhindawas Bird Sanctuary, a man-made wetland designated as a protected area in the year 1986, is the largest wetland in the state of Haryana (412 ha) with a periphery of 12 km (28°28′00″ to 28°36′00″ N; 76°28′00″ to 76°38′00″ E).
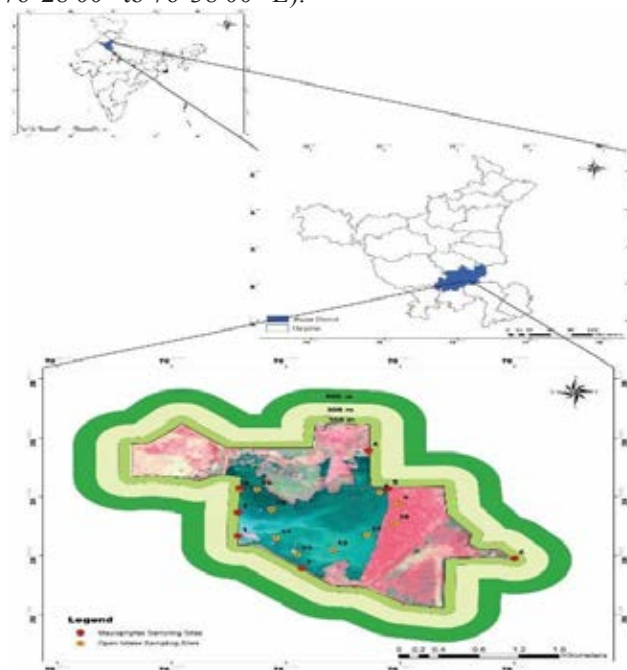
Fig 1. Study area maps showing Bhindawas wetland and sampling sites

Data Collection

Sampling was conducted during May, September and December for 2014 and 2015. *In-situ* spectral measurements were collected on a survey boat within solar noon (i.e. 1000 to 1400 hours) during each survey. Hyperspectral (approximately 512 bands with sampling interval of ~0.3 nm and spectral resolution of ~1.4 nm) water irradiance was measured with a SVC GER1500 spectroradiometer having a range of 350 to 1050 nm.
Sample points (shown in fig 1) within the seven transects perpendicular to the shore covering dominant macrophyte

species were identified for homogeneous patches of macrophyte vegetation (emergent, submerged and floating species). Eight macrophyte species *Ageratum conyzoides, Phragmites karka, Cyperus alopecuroides, Typha sp., Anisomeles indica, Paspalum paspaloides, Achyranthus aspera, Alternanthera sessilis and Cynodon dactylon*. Reflectance $R(\lambda)$ was calibrated by measuring the upwelling radiance of a white Spectralon© panel and a custom software package "GER 1500 PC Data Acquisition Software" compared the signals from the two and generated a normalized percent reflectance.

Sample analysis
At each sampling station, the following water quality parameters were measured: conductivity (Cond.), temperature, pH, secchi depth (SD), turbidity, chlorophyll-a (Chl-a) and total suspended solids (TSS) using laboratory procedures in consistent with Standard Methods for Examination of Water and Wastewater [9].

Spectral analysis
After pre-processing, spectral data were smoothed using Savitzky-Golay (SG) filter. In this study, following Tsai and Philpot (2002) [10], first derivative was estimated by dividing the difference between successive spectral values by the wavelength interval using the following equation:

$$\frac{dr}{d\lambda} = \frac{r(\lambda_i) - r(\lambda j)}{\Delta \lambda} \qquad (i)$$

Statistical analysis
For statistical analysis, reflectance values between 400-800 nm wavelength range were included. The dataset was normalized by subtracting the spectrum mean from each spectrum. The principal components extracted using PCA were then correlated to the concurrently measured optically active components. Correlation analysis was also applied to the measurements of optically active water parameters. Furthermore, to explore the relationships between the spectral reflectance and optical parameters Canonical Correspondence Analysis (CCA) was applied. Bio-optical models were developed using stepwise linear regression.

3. RESULTS AND DISCUSSION
Wetland water quality
Table 1 Descriptive statistics of bio-optical parameters

Parameters	SI Unit	Min	Max	Mean	SD
Temp	°C	13	34.6	26.76	8.14
SD	m	0.24	1.35	0.59	0.26
Cond.	µS/cm	208	357	246.9	40.6
Chl-a	µg/l	1.14	107.5	22.76	19.75
TSS	mg/l	17.8	415.8	173.91	135.9
Turbidity	NTU	0.81	35.15	6.06	6.65
TOC	mg/l	0	13	2.59	3.7

Despite the variability observed in water column reflectance, a constant spectral pattern is observed typical of Case II waters (Fig. 2). Spectra characteristically show a peak reflectance around 570 nm, caused by minimal absorbance by phytoplankton pigments and backscattering by suspended matter [11]. A second reflectance peak near 700 nm results from phycocyanin

absorption at around 675 nm and strong water absorption at longer wavelengths ($\lambda > 700$ nm). As compared to other spectral regions, the $R(\lambda)$ in the blue region (400-500 nm) was lower and exhibited small variation as compared to the green, red and infrared (NIR) regions suggesting strong absorption by organic matter as well as phytoplankton's in this region.

Principal component analysis of the reflectance dataset resulted in three dominant principal components first component accounts for 84% of the total variance, while the second and third components account for 10.7% and 4% respectively. The interpretation of the components is amalgamated with a correlation analysis performed between the water quality parameters characterizing the wetland water and the amplitude of the components.
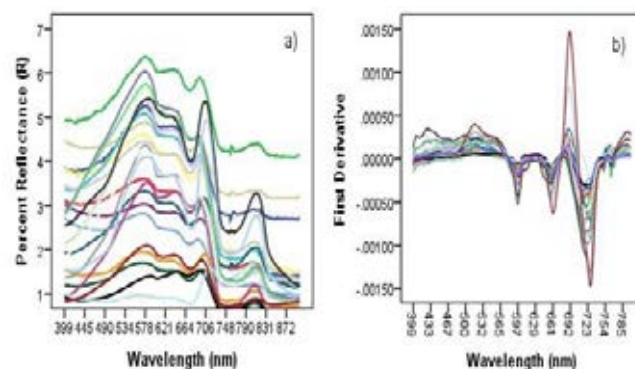
Fig 2 Reflectance Spectra of Bhindawas wetland-a) percentage reflectance b) first derivative spectra.

The regression models developed using step-wise linear regression for bio-optical parameters including Chlorophyll-a, TSS and turbidity were examined and evaluated based on the coefficient of determination (R^2), root mean square error (RMSE) and mean square error (MSE). The log-transformed data were used in this study for the development of models for Chl-a. In this study, the most suitable model for TSS is derived using combination of R_{755} and R_{758} explaining the highest variation in TSS concentration ($R^2 = 0.83$, RMSE = 62.63 mg/l). The best fitting model identified for Chl-a is derived using R'_{675} and R'_{743} with value of $R^2 = 0.80$ and RMSE = 0.12. The most suitable model for retrieval of turbidity in this research is derived using a combination of R_{596}, R_{599} and R_{615} with a $R^2 = 0.55$ and RMSE = 5.34 NTU.

Reflectance spectra of Macrophytes
Analysis of reflectance spectra indicates that macrophyte species exhibit typical vegetation spectra with distinct red and near infra-red boundary. The variation observed in the reflectance spectra of different macrophytes can be attributed to species-specific factors such as canopy structure, water content, chlorophyll concentration, plant vigor and leaf orientation (Pu. 2008)[12]. In addition to these factors, Artigas (2003)[13] suggested that the spectral response of macrophyte species is a function of the phenological stage, season and light conditions categorized as environmental factors.
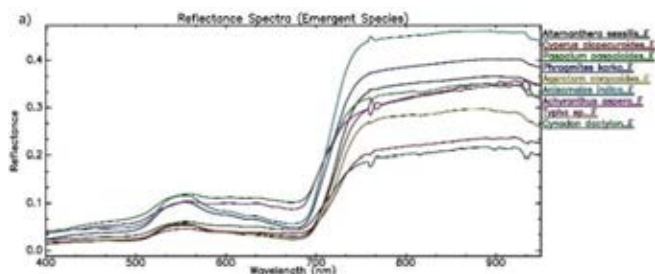
Fig 3 Reflectance spectra of wetland macrophytes.

The first derivative spectra of different macrophytic were found to have similar features with maxima and minima occurring at almost similar wavelengths with variable magnitude. First derivative spectrum is characterized by two prominent peaks indicating an increase in spectral values at 520 and 700 nm. The peak at 520 nm indicates chlorophyll reflectance whereas the peak at 720 nm designates the red-edge phenomenon.

The magnitude and position of the red-edge peak was derived for each of the macrophyte species. *Ageratum conyzoides* had the highest red-edge maximum at 722.32 nm with a value of 0.00879 while *Cynodon dactylon* was lowest (0.00274) at 698.84 nm. Second derivative spectra show a pronounced absorption feature in the red region (685-695 nm wavebands) whereas the NIR region has a distinct reflectance feature in the 720-740 nm region for different macrophytes.
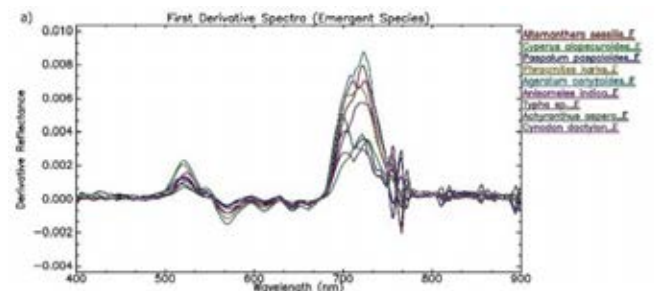
Fig 4 First derivative spectra of wetland macrophytes.
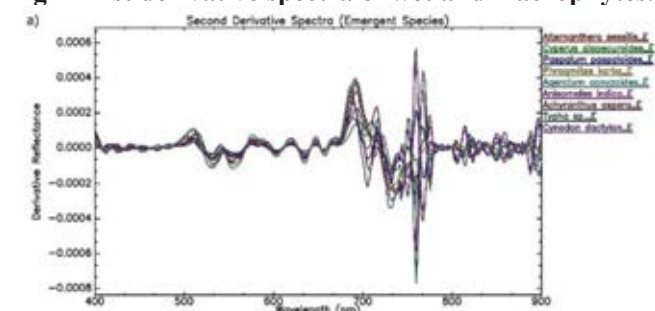
Fig 5 Second derivative spectra of wetland macrophytes

The maximum absorption and reflectance features have values within a narrow range i.e. +0.0006 to -0.0008. The steepest slope was observed for *Ageratum conyzoides* whereas lowest values were seen for *Cyperus alopecuroides*. Despite the similarity, differences can be observed in terms of absorption depth and absolute reflectance. Spectral characteristics of each of the species vary according to their phenological stages [13].

4. CONCLUSIONS

The availability of retrieval algorithms for water constituents based on spectral signatures measured by satellite sensors and aerial platforms is the essence for remote sensing of water quality over large spatial areas. Several retrieval algorithms have been identified in the study to retrieve the concentrations of bio-optical properties in the wetland water. This clearly indicates that hyperspectral sensor can be a reliable tool for monitoring water quality in terms of its bio-optical properties. Present study has brought out vividly the utility of in-situ hyperspectral data in wetland condition assessment. Further research is required to be carried out using orbital hyperspectral data for wetland health and integrity assessment.

REFERENCES

1. Ustin, S. L., Roberts, D. A. R. A., Gamon, J. A., & Green, R. O. (2004). Using Imaging Spectroscopy to Study Ecosystem Processes and Properties. *BioScience*, *54*(6), 523–534.
2. Schmidt, K. S., & Skidmore, A. K. (2003). Spectral discrimination of vegetation types in a coastal wetland. Remote Sensing of Environment, 85(1), 92–108.
3. Thiemann, S., & Kaufmann, H. (2002). Lake water quality monitoring using hyperspectral airborne data - A semiempirical multisensor and multitemporal approach for the Mecklenburg Lake District, Germany. *Remote Sensing of Environment*, *81*(2–3), 228–237.
4. Froidefond, J., Gardel, L., Guiral, D., & Parra, M. (2002). Spectral remote sensing reflectances of coastal waters in French Guiana under the Amazon influence Spectral remote sensing reflectances of coastal waters in French Guiana under the Amazon influence. *Remote Sensing of Environment*, *80*, 225–232.
5. Stumpf, R. P. (2001). Applications of Satellite Ocean Color Sensors for Monitoring and Predicting Harmful Algal Blooms. *Human and Ecological Risk Assessment: An International Journal*, *7*(5), 1363–1368.
6. Tilley, D. R., Ahmed, M., Son, J. H., & Badrinarayanan, H. (2003). Hyperspectral reflectance of emergent macrophytes as an indicator of water column ammonia in an oligohaline, subtropical marsh. *Ecological Engineering*, *21*(2–3), 153–163.
7. Gitelson, A. A., Schalles, J. F., & Hladik, C. M. (2007). Remote chlorophyll-a retrieval in turbid, productive estuaries: Chesapeake Bay case study. *Remote Sensing of Environment*, *109*(4), 464–472.
8. Everitt, J. H., Yang, C., Summy, K. R., Glomski, L. M., & Owens, C. S. (2011). Evaluation of hyperspectral reflectance data for discriminating six aquatic weeds. *Journal of Aquatic Plant Management*, (49), 94–100.
9. APHA. (2005). Standard methods for the examination of water and wastewater. *American Public Health Association (APHA): Washington, DC, USA*, 1–2671.
10. Tsai, F., & Philpot, W. D. (2002). A derivative-aided hyperspectral image analysis system for land-cover classification. *Ieee Transactions on Geoscience and Remote Sensing*, *40*(2), 416–425.
11. Gitelson, A. (1992). The peak near 700 nm on radiance spectra of algae and water: relationships of its magnitude and position with chlorophyll concentration. *International Journal of Remote Sensing*, *13*(17), 3367–3373.
12. Pu, R. (2008). An Exploratory Analysis of in Situ Hyperspectral Data for Broadleaf Species Recognition. *The International Archives of Photogrammetry, Remote Sensing and Spatial Infromation Sciences. Vol. XXXVII Part B7*, 255–260.
13. Artigas, F. J., & Yang, J. (2006). Spectral discrimination of marsh vegetation types in the New Jersey Meadowlands, USA., *26*(1), 271–277.

O6-13

湖沼データの整備，提供及び活用

沼田 佳典[1]，根本 正美[1]，稲澤 保行[1]，四野宮 良周[1]，林 諒祐[1]

[1]国土交通省国土地理院応用地理部地理調査課

キーワード：湖沼データ，数値データ，湖沼画像データ

抄録

　国土交通省国土地理院では，平成 29 年（2017 年）3 月 1 日に国土地理院ウェブサイトから湖沼データの無償ダウンロード提供を開始しました．湖沼データは湖底地形，底質，水生植物の分布などに関する数値データ及び数値データを元に作成した地図形式の湖沼画像データから構成されています．湖沼データを活用することにより，湖沼を詳細で定量的，視覚的あるいは立体的に把握でき，湖沼に対する各種取り組みに対して有用に活用できるものと期待できます．

1．はじめに

　国土交通省国土地理院は，湖沼の利用，開発，保全の各種計画の策定等，様々な業務の基礎資料として活用されることを目的に，昭和 30 年（1955 年）から湖沼調査を実施し，その成果は紙地図の「湖沼図」として取り纏めてきました．現在，湖沼図に代わる数値データとして湖沼データの整備・提供を進めています．数値データ化することで多様な表現が可能となり，湖沼を詳細かつ定量的，視覚的または立体的に監視，把握，解析できるようになりました．

2．方法

　全国の概ね 1km² 以上の 79 湖沼を対象に，以下の湖沼調査を実施してきました．（図1及び表1）

①湖底地形調査：測量船に搭載した音響測深機で水深を測定します．船の位置情報は GNSS 衛星により求められます．この際，水中音速度計測や水位観測の結果を使って水深データを補正します．

②底質調査：湖底の表層物質を採取して粒度分析により分類し，底質の分布を調査します．

③水生植物調査：空中写真判読や現地調査により，水生植物の分布状況を調査します．

　これらの調査結果を以下の各データ形式で取りまとめたものが湖沼データです．①～④は「数値データ」，⑤の「湖沼画像データ」と区分しています．

①GML 形式：湖底地形（水深点，等深線，水深グリッド，湖岸線），底質，水生植物等の各データを地理情報標準（JPGIS2014）準拠で作成しています．

②シェープファイル形式：GML 形式のものをシェープファイル化したものです．

③TIFF 形式：水深グリッドを TIFF 形式にしたもので，厳密には位置情報を持った GeoTIFF 形式です．

④CSV 形式：水深グリッドを X，Y，Z 形式かつ CSV 形式にしたデータで，グリッド間隔は 10m です．

⑤PDF：地図形式の画像データで PDF 形式です．湖沼部を段彩表示するとともに，湖沼周辺部は最新の電子地形図（タイル）を使用しています．多色表示かつ縮尺 1 万分 1 です．また，1 枚の用紙で湖沼全域を表示したより小縮尺のものも作成しています．

図 1　湖沼調査を実施した湖沼

表1 湖沼データの提供開始日等（平成30年4月現在）

	湖沼の名称	都道府県	面積(km2)	提供開始日		湖沼の名称	都道府県	面積(km2)	提供開始日
1	クッチャロ湖（大沼）	北海道	13.40	（未提供）	42	桧原湖	福島	10.70	（未提供）
2	クッチャロ湖（小沼）	北海道	0.00	（未提供）	43	小野川湖	福島	1.72	（未提供）
3	ポロ沼	北海道	1.97	（未提供）	44	秋元湖	福島	3.62	（未提供）
4	ペンケ沼	北海道	1.27	平成29年9月1日	45	北浦	茨城	35.04	平成30年3月30日
5	パンケ沼	北海道	3.55	平成29年9月1日	46	外浪逆浦	茨城・千葉	5.93	平成30年3月30日
6	サロマ湖	北海道	151.59	（未提供）	47	霞ヶ浦	茨城	168.22	平成30年3月30日
7	能取湖	北海道	58.20	（未提供）	48	牛久沼	茨城	3.55	（未提供）
8	網走湖	北海道	32.28	平成29年3月1日	49	中禅寺湖	栃木	11.90	（未提供）
9	コムケ湖	北海道	4.84	（未提供）	50	西印旛沼	千葉	9.43	（未提供）
10	濤沸湖	北海道	8.19	（未提供）	51	北印旛沼			（未提供）
11	藻琴湖	北海道	0.98	（未提供）	52	芦ノ湖	神奈川	7.03	（未提供）
12	風蓮湖	北海道	59.01	（未提供）	53	河北潟	石川	4.20	（未提供）
13	温根沼	北海道	5.72	平成29年9月1日	54	柴山潟	石川	1.92	平成29年9月1日
14	屈斜路湖	北海道	79.54	（未提供）	55	木場潟	石川	1.13	平成29年9月1日
15	厚岸湖	北海道	32.31	（未提供）	56	北潟湖	石川・福井	2.16	平成29年9月1日
16	摩周湖	北海道	19.22	（未提供）	57	水月湖	福井	4.18	（未提供）
17	阿寒湖	北海道	13.25	（未提供）	58	三方湖	福井	3.58	（未提供）
18	塘路湖	北海道	6.27	（未提供）	59	久々子湖	福井	1.40	（未提供）
19	達古武湖	北海道	1.31	（未提供）	60	日向湖	福井	0.93	（未提供）
20	シラルトロ沼	北海道	1.72	平成29年9月1日	61	菅湖	福井	0.91	（未提供）
21	火散布沼	北海道	3.76	平成29年9月1日	62	山中湖	山梨	6.57	（未提供）
22	然別湖	北海道	3.59	平成29年9月1日	63	河口湖	山梨	5.48	（未提供）
23	支笏湖	北海道	78.48	（未提供）	64	本栖湖	山梨	4.70	（未提供）
24	洞爺湖	北海道	70.72	（未提供）	65	西湖	山梨	2.10	平成29年3月1日
25	倶多楽湖	北海道	4.70	（未提供）	66	精進湖	山梨	0.51	平成29年3月1日
26	ウトナイ湖	北海道	2.10	平成29年9月1日	67	諏訪湖	長野	12.81	（未提供）
27	大沼	北海道	5.31	（未提供）	68	野尻湖	長野	4.45	平成29年9月1日
28	小沼	北海道	3.80	（未提供）	69	浜名湖	静岡	64.91	（未提供）
29	内沼	青森	62.12	平成30年2月28日	70	猪鼻湖	静岡	5.36	（未提供）
30	小川原湖	青森		平成30年2月28日	71	琵琶湖	滋賀	669.23	（未提供）
31	姉沼	青森	1.57	平成30年2月28日	72	余呉湖	滋賀	1.75	（未提供）
32	十和田湖	青森・秋田	61.11	（未提供）	73	久美浜湾	京都	7.18	（未提供）
33	十三湖	青森	17.82	（未提供）	74	阿蘇海	京都	4.80	（未提供）
34	万石浦	宮城	7.30	平成30年2月28日	75	湖山池	鳥取	6.99	（未提供）
35	伊豆沼	宮城	3.31	平成29年9月1日	76	東郷池	鳥取	4.05	（未提供）
36	内沼	宮城	1.05	平成29年9月1日	77	中海	鳥取・島根	85.68	（未提供）
37	井土浦	宮城	0.40	（未提供）	78	宍道湖	島根	79.25	（未提供）
38	鳥の海	宮城	1.35	（未提供）	79	池田湖	鹿児島	10.91	（未提供）
39	八郎潟調整池	秋田	27.75	（未提供）	80	鰻池	鹿児島	1.20	（未提供）
40	田沢湖	秋田	25.75	（未提供）		計		2,235.33	
41	猪苗代湖	福島	103.24	（未提供）					

3. 結果

平成29年（2017）年3月1日から，以下に示す国土地理院のウェブサイトで湖沼データの無償ダウンロード提供を行っています．（図2，図3及び図5）

http://www.gsi.go.jp/kankyochiri/lakedata.html

図2 湖沼データのダウンロードサイト

平成30年（2018年）4月現在，湖沼調査を実施した全国の80湖沼中，22湖沼の湖沼データの提供を開始しました．霞ヶ浦は，北浦及び外浪逆浦とともに平成30年（2018年）3月30日に提供を開始しました．（図5）

ウェブ地図の「地理院地図」でも，「地理院タイル（湖沼データ）」として湖沼データを閲覧できます．（図4）

地理院地図は，各種地理情報を階層的に表示できる上，3D 表示も可能です．ただし， 地理院地図自身では湖沼データの3D表示が現在できないため，他のGISソフトウェアが必要です．

図3
数値データ
「小川原湖」

図4
地理院タイル
（湖沼データ）
「西湖」

4. 考察

　霞ヶ浦の湖沼データを使って地形的性質を見たところ，局所的に何カ所かの窪みが存在しますが，水深は概ね10m以下で全体的に浅く，最深部は11.5mでした．また，ヒストグラムで見ると，水深 4m〜6m の範囲が全体の55%を占めることが分かりました．（図5及び図6）

図5　湖沼画像データ「霞ヶ浦」

図6　霞ヶ浦の水深ヒストグラム

　湖沼データを使って湖底地形の断面図を作成することもできます．断面図は湖底の地形的特徴を詳細に把握するのに効果的な資料になります．（図7）

図7　図4の赤線位置の断面図
（縦方向と横方向の縮尺は異なる）

　湖沼の面積や湖岸線は容易に把握できますが，湖底地形の詳細な形状や深度分布の定量的把握は容易ではなく，湖沼データが有用であることが分かりました．
　等深線の GML や CSV のデータを使えば，湖底地形
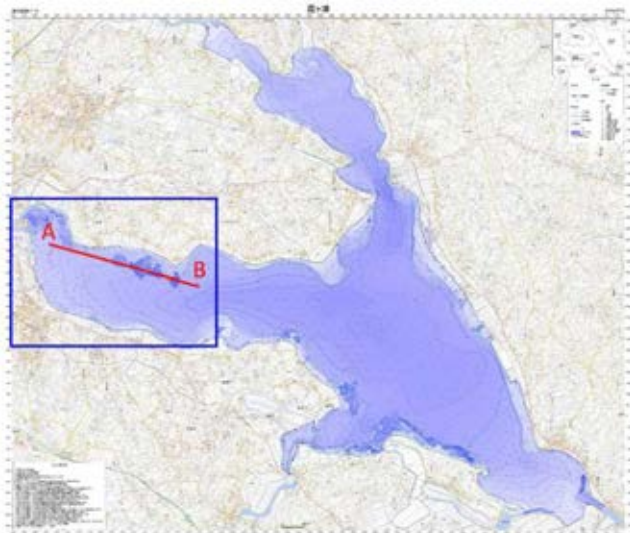
の傾斜分布，方位分布，谷線などの二次加工した地理情報も作成でき，流入土砂の流送や堆積などの各種シミュレーションに役立つと考えています．土浦市付近の霞ヶ浦の傾斜を見ると大部分が平坦ですが，凹地部分では最大 15°程度の傾斜がありました．（図8）
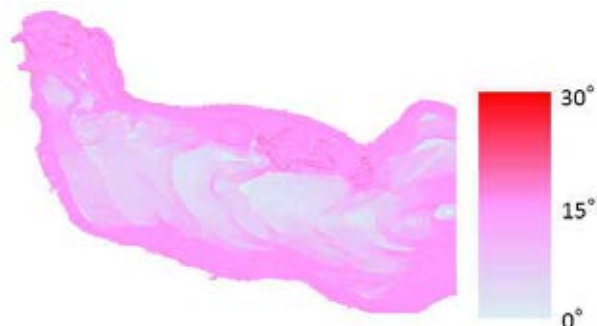
図8　図4の青線範囲の傾斜分布図

　更に，湖底地形データに別に整備された各種データを組み合わせれば水深との相関情報を得ることもでき，湖沼環境対策などで効果的であると考えられます．
　陸域の航空機や人工衛星から撮影した画像の 3D 表示には高い視覚性がありますが，湖沼データを活用すれば湖沼部の 3D 表示も可能になり，視覚的・立体的な把握に効果的であることが分かりました．なお，特殊なメガネをかけて見ると立体的に見られる地図による手法もあります．（図9）
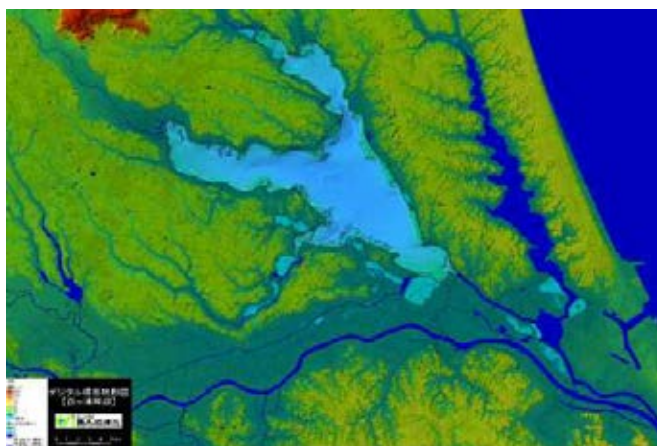
図9　霞ヶ浦周辺のデジタル標高地形図
（ChromaDepth3D メガネで立体的に見える）

5. 結論

　湖沼データを活用して湖沼の詳細かつ定量的，視覚的，立体的な把握が可能になりました．霞ヶ浦を初めとする全国の湖沼での各種取り組みに対し，湖沼データは有意義に貢献できるものです．関係機関における湖沼データの活用をよろしくお願いします．

O6-14

Long-Term Monitoring of Lake Surface Area Change in Indonesia from Global Surface Water Data

Rossi Hamzah[1,4], Bunkei Matsushita[2], and Takehiko Fukushima[3]

[1]Graduate School of Life and Environmental Sciences, University of Tsukuba, Tsukuba, Ibaraki, Japan,
[2]Faculty of Life and Environmental Sciences, University of Tsukuba, Tsukuba, Ibaraki, Japan,
[3]Kasumigaura Environmental Science Center, Tsuchiura, Ibaraki, Japan
[4]Indonesian National Institute of Aeronautics and Space, Jakarta, Indonesia

Keywords: Lake monitoring, Surface Area changes, Landsat, Google Earth Engine

ABSTRACT

Currently, the conditions of lakes in Indonesia have changed in terms of water surface area, especially for the main lake (larger than 10 km^2). A manual method to extract the water surface area for long-term monitoring requires time, is costly and requires a lot of resources. Nowadays, with the development of digital image processing, the manual method is no longer effective and efficient. In this study, Global Surface Water provided by Google Earth Engine combined with simple polygon masking was used to identify lakes larger than 10 km^2. Results from this study show that total water surface area has increased for inland water body in Indonesia from the year 1988 until 2015. Some because of new water body formed from the former mine sites. In the other hand, some lakes decreased their water surface area. Lake Limboto, in the north side of Sulawesi Island, decreased by 12.8 km^2 from 2001 until 2014. The objectives of this study are to obtain long-term monitoring water surface area for all main lakes so that it can be used to update lake information in Indonesia.

1. INTRODUCTION

Indonesia consists of 17,504 islands with 1,905 million km² land area. With this separated land and a wide area, effective and efficient ways to monitor all resources are needed. Accurate maps of surface water are essential for many environmental applications, such as lakes monitoring. The assessment of the role of lakes requires good estimates of the areal extent and shape of water bodies. Upscaling to large regions, except in limited areas where precise maps are available, so far depends on statistical estimates of the number and size of lakes [1].

Precise estimation of surface water using satellite imagery remains a challenging task due to the sensor limitations, complex land cover, topography, and atmospheric conditions [2]. There are many lakes in Indonesia, some are facing drought, water loss, and decreasing water surface area.

Calculation and monitoring temporal change for all lakes in Indonesia is very expensive if done manually. In the other hand, using remote sensing satellite data is time-consuming to identify the main lakes by manual digitation. Especially for a large number of lakes and small size water surface area. Join Research Center of European Commission already provide Global Water Surface [3] through Google Earth Engine data catalog. The problem is that the water body information is mixed for all types such as lake, reservoir, river and coastal object. Therefore the objectives of this study are: separation of all waterbody types (lake, reservoir, river and coastal object) from Global Surface Water data, calculate water surface area and count the number of all lakes larger than 10 km^2. In addition monitoring spatial and temporal change for all lakes in Indonesia.

2. METHOD

The research area of this study is Indonesia inland water surface. Global Water Surface was used as the main input to identify main lakes in Indonesia. This data was extracted and processed using Landsat TM, ETM and OLI from 1982 until 2015. There is much information provided by Global Water Surface, yearly water history which consists of permanent water and seasonal water.

High-resolution satellite data from Google Maps and Google Earth were used for validation of all the lakes identified. River and coastal object masking were built to separate from other water bodies. All processing was done by Python arcpy.

3. RESULTS

The permanent water surface was used as main data input in the processing to identify all lakes larger than 10 km^2. Years 1984 – 1987, 1992 - 1993 and1998 were not included in the processing because the water surface did not cover all inland Indonesia area. River and coastal object were separated from permanent water to reduce the waterbody types. Some river in Kalimantan island and Irian Jaya island have big water surface area. Many pond

and paddy fields are spread along north coast Java island.

Figure 1 shows processing results from water surface area after separating into waterbody types. Water surface with seasonal data is very dynamic, and in this data, it is also included seasonal water body for all types. If we see the differences with permanent water, the pattern is not so different. The differences occur very prominently after the separation of the river and coastal water bodies. Although small, the water surface area seems to increase significantly from 1988 until 2015.
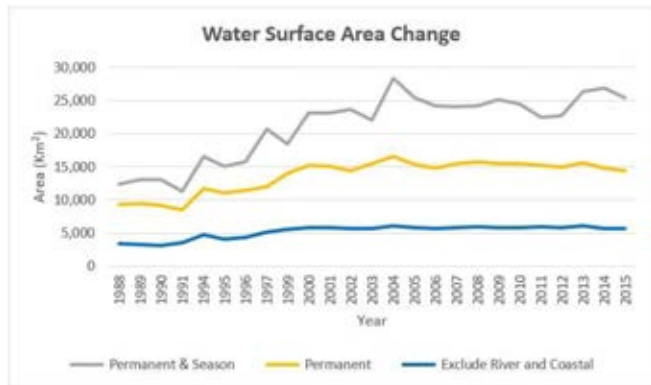
Fig. 1 Total water surface area change over years

48 lakes were found with an area larger than 10 km^2 (Table 1). Most of the lakes are on the Irian Jaya island. Compared to the number of lakes from [4] in [5], there is a difference in the number of lakes on the Sumatera, Kalimantan, Nusa Tenggara, and Mollucas Islands.

Table 1 Number of main lakes

Location/Island	Lake >10 km^2
Sumatera	9
Java and Bali	1
Kalimantan	8
Sulawesi	9
Nusa Tenggara (West and East)	2
Irian Jaya	16
Mollucas	3
Total	48

4. DISCUSSION

Even though the total water surface area is increasing, some lakes are decreasing their water surface area. One of the cases is happening in Lake Limboto, reduce by 12.8 km^2 from 2001 to 2014 (Table 2). This value was calculated from permanent water only. As shown in figure 2, seasonal water surface area changes dynamically, but still in the range between 20 – 45 km^2. Water surface area of Lake Limboto changes every two to four years decreasing and increasing. But with a small area, significantly reduce for each year. With this temporal change of surface area, we can monitor all changes happening for all main lake in

Indonesia.
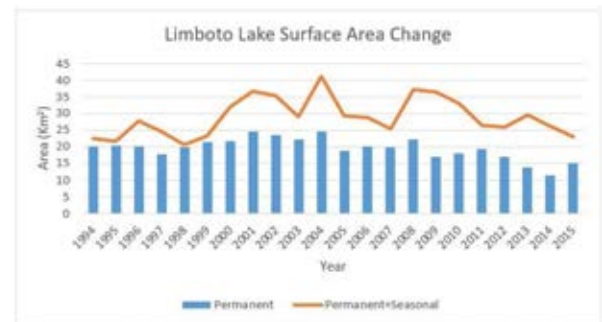
Fig. 2 Water surface area change of Limboto Lake

Table 2 Limboto Lake water surface area decrease

Year	Area (km^2)	Change (km^2)		
2001	24.44	-2.25		
2003	22.19	-2.12		
2006	20.07	-0.15		
2007	19.92	-1.9		-12.8
2010	18.02	-1.12		
2012	16.9	-3.31		
2013	13.59	-1.94		
2014	11.65			

5. CONCLUSION

Over the year 1988 until 2015, permanent water increased significantly even though in a small value. In the last year of this study, 2015, it was found 48 main lakes spread over Indonesian Islands. In the opposite side, some lakes face water loss and decreasing water surface area (e.g: Lake Limboto). Lake Limboto from 2001 until 2014 already lost 12.8 km^2 of its water surface area. New water surface formed from the former mine sites. These results are expected to be additional information to save all lakes decreasing its water surface area in Indonesia.

REFERENCES

[1] C. Verpoorter, T. Kutser, and L. Tranvik: Automated mapping of water bodies using Landsat multispectral data, Limnol. Oceanogr.: Methods, Vol. 10, pp. 1037–1050, 2012

[2] G. Donchyts, J. Schellekens, H. Winsemius, E. Eisemann, and N.C. van de Giesen: A 30 m Resolution Surface Water Mask Including Estimation of Positional and Thematic Differences Using Landsat 8, SRTM and OpenStreetMap : A Case Study in the Murray-Darling Basin, Australia, Remote Sensing, Vol. 8(5), pp. 1-22, 2016.

[3] J. F. Pekel, A. Cottam, N. Gorelick, and A. S. Belward: High-resolution mapping of global surface water and its long-term changes, Nature, Vol. 540, pp. 418-422, 2016.

[4] T. Uchida: Study on the Characteristics of inland Water Body in Indonesia. Investigation for Realitical Technology of Tropical Area, Research and Development Center for Limnology-

LIPI in the Cooperation with Japan International Cooperation Agency, pp. 56, 1997.

[5]   Sulastri: Inland water resources and limnology in Indonesia, Tropics, Vol. 15 (3), pp. 285-295, 2006.

O6-15

帰還困難区域に生息する渓流魚の放射性セシウムのモニタリングと標識放流実験による渓流魚の ^{137}Cs 蓄積速度の推定

樽井 美香[1], 中里 亮治[1], 鈴木 貴大[1, 2], 川上 拓磨, Park Soeun[1], 櫛井 優志[1],

苅部 甚一[1, 3], 鈴木 仁根[4], 加藤 健一[4], 竹高 慎祐[1], 桑原 祐史[1]

[1]茨城大学 広域水圏センター, [2]東京建設コンサルタント, [3]近畿大学, [4]室原川・高瀬川漁協

キーワード：ヤマメ, イワナ, 森林小河川, ^{137}Cs のモニタリング, 標識放流実験

抄録

帰還困難区域の空間線量率の異なる 4 地点の森林河川で, 渓流魚のヤマメとイワナの ^{137}Cs 濃度をモニタリングした。また, ヤマメとイワナの標識放流実験により, 2 魚種の ^{137}Cs 蓄積速度を調べた。その結果, ヤマメとイワナに含まれる ^{137}Cs 濃度は, 2 魚種ともに環境中の放射能強度が高い地点ほど有意に高かった。空間線量率の最も高い地点 D で採捕した 2 魚種の ^{137}Cs 濃度は, 2016 年〜2017 年度の 2 年間で, ヤマメとイワナでそれぞれ 855-27,738 Bq/kg と 651-18,865 Bq/kg の範囲にあった。いずれの地点・魚種ともに ^{137}Cs 濃度の明瞭な減少傾向は認められず, 福島第一原発事故から約 7 年が経過した現在では 2 魚種の ^{137}Cs 濃度は平衡状態に達していると推測された。

　2016 年に実施した標識放流実験の結果, ヤマメの ^{137}Cs 蓄積速度は, 線量の最も低い地点 A と最も高い地点 D でそれぞれ 2.5 Bq/kg/day と 24.9 Bk/kg/day であり(実験期間 150 日), 空間線量率の高い地点 D において有意に速かった。またイワナの蓄積速度はヤマメよりも有意に遅かった。

1. はじめに

　2011 年 3 月の東京電力福島第一原子力発電所事故により, 環境中へ多量の放射性物質が放出された。事故から約 7 年が経過した現在でも, 避難指示区域内およびその近傍の河川に生息するほぼすべての内水面魚種について採捕・出荷の制限・自粛がなされている。避難指示解除後の地域の再活性化と内水面漁業の復興のカギの一つとして, ヤマメやイワナに代表される森林小河川での渓流釣りや, より下流側でのアユ釣りなどのいわゆる遊漁活動の復活があげられており, 地元の漁業組合関係者, 地域行政関係者や住民の方々も強く熱望している。しかしながら, 避難指示地域において遊漁対象となる魚類については, 生息地環境を含めたそれらの放射性セシウム濃度の現状が十分調べられておらず, 異なる空間線量環境下における魚への放射性セシウム蓄積速度の差異やそれをもたらす理由などが未解明である。さらに, 今後の放射性セシウムの推移や収束時期の予測等など多くの課題についても手つかずのままである。被災地での遊漁活動を復興・復活させるためには

上記のことを十分に理解・把握しながら, 適切な方策を立案することが重要と思われる。

　そこで私ども茨城大学広域水圏センターの陸水生物研究グループでは, 地元の漁業組合と共同で 2015 年 3 月から 2018 年の現在まで, 福島県の避難指示区域内(帰還困難区域)にある空間線量率の異なる複数の森林河川を研究フィールドとして以下に述べる 2 つの研究を実施している。

①魚を含めた生物群集と生息環境中の放射性セシウム濃度の現状を把握することを目的とした, 遊漁対象魚種のヤマメとイワナ, 大型無脊椎動物および河川環境試料の放射性セシウム濃度のモニタリング。また渓流魚の主要な餌資源を明らかにするための, 捕獲した魚類の胃内容物分析。

②異なる空間線量環境下における魚への放射性セシウム蓄積速度の差異の有無を明らかにするための「標識放流実験」。この実験は放射性セシウムを含まない養殖イワナ・ヤマメを異なる空間線量をもつ河川に放流し, 定期的に再捕獲することで放射性セシ

ウムの蓄積速度（見かけの増加量）を評価するものである。

　今回の発表では，2015 年から現在まで実施している帰還困難区域の森林河川に生息する代表的な渓流魚であるヤマメとイワナの ^{137}Cs 濃度のモニタリング結果を報告し，さらに異なる空間線量環境下での当該魚種への ^{137}Cs の蓄積速度を評価するための標識放流実験を実施した結果について報告する。

2.　方法
渓流魚および河川環境試料の放射性セシウム濃度のモニタリング

　避難指示区域内にある山地渓流の 4 地点（地点 A, B, C, D）において定期的に空間線量率の測定と試料採取を行った。河川環境試料として河川近傍の山土（表層約 50 mm），河床堆積物（川砂），水底落葉および河川水を採取した。渓流魚のヤマメとイワナはミミズやブドウ虫を餌とした釣りによって採捕し，冷蔵して研究室に持ち帰った。測定の前処理として，魚類試料についてはホールボディーの放射性セシウム分析後に可食部のみを U8 容器に充填した。河川水は，カートリッジ型フィルタ装置 [1], [2], [3] によってろ過・濃縮を行った。処理後の河川環境試料および魚類は，Ge 半導体検出器（CANBERRA 社製）を用いて放射性セシウム濃度を測定した。これらの調査は地点 A，B，C では 2015 年 3〜5 月から，地点 D では 2016 年 3 月から実施した。

渓流魚の標識放流実験

　標識放流実験は，4 定点の中では空間線量率の最も低い地点 A と最も高い地点 D の 2 か所を実験フィールドとして，2016 年 5 月と 2017 年 5 月に実施した。また晩秋から厳冬期にかけての水温の低い時期における ^{137}Cs の蓄積速度を調べるために，2017 年 10 月に地点 D でのみ放流実験をした。各実験ともに魚類・甲殻類用麻酔剤 FA100 で麻酔後にイラストマー蛍光タグ（NMT 社製）で標識した養殖イワナとヤマメを各地点に 100〜200 尾程度放流した。ちなみに，これらの養殖魚には ^{137}Cs がほとんど含まれていない（5 Bq/kg 以下）。これらの魚は釣りによって定期的に再捕獲した。採捕した魚は速やかに冷蔵保温して実験

室に持ち帰り，Ge 半導体検出器による放射性セシウム分析を行うまで冷凍保存した。

　また 2018 年 5 月中旬には地点 D において個体識別が可能な VI タグ（NMT 社製）を用いた放流実験を実施する予定であり，これにより個体ごとの ^{137}Cs 蓄積速度や成長速度のモニタリングが可能となる。

3.　結果と考察
避難指示区域内の森林河川に生息する渓流魚の ^{137}Cs 濃度の推移

　2017 年 3 月〜12 月の各地点の空間線量率の平均値は地点 A，B，C，D でそれぞれ約 0.4，1.2，2.4，3.1 μSv/h であり，空間線量率の強度は地点 D＞地点 C＞地点 B＞地点 A の順に高かった。各種環境試料も同様の傾向であり，地点間での環境試料の放射性セシウム濃度の強度の違いが各地点での空間線量率の差に影響しているものと考えられた。2015 年〜2017 年度までの山土，水底落葉，川砂，河川水中の溶存 ^{137}Cs 濃度の推移をみると明瞭な減少は見られなかった。

　ヤマメとイワナに含まれる ^{137}Cs 濃度は，2 魚種ともに環境中の放射能強度が高い河川ほど有意に高かった（K-W test，p<0.01；地点 D＞地点 C＞地点 B＞地点 A，Steel-Dwass，p<0.01）。空間線量率のもっとも低い地点 A で採捕した 2 魚種の ^{137}Cs 濃度は 2015 年〜2017 年度までの 3 年間でヤマメおよびイワナでそれぞれ 102-3,829 Bq/kg と 73-2,260 Bq/kg の範囲にあった。また 3 年間に採捕されたヤマメ・イワナの平均値はそれぞれ 581 Bq/kg と 485 Bq/kg であり，魚種による ^{137}Cs 濃度の統計的な有意差はなかった。

　空間線量率の最も高い地点 D で採捕した 2 魚種の ^{137}Cs 濃度はヤマメとイワナで 855-27,738 Bq/kg と 651-18,865 Bq/kg の範囲にあり，2016 年〜2017 年度までの 2 年間に採捕された各魚種の平均値はそれぞれ 5,137Bq/kg と 4,083 Bq/kg であった。魚種による ^{137}Cs 濃度の平均値に統計的な有意差は見られなかった。本研究での調査期間内で，いずれの地点・魚種ともに ^{137}Cs 濃度の明瞭な減少傾向は認められず，福島第一原発事故から約 7 年が経過した現在では 2 魚種の Cs 濃度はほぼ平衡状態に達しているものと推測された。

標識放流実験によるヤマメとイワナの 137Cs 蓄積速度

の推定

2016 年 5 月の放流実験の結果を図 1 と図 2 に示した。いずれの魚種とも放流後の経過日数が多い個体ほど ^{137}Cs 濃度が高かった。個体によってその濃度には差異が見られたものの，放流後から 150 日まではほぼ直線的に濃度が増加した。その直線の傾きから計算した一日当たりの見かけ上のヤマメの ^{137}Cs 蓄積速度は，地点 A と地点 D でそれぞれ 2.5 Bq/kg/day と 24.9 Bk/kg/day であり，空間線量率の高い地点 D において有意に速かった。
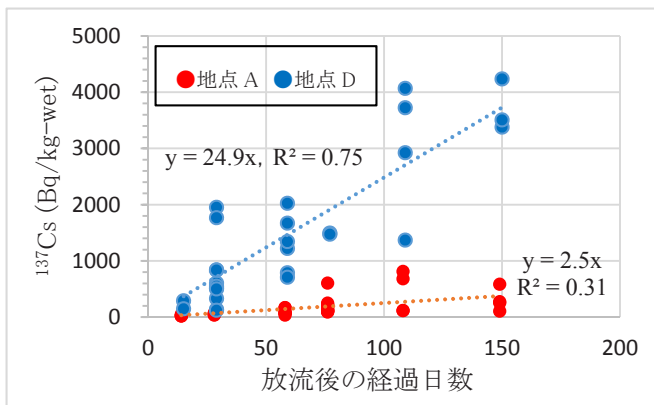
図1　2016 年 5 月に地点 A と D に放流した"ヤマメ"の
**　　　^{137}Cs濃度の推移.**
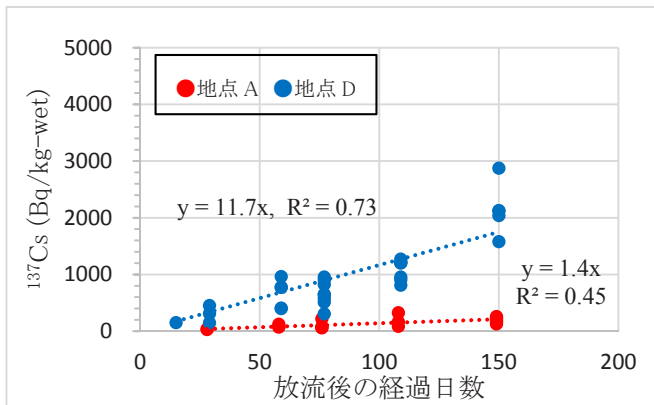
図2　2016 年 5 月に地点 A と D に放流した"イワナ"の
**　　　^{137}Cs濃度の推移.**

一方，イワナの場合は，ヤマメと同様に空間線量率の高い地点 D においてその蓄積速度は速かったが，見かけ上の蓄積速度はヤマメと比較して有意に低く，地点 A と地点 D でそれぞれ 1.4 Bq/kg/day と 11.7 Bq/kg/day であった。このように ^{137}Cs 蓄積速度が魚種間で異なったことは非常に興味深いが，現在のところ，この理由については不明であり，今後の検討課題としたい。

2017 年 5 月の放流実験も 2016 年とほぼ同様の結果となった。また 2017 年 10 月に地点 D で実施した放流実験での 1 日あたりの ^{137}Cs 蓄積速度は，5 月の値とは大きく異なり，ヤマメ・イワナともに約 2.8 Bq/kg/day と極めて低かった（表 1）。この理由は実験の期間である 2017 年 10 月末から翌年 3 月までの低い水温（0.5～11.5℃）により魚の活性が低下したため，利用可能な餌資源や水経由での 137Cs の取り込み量が低下したためと推測された。ちなみに地点 D における 2017 年 5 月下旬～10 月上旬までの 133 日間における水温は 12.3～17.6℃の範囲であった。

表1　地点 D における 1 日あたりの ^{137}Cs 蓄積速度(Bq/kg/day)

放流した時期	放流期間	ヤマメ	イワナ
2016 年 5 月中旬	150 日	24.9	11.7
2017 年 5 月下旬	133 日	26.0	17.8
2017 年 10 月下旬	147 日	2.9	2.8

4.　結論

2015 年から 3 年にわたる帰還困難区域でのモニタリング結果から，震災後 7 年が経過した現在でも渓流魚に含まれる ^{137}Cs 濃度は収束することはなく，高いレベルで平衡状態に達していると考えられた。また放流実験から空間線量の高低や魚種による ^{137}Cs の蓄積速度にも差があることが明らかとなり，これらの成果が遊漁活動の再開方法を模索する上での何らかのヒントになるかもしれない。

本発表では，VI タグでの個体識別をした放流実験の結果についても合わせて報告する予定である。

引用文献

[1]　T. Yasutaka, Tsuji, H., Kondo, Y., and Suzuki, Y. "Developemnt of Rapid Monitoring for Dissolved Radioactive Cesium with a Cartridge Type of Prussian blue-impregnated Nonwoven Fabric". BUNSEKI KAGAKU 62, 499-506, 2013.

[2]　H. Tsuji, Kondo, Y., Suzuki, Y., and Yasutaka, T. "Development of a method for rapid and simultaneous monitoring of particulate and dissolved radiocesium in water with nonwoven fabric cartridge filters". Journal of Radioanalytical and Nuclear Chemistry 299, 139-147, 2014.

[3]　T. Yasutaka, Kondo, Y., Suzuki, Y., Takahashi. A., and Kawamoto,T. "Rapid quantification of radiocesium dissolved in water by using nonwoven fabric cartridge filters impregnated with potassium zinc ferrocyanide". Journal of Nuclear Science and Technology 50, 792-800, 2015.

O6-16

Evaluation of anthropogenic impacts on reservoir water quality: A case study in a reservoir catchment in southern Taiwan

Wan-Ru Chen[1], Chia-Chen Chung[1], Chun-Ying Chao[1], Wen-Yi Wei[2], Wen-Chieh Huang[2]

[1]Department of Environmental Engineering, National Cheng Kung University, Taiwan, [2]Environmental Protection Administration Executive Yuan, Taiwan

Keywords: reservoir catchment, human activity, BPA, pesticide, OTC, water quality

ABSTRACT

Recently, the need for high quality finished water has brought the land-use management around reservoir catchment area to the public attention. Human activities would damage the source water quality by different levels based on the types of activities. The objective of this study is to evaluate the impacts of anthropogenic sources on water quality around the reservoir catchment area by monitoring the occurrence of selected contaminants, including four pesticides (glyphosate, glufosinate, fenthion and thiophanate-methyl), one antibiotics (oxytetracycline) and one endocrine disrupting substance (bisphenol A) to reflect the pollution from agricultural run-off, aquaculture wastes and domestic sewage, respectively. Basic water quality parameters were also acquired to examine the relation between water qualities and the occurrence of trace organic pollutants. Samples were collected every month from March to July in 2017 near a reservoir located in southern Taiwan. Results showed bisphenol A exists ubiquitously and glyphosate concentration varies along with farmer's behavior. Glyphosate concentration was positively correlated to ammonia nitrogen and total phosphorus and inversely correlated to dissolved oxygen. As for oxytetracycline, its polluted area was not as wide as bisphenol A and glyphosate, indicating the aquaculture activities was limited in the area. Overall, this study revealed that the occurrence of selected contaminants can be surrogates to indicate human pollution. This approach can be applied to other reservoir. The results from this study can provide the government better land use managements in catchment area.

1. INTRODUCTION

In recent years, considerable attention of land-use management around reservoir catchment areas have been raised because of the need of high quality finished water. If no restriction is enforced around the reservoir catchment areas, pollution derived from anthropogenic activities may lead to drinking water source contamination.

This research aims to evaluate the anthropogenic impacts on a reservoir catchment by monitoring the occurrence of selected trace organic compounds including four pesticides, one antibiotics and one endocrine disrupting substance which serve as surrogates to reflect the pollution from agricultural run-off, aquaculture wastes and domestic sewage, respectively. Four pesticides include glyphosate, glufosinate, fenthion and thiophanate-methyl which are applied popularly in the field for decades due to their short half-life in the environment (Table 1). The selected endocrine disrupting substance is bisphenol A (BPA) which commonly exists in plastic products. The selected antibiotics is oxytetracycline (OTC) which is widely applied in animal feeds to control bacterial infection. Water quality including pH, dissolved oxygen (DO), ammonia-nitrogen (NH_3-N) and total phosphorus (TP) was monitored to examine any relation between water

Fig. 1 Study area and sampling sites

quality and the trace organic pollutants. Study area is located at Yanchao District, Kaohsiung in southern Taiwan (Fig. 1), which is Agongdian reservoir serving water for about 127,000 population. The results from this study can be provided for the government to develop proper policies to regulate the land use of water source protection area.

2. METHOD

Liquid chromatography equipped with a C18 (Acclaim 120 series, 3μm, 4.6×150 mm) was used to carry out the separation. Fluorescence detector was used to quantify BPA and triple quadrupole tandem mass spectrometry was for pesticides and OTC.

32% of Agongdian reservoir catchment area is orchards and minor area is used for aquaculture. Only 10% is occupied by household. There are 10 sampling sites, 7 sites along Wanglai Creek and 3 sites along Zhuoshui Creek. Samples were taken once a month, from March to July in 2017, four times in total, and 40 samples in total.

3. RESULTS AND DISCUSSIONS

Occurrence of pesticides

Glyphosate has been widely used as non-selective herbicides since 1970s, so it has been frequently detected in 50% of the surface water samples [4-5]. Similar occurrence ratio (50%) was acquired in this study (Table 1). It was also found that the occurrence of glyphosate was higher in summer season (May and July) with detection frequency up to 80% and lower in March (16.7%) and April (25%). As for glufosinate and thiophanate-methyl, they were detected from April to July, with increasing concentration when the weather became warmer. The above correlation could be attributed to chemical weed and pest control strategy in summer, so the occurrence of agrochemicals in surface water is strong correlated to farmer behavior. W6 located at the intensive agricultural area where glyphosate concentration was positively correlated to NH_3-N and TP and adversely correlated to DO (Fig. 2). W3, W4, W5 and Z3 also showed similar correlation inferring that agriculture activities resulted in the residue of pesticides and bad water quality.

Occurrence of OTC

The detection frequency of OTC was 22.5% with maximum concentration 1.9 µg/L (Table 1). Only four sampling sites (W1, W3, W5 and W6) were found with OTC. It was previously reported OTC appeared in rivers with high nitrogen and phosphorus when aquacultural land use predominated [7]. However, the correlation was not observed in this study due to insignificant aquaculture activity in Agongdian reservoir catchment area.

Occurrence of BPA

BPA was detected in 55% of 40 samples with maximal concentration 0.41 µg/L (Table 1). Sub-ppb level of BPA was found nearly in all sampling sites. Lee et al. (2013)

Table 1 Half life and monitoring results (Unit: µg/L)

Compound	Half-life (day)	Conc. range	Detection [a]	MDL [b]
Glyphosate	>35 [1]	ND[c]-4.53	20/40	0.12
Glufosinate	-	ND-1.23	11/40	0.12
Fenthion	4.6 [2]	ND	0/40	16.62
Thiophanate-methyl	-	ND-0.12	5/40	0.01
OTC	2.7-6.5 [3]	ND-1.90	9/40	0.25
BPA	2.5-4 [6]	ND-0.41	22/40	0.01

[a]: Detected samples/all samples. [b]: Method detection limit. [c]: Lower than MDL marked as ND. -: not available.
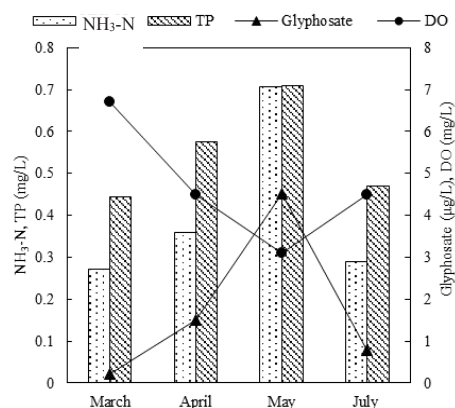
Fig. 2 The relations between water quality and glyphosate
(W6 sampling site)

indicated that BPA had negative correlation between DO and pH, but had positive correlation with NH_3-N in rivers [8]. However, those relations were not observed because of less industrial pollution and population in the studied area.

4. CONCLUSION

Results showed BPA existed everywhere and glyphosate concentration varied along with farmer's behavior. The relation between water quality and glyphosate might result from the domination of agriculture activities. As for OTC, its polluted area was not as wide as BPA and glyphosate, indicating the aquaculture activities was limited in the study area. Overall, this study revealed the occurrence of selected contaminants can be used as surrogates to reflect human pollution. This approach can be applied to other reservoir catchments. The results from this study can be provided to the government for better land use managements in the catchment area.

5. REFERENCE

[1] Kollman, W.; Segawa, R., Interim report of the pesticide chemistry database. *Environmental hazards Assessment Program*, 1995.
[2] Lacorte, S.; Lartiges, S. B.; Garrigues, P.; Barcelo, D., Degradation of Organophosphorus Pesticides and Their Transformation Products in Estuarine Waters. *Environmental Science & Technology*, *29* (2), 431-438, 1995.
[3] Xuan, R.; Arisi, L.; Wang, Q.; Yates, S. R.; Biswas, K. C., Hydrolysis and photolysis of oxytetracycline in aqueous solution. *Journal of Environmental Science and Health, Part B*, *45* (1), 73-81, 2009.
[4] Hanke, I.; Singer, H.; Hollender, J., Ultratrace-level determination of glyphosate, aminomethylphosphonic acid and glufosinate in natural waters by solid-phase extraction followed by liquid chromatography–tandem mass spectrometry: performance tuning of derivatization, enrichment and detection. *Analytical and Bioanalytical Chemistry*, *391* (6), 2265-2276, 2008.
[5] Skark, C.; Zullei-seibert, N.; Schöttler, U.; Schlett, C., The Occurrence of Glyphosate in Surface Water. *International Journal of Environmental Analytical Chemistry*, *70* (1-4), 93-104, 1998.
[6] Staples, C. A.; Dome, P. B.; Klecka, G. M.; Oblock, S. T.; Harris, L. R., A review of the environmental fate, effects, and exposures of bisphenol A. *Chemosphere*, *36* (10), 2149-2173, 1998.
[7] Yang, S.; Carlson, K., Evolution of antibiotic occurrence in a river through pristine, urban and agricultural landscapes. *Water Research*, *37* (19), 4645-4656, 2003.
[8] Lee, C.-C.; Jiang, L.-Y.; Kuo, Y.-L.; Hsieh, C.-Y.; Chen, C. S.; Tien, C.-J., The potential role of water quality parameters on occurrence of nonylphenol and bisphenol A and identification of their discharge sources in the river ecosystems. *Chemosphere*, *91* (7), 904-911, 2013.

O6-17

琵琶湖南湖で検出される大腸菌の起源推定

井原 賢 [1], 劉 思瑶 [1], 田村 太一 [1]、馬 緻宇 [1]、林 東範 [1]、山下 尚之 [2]、田中 宏明 [1]

[1]京都大学, [2]愛媛大学

キーワード：琵琶湖，大腸菌，全ゲノム解析、起源推定

抄録

現在、日本では衛生学的水質基準として大腸菌群から大腸菌への変更が検討されている。しかし、水環境から検出される大腸菌のうちどれくらいがヒト糞便由来であるのか、よくわかっていない。本研究は、琵琶湖南湖および下水処理場由来の大腸菌の全ゲノム塩基配列を解読して比較することで、琵琶湖南湖の大腸菌のどれくらいがヒト糞便由来なのか、ヒト以外の動物由来の大腸菌はどれくらいいるのか推測した。その結果、琵琶湖から検出される大腸菌の由来は下水が主ではなく家畜や水鳥の寄与が高いと示唆された。

1. はじめに

日本では、水環境における衛生学的水質基準として大腸菌群が長らく用いられてきた。しかしながら、土壌由来の大腸菌群も検出してしまうため、正確に糞便汚染を示しているとは言えない。そのため、現在、大腸菌群から大腸菌への環境基準の変更の検討が進んでいる。変更が検討されている大腸菌についても、ヒト以外の様々な温血動物の腸管から排出されたり、環境中での増殖の可能性が指摘されており、糞便汚染指標としてどこまで有効か、さらなる検証が必要である。そのためには、環境水から検出される大腸菌が果たして下水由来の大腸菌と同じ系統なのか否かの検証が必要である。一口に大腸菌と言っても、遺伝子の種類や塩基配列の変異のパターンによって多くの系統に分類される [1), 2)]。

疫学の分野ではゲノム塩基配列に基づいて大腸菌の分類を行う方法の一つに Multi Locus Sequence Type (MLST)がある。MLST では特定の遺伝子群の型(allele)の違いに基づいて大腸菌が sequence type (ST)として分類できる。もともとは特定の複数の遺伝子の配列を個別の PCR とサンガーシーケンス法によって解読して ST を決定していたが、近年は次世代シーケンサーの低コスト化によって、大腸菌の全ゲノムを解読してしまい(whole genome sequencing: WGS)、その塩基配列情報から MLST を実施することも現実的となった。また、WGS で得られる全ゲノムの塩基配列から系統樹を作成し、細菌の株がどれくらい近縁であるのかを推定することも可能となってきている [3)]。疫学だけでなく環境分野の研究においても、河川水から単離された病原性大腸菌の遺伝子的特徴の詳細な解析にこれらの方法が利用され始めている [4)]。

本研究は、琵琶湖南湖および周辺下水処理場から単離される大腸菌がどれくらい類似しているのか調べることを目的とした。そのために、大腸菌の全ゲノム塩基配列を次世代シーケンサーを用いて解読し、MLST 解析および k-mer 系統樹、single nucleotide polymorphisms (SNPs)系統樹の作成を行った。

2. 方法

2.1 採水、大腸菌の培養

琵琶湖南湖および周辺下水処理場で採水を行った。琵琶湖南湖では、2017 年 3 月に 11 地点で採水を行い、XM-G 寒天培地によって大腸菌を単離した。また、琵琶湖南湖周辺に位置する 3 か所の下水処理場で 2016 年 12 月および 2017 年 3 月に放流水を採水し、同じく XM-G 寒天培地によって大腸菌を単離した。形成された青色コロニーはシングルコロニーを選択して爪楊枝でピックアップし、新しい XM-G 寒天培地でさらに培養した。コロニーの密度が高くてシングルコロニーが得られない場合には、PBS によって希釈し XM-G 寒天培地で培養することでシングルのコロニー(株)を得た。

2.2 大腸菌からのゲノム DNA 抽出

大腸菌のゲノム DNA は DNeasy Blood & Tissue Kit (Qiagen)を用いて抽出した。琵琶湖南湖水由来の株 14 個、下水処理場流入水および放流水由来の株をそれぞれ 9 個および 15 個から DNA を抽出した。抽出した DNA の濃度は Qubit 2.0 Fluorometer (Invitrogen)を用いて測定し、ライブラリーの調整に供した。

2.3 ライブラリーの調整

五味らの報告 [4)]に従い、イルミナの Nextera XT DNA library prep kit を用いてライブラリーを作成した。ライブラリーの品質の確認および定量は Agilent2100 バイオアナライザ(Agilent)を用いた。

2.4 次世代シーケンサー、データ解析

イルミナ社製の次世代シーケンサーMiSeq を用いて大腸菌全ゲノムの塩基配列を解読した(paired-end read, 600 cycle)。得られたリードから市販の解析ソフト CLC Genomics Workbench (CLC bio) を用いて de-novo assembly により contig を作成し、各株毎に全 contig のトータルの長さを確認した。大腸菌のゲノムサイズ(約 500 万塩基)に該当する株の数は琵琶湖南湖水由来は 15 株下水処理場流入水は 9 株、放流水は 15 株であった。これらの株について、市販の解析ソフト Microbial Genomics Module (CLC bio) を用いて、MLST 解析、k-mer 系統樹、および SNP 系統樹の作成を行った。Microbial Genomics Module は Warwick Medical School (Coventry, UK)から提供されている大腸菌の MLST scheme に基づいて MLST 解析を実施してくれる(7 つの遺伝子の allele の組み合わせから ST 番号を決定)。また、K-mer 系統樹の作成では、各大腸菌株の contig から k-mer (長さ k 塩基)の断片配列のセットを作成し、そのセットが大腸菌株の間でそのくらい類似しているかを数値化して系統樹を作成する。配列が似通った株ほど同じ配列の k-mer を共有していることに基づく系統樹作成方法である。以上の解析から、琵琶湖南湖水から単離した大腸菌と下水処理場放流水から単離した大腸菌の ST の比較および、ゲノム配列がどれくらい似ているのか考察を行った。

3. 結果

琵琶湖水、放流水、糞便株由来の大腸菌(黒字、実線表記)と従来から系統分類の代表として用いられている大腸菌 reference 株(灰色字、点線)の全ゲノム情報を合わせて k-mer 系統樹を作成した(図 1)。琵琶湖水、放流水由来の大腸菌の株名は採水時期と水試料、株番号で表示(例:2017July_Biwa3)。株毎に宿主特異的マーカー遺伝子の保有状況、系統分類(A, B1, B2, C, D, E, F)2)を表記。どの Phylogroup に属するかは Clermont et al.(2015)[1]および Kaas et al (2012)[2]に従った。糞便株(DRR で始まる株名)の宿主、およびは宿主特異的なマーカー遺伝子の保有状況は五味らの報告に基づいて記載[4]。

放流水由来の大腸菌は系統 A が最も多く 12 株中 5 株(42%)だった。これに対して琵琶湖水由来の大腸菌は系統 A はゼロで、系統 B1 が最多で 12 株中 7 株(58%)だった。ヒト糞便由来の株は 9 株中 4 株(44%)が系統 A に分類されている。放流水由来と類似した系統である。トリ糞便由来の株は 5 株中 4 株(80%)が B1 に分類された。琵琶湖水と類似した系統である。

放流水由来の大腸菌はヒトマーカーを保有している株が最も多く 4 株、ついで 3 株がトリマーカーを保有していた。これに対して琵琶湖水由来の大腸菌はヒトマーカーを保有する株はゼロで、トリマーカーを保有する株が 5 株であった。ウシマーカーを保有する大腸菌が 1 株見られた。他の採水月でもおおむね同様の結果が得られた。
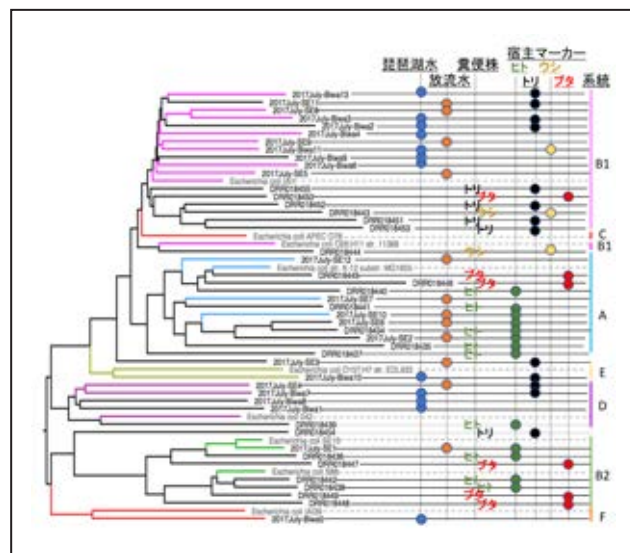
図 1 琵琶湖水、下水処理場放流水、および糞便株由来の大腸菌の k-mer 系統樹(2017 年 7 月採水の例)

4. 考察

生活排水を含む放流水由来の大腸菌が、系統樹上の位置関係でも系統の分類でも宿主マーカー遺伝子の保有状況でもヒト糞便由来の大腸菌に最も類似している結果は理解しやすい。これに対して、琵琶湖水由来の大腸菌はトリ糞便由来の大腸菌と最も類似しており、その由来は下水と異なる可能性(家禽、水鳥等)が示唆された。

5. 結論

琵琶湖から検出される大腸菌の由来は下水が主ではなく家畜や水鳥の寄与が高いと示唆された。

引用文献

[1] Clermont O. et al., Guide to the various phylogenetic classification schemes for *Escherichia coli* and the correspondence among schemes. 2015, *Microbiology* 161, 980-988.

[2] Kaas R. et al., Estimating variation within the genes and inferring the phylogeny of 186 sequenced diverse *Escherichia coli* genomes. 2012, *BMC Genomics* 13, 577.

[3] Leekitcharoenphon P. et al., Evaluation of whole genome sequencing for outbreak detection of *Salmonella enterica*. 2014, *PLOS ONE*, 9, e87991.

[4] Gomi R. et al., Whole-genome analysis of antimicrobial-resistant and extraintestinal pathogenic *Escherichia coli* in river

water. 2017, *Appl. Environ. Microbiol.* 83, e02703-16.

O6-18

Estimation of Dissolved Oxygen Deficiency in Aquatic Environments with Time Spread Based on Dissolved Methane and Nitrous Oxide Measurements

Yuzuru Kimochi[1] and Hitoshi Tanaka[1]

[1]Center for Environmental Science in Saitama, Japan

Keywords: dissolved oxygen (DO), dissolved nitrous oxide (DN$_2$O), dissolved methane (DCH$_4$), hypoxia/anoxia,

aquatic environment monitoring

ABSTRACT

We constructed and proposed a method to estimate the dissolved oxygen (DO) deficiency in aquatic environments with time spread ranging from hours to an entire day, with measurement of dissolved methane (DCH$_4$) and nitrous oxide (DN$_2$O). Based on the results of the water purification experiment, the determination threshold of the DO deficiency in this method was set to 0.025 mgC/L and 0.003 mgN/L for DCH$_4$ and DN$_2$O, respectively. Next, the threshold value was verified from continuous monitoring in actual ponds and data of past literature. As a result, although it may be necessary to set a value for each field, since at least detection of DCH$_4$ reflects the occurrence of an anaerobic environment, the method can be used for screening of a detailed investigation site related to DO depletion. In this way, the most important merit of our method is that it can be used to estimate previous DO levels especially, without the need for continuous DO monitoring. In addition, as sampling of dissolved gases by the headspace method is simple, a large number of gas samples can be collected efficiently by field survey and analyzed collectively by laboratory etc. It can be analyzed with GC-FID for CH$_4$ and GC-ECD for N$_2$O: both analytical instruments are relatively inexpensive and easy to introduce. Applying this method to similar lakes can be expected if knowledge about thresholds is accumulated and diversified in various regions, climate, lake size (breadth and depth), eutrophication level, etc.

1. INTRODUCTION

Lack of DO, roughly below 2 mg/L, has severe impacts on aquatic organisms, especially benthic organisms. However, when the hypoxia/anoxia occurrence is relatively short, or DO frequently change, the current DO value does not indicate whether there was a period of hypoxia/anoxia in the past, or if it will occur in the near future.

In this study, we constructed and examined a method to estimate DO conditions in aquatic environments with time spread ranging from a few hours to an entire day, based on current values of dissolved gases, including CH$_4$ and N$_2$O[1]. This method was evaluated based on previous knowledge concerning the behavior of DO, DCH$_4$, DN$_2$O, and water quality, especially of nitrogen compounds in a wastewater treatment process, in which DO concentrations, ranging from oxic to anoxic/anaerobic levels, were artificially controlled. Based on an in situ wastewater treatment experiment, we set the threshold in order to determine that the previous DO condition for DCH$_4$ and DN$_2$O. We then verified the method and each threshold based on an investigation in small ponds as well as on previous studies. Finally, we propose to investigate whether the method can be put to practical use or to accumulate and organize surveys and knowledge in various lakes.

2. MATERIALS AND METHOD

Microbial metabolic reactions in aquatic environments ranging from oxic to anaerobic

Metabolic reactions in aquatic microorganisms vary according to the environment, which ranges from oxic to anoxic (anaerobic). Dynamics of carbon and nitrogen by microbial metabolism in a lake is shown in Fig. 1.

Theoretical behavior of DCH$_4$ and DN$_2$O, which reflect DO deplete conditions

N$_2$O is produced under both decreased and increased levels
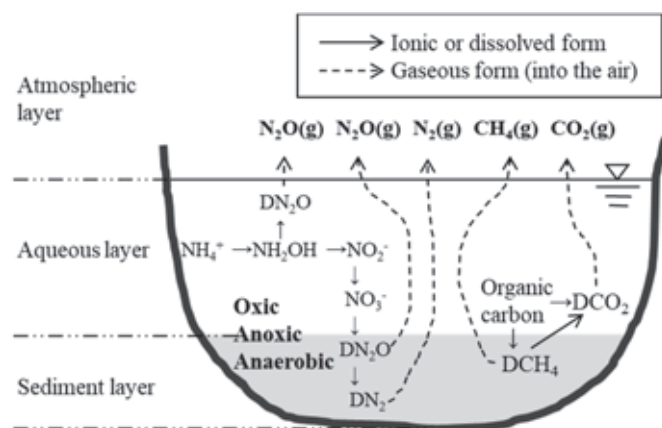
Fig. 1 Dynamics of carbon and nitrogen by microbial metabolism in a lake

of DO: DN_2O can be positioned as a factor determining micro-oxic and anoxic conditions. CH_4 is produced only under anaerobic conditions, and is easily depleted with an increase in the DO concentration. Since the solubility of CH_4 in water is very low, which indicated that it is highly volatile, it is difficult to detect DCH_4 in aquatic environments. In other words, CH_4 detection in aquatic environment means serious DO lacking due to anaerobic conditions. Model behavior of both substances according to DO decrease and increase is assumed in Fig. 2.

Development of a method to estimate previous DO levels in aquatic environments by measuring current DCH_4 and DN_2O values

Here, we propose a new method to estimate of previous DO levels in aquatic environments using DCH_4 and DN_2O (Table 1). The assumed cases are as follows.

Case 1: Detection of neither DCH_4 nor DN_2O

The condition might not have been due to the lack of DO, we labeled it as "negative", indicating that there was no risk of occurrence of anoxic conditions.
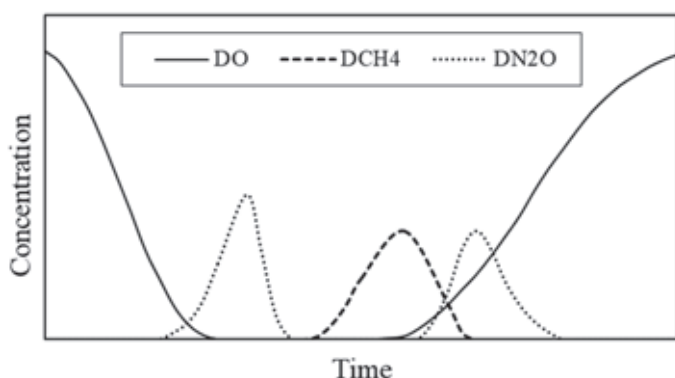
Fig. 2 Model behavior of DCH_4 and DN_2O according to changes in DO levels.

Case 2: Detection of DN_2O and non-detection of DCH_4

Presence of DN_2O indicates low DO concentrations; we labeled it as "false-positive", indicating that the area was likely hypoxic in the past. Such regions would require continuous monitoring of DO.

Case 3: Detection of DCH_4

Presence of DCH_4 indicates that the area was previously anaerobic, thus, we labeled this region as "positive". Such areas require improvement in DO levels.

Assumption of the threshold of DCH_4 and DN_2O based on the wastewater treatment experiment

In wastewater treatment process, decrease and increase in DO levels in the treatment tank can be regarded as similar to its behavior in aquatic environments. In setting the threshold of DCH_4 and DN_2O, we used the data of the domestic wastewater treatment experiment[2].

Verification of the threshold of DCH_4 and DN_2O by continuous monitoring in actual ponds

We verified the threshold of DCH_4 and DN_2O by minute monitoring of DO, DCH_4, DN_2O as well as the water quality in small ponds. There are two ponds: the pond A (rectangle shape, 1mW x 7mL x 1mD) and the pond C (oval shape, 18mW x 42mL x 1.2mD). As sediment accumulated on the bottom of every pond, actual water depth of the ponds A and C was 0.6m and 0.8m, approximately. Monitoring was made at the bottom layer, almost 5cm above the surface of the sediment in the pond A (St. 1) and the pond C (St. 2). General water quality of the ponds was about 10mg/L of DOC and 0.5mg/L of T-N, with almost no difference by the sampling station.

Test decision of lake environment on the data in previous researches by the new estimation method

Test decision of lake environment in some countries was made on the data in previous reports based on the threshold of DCH_4 and DN_2O, set on the wastewater experiment.

Table 1 Estimation of previous DO concentrations in aquatic environments by measuring DN_2O and DCH_4

DCH_4, DN_2O	Decision	Remarks
All non-detection	Negative (No risk)	Oxic condition including past few hours
Detection of DN_2O and non-detection of DCH_4	False-positive (Need for DO continuous monitoring)	Suspicion of hypoxic/anoxic/anaerobic condition (Even if present DO is sufficient, it might have decreased to nearly zero in the past)
Detection of DCH_4	Positive (Need for improvement of DO condition)	Occurrence of anaerobic condition for several hours in the past (Detection of CH_4 means existence of a few hours of 0mg/L DO in the past)

3. RESULTS AND DISCUSSION

Verification of theoretical behaviors of each substance and consideration of the new estimation method through a wastewater treatment experiment

Based on the results obtained from experiments on water treatment of anoxic/oxic process, threshold values for judging the state of oxygen deficiency were temporarily set. The behavior of each gas in the reaction tank was similar to that shown in Fig. 2. The threshold to estimate previous deplete DO conditions would be 0.003 mg N/L (100 nmol/L) for DN_2O, and 0.025 mg C/L (2,000 nmol/L) for DCH_4. In particular, DCH_4 detection at this level would indicate previous continuous conditions of DO at 0 mg/L.

Verification of the threshold of DCH_4 and DN_2O by continuous monitoring in actual ponds

In terms of DO, it decreased during the night, and increased in the daytime up to 14mg/L at St. 1. On the other hand, there was almost no DO at St. 2. As for DCH_4, we couldn't necessarily observe the phenomenon that DCH_4 increase with DO decrease or DCH_4 decrease with DO increase, at St. 1. However, it could be said with certainty that DCH_4 was always greater than the threshold of 0.025mgC/L, regardless of the DO value. Similarly, DCH_4 was always extremely high at St. 2. As for DN_2O, it was always less than the threshold of 0.003mgN/L at both of St. 1 and St. 2. From these results, at least the DCH_4 value would be useful tool in order to determine and screen the required minute investigation site.

Test decision of lake environment on the data in previous researches by the new estimation method

Results of test decision on the environment of several pond and lakes in previous studies are summarized in Table 2. It can be considered that we could almost determine the lake environment in the literature using this method based on provisionally set threshold. Though the threshold value itself needs further study, the usefulness of this method in determining the lake environment was suggested.

4. CONCLUSION

A method to estimate DO deficiency in aquatic environments with time spread with measurement of DCH_4 and DN_2O proposed,. Applying this method to similar lakes can be expected if knowledge about thresholds is accumulated and diversified in various regions, climate, lake size, eutrophication level, etc. We hope that many researchers will examine this new method in various fields, and that it will contribute to the conservation and improvement of aquatic environments globally.

REFERENCES

[1] Kimochi, Y. and Tanaka, H., *Japanese J. Wat. Treat. Biol.*, Vol. 53, No. 4, pp. 95-109, 2017.

[2] Jono, K., Sano, A., Ogura, et. al., *J. Wat. Environ. Technol.*, Vol. 12 (4), 379-388, 2014.

[3] Hashimoto, S., Sun, H. Y., Nakamura, T., et. al., *Geochem. J.*, Vol. 27, pp. 117-123, 1993.

[4] Nojiri, Y., Final report of the Global Environmental Research Project, Ministry of the Environment, Japan, 1995.

[5] Wang, S., Yeager, K. M., Wang, G., et. al., *J. Environ. Qual.*, Vol. 39 September-October, pp. 1858-1863, 2010.

[6] Miettinen, H., Pumpanen, J., Heiskanen, J. J., et. al., *Boreal Environ. Res.*, Vol. 20, pp. 75-89, 2015.

Table 2 Test decision of water environment on the data obtained by previous studies

Field	Condition	DO (mg/L)	DCH_4 [mgC/L (nM)]		DN_2O [mgN/L (nM)]		Decision	References
Lake Kasumigaura	Eutrophic	Oxic			Max. 0.0006 (22)	Min. 0.0003 (10)	Negative	Hashimoto et. al. 1993 [3]
			Max. 0.012 (1,000)	Min. 0.0006 (50)				Nojiri et. al. 1995 [4]
Lake Tahihu	Eutrophic	Oxic	Max. 0.0010 (83)	Min. 0.0001 (10)	Max. 0.0031 (110)	Min. 0.0013 (47)	False-positive	Wang et. al. 2010 [5]
			0.0005 (38)	0.0002 (15)	0.0013 (46)	0.0010 (35)		
Lake Kuivajärvi	Mesotrophic	0	Min. 0.08 (6,000)		Min. 0.006 (200)		Positive	Miettinen et. al. 2015 [6]

O6-19

Source estimation of veterinary drugs in Yodo River watershed, Japan

Seiya Hanamoto*, Norihide Nakada, Naoyuki Yamashita, and Hiroaki Tanaka

Research Center for Environmental Quality Management, Graduate School of Engineering, Kyoto University
*Present address: Water Quality Research Team, Water Environment Research Group, Public Works Research Institute

Keywords: veterinary drugs, source estimation, field study, livestock population, human population

ABSTRACT

Twelve veterinary drugs were monitored at four rivers in Yodo River watershed, Japan over 17 sampling events. Among the five frequently detected veterinary drugs, mass flux in the river was significantly correlated with human population in the catchment for three veterinary drugs substantially used by humans, sulfamethoxazole, trimethoprim, and sulfadimethoxine. Sources of the three would be sewage treatment plants and household septic tanks. On the other hand, mass fluxes of the remaining two, sulfamonomethoxine and lincomycin, in the rivers showed positive correlation with swine population in the catchment, although sulfamonomethoxine is equally used in both cattle and swine farming. This was attributable to application of cattle excrement as manure, and lability of sulfamonomethoxine during composting processes. The major source of the two would be on-site treatment facilities of swine urine.

1. INTRODUCTION

Veterinary drugs are one of the most noticeable emerging contaminants due to their potential risks to aquatic organisms, and they have been widely detected in surface waters[1]. Therefore, source identification and mass loading prediction should be conducted to develop reduction strategies of the veterinary drugs. However, most studies only reported qualitative outcomes for their sources.

We therefore conducted this study to provide quantitative source characterization of veterinary drugs in the Yodo River watershed, Japan. We monitored 12 veterinary drugs at four rivers in the watershed over five months. The sources of veterinary drugs were evaluated by linking their mass fluxes in rivers with human or livestock populations in catchment areas and flow rate patterns.

2. METHOD

Yodo River watershed (8,240 km^2) comprises residential area (21%), agricultural land (25%), forest (47%), and others (7%). The population is approximately 12,000,000, of which approximately 95% use the sewer system in the watershed. Human and livestock populations in catchment areas of sampling sites are summarized in Table 1. Human and livestock population were obtained from Ministry of the Environment[2] and Ministry of Agriculture, Forestry and Fisheries[3], respectively.

Field surveys were conducted in the middle basin of the watershed. Surface water samples were collected from the Katsura River (Miyamae Bridge), the Uji River (Ujigokou Bridge), the Kizu river (Kizugokou Bridge), and the Yodo River (Hirakata Bridge) approximately weekly between October 2009 and February 2010, yielding a total of 17 sampling events. Samples were collected using a grab in a stainless steel bucket. The samples were stored in amber glass bottles with 1.0 g/L ascorbic acid in darkness and taken to the laboratory. The 12 selected veterinary drugs in the dissolved phase were concentrated by solid-phase extraction, measured by UPLC-MS/MS, and quantified by the absolute calibration method[4]. Signal to noise ratios (S/N) of 3 were used as the detection limit. The flow rates at sampling sites were obtained from the Ministry of Land, Infrastructure and Transport[5].

Table 1 Human and livestock populations in catchment areas of sampling sites.

	Human	Cattle	Swine
Katsura River	125,285	3,675	4,895
Uji River	1,758,892	18,952	7,704
Kizu River	390,907	7,810	26,600
Yodo River	4,088,883	33,040	40,055

3. RESULTS

Among the 12 selected veterinary drugs, sulfamethoxazole, sulfadimethoxine, trimethoprim, sulfamonomethoxine and lincomycin were frequently detected (> 50%) in more than one river. Concentrations of the former three drugs were in the same order of magnitude among rivers, while those of the Kizu River were much higher than the other rivers for the latter two drugs and thiamphenicol (Figure 1).
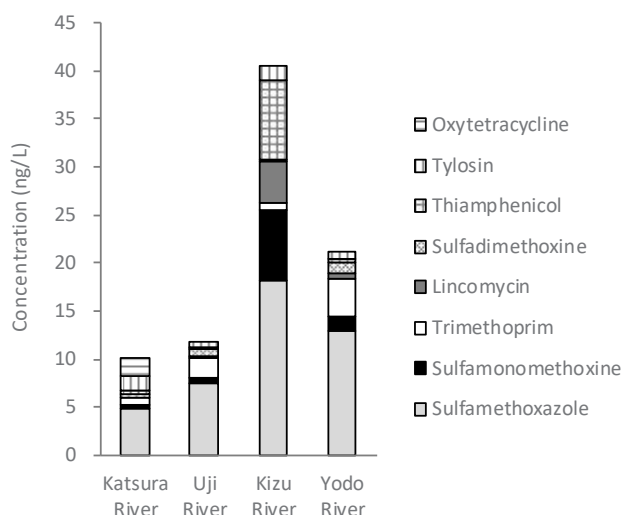
Fig. 1 Concentrations of veterinary drugs in study area. Vertical bars denote means of 17 samplings. Tiamulin, sulfadimidine, sulfamerazine, and ceftiofur were not shown due to their low concentrations (<1 ng/L).

Since the five frequently detected veterinary drugs are relatively conservative during river transport in this watershed[6], their mass fluxes in a river indicate total mass loadings at sources located in the catchment area. Among the five drugs, the mass fluxes in rivers were significantly correlated with human population in the catchment area for sulfamethoxazole, trimethoprim, and sulfadimethoxine (Table 2 and Figure 2A). This is attributable to their substantial usage by humans[7]. Therefore, sources of the three drugs would be sewage treatment plants (STPs) and household septic tanks.

On the other hand, mass fluxes of sulfamonomethoxine and lincomycin in rivers showed positive correlation with swine population in the catchment (Table 2 and Figure 2B). As lincomycin is mostly used for swine farming[8], the correlation reflects its usage. However, sulfamonomethoxine is equally used for both cattle and swine, indicating existence of influential factors determining the sources other than usage. Though both feces and urine of cattle are mostly applied to agricultural land as manure after composting or storage, approximately 60% of swine urine is discharged to the aquatic environment via on-site treatment facilities[9]. Therefore, given the correlation with swine population, runoff of land-applied manure does not have appreciable impact for sulfamonomethoxine, compared with discharge from on-site treatment facilities of swine urine. This would be mostly attributed to lability of sulfamonomethoxine during composting process (removal >98%, measured at several cattle farms in Japan by the Research Institute for Animal

Science in Biochemistry and Toxicology[10]). Low contribution of the runoff is complemented by the lack of correlation between mass flux in a river and its flow rate ($p > 0.05$ for four studied rivers, for both sulfamonomethoxine and lincomycin, data not shown). Therefore, on-site treatment facilities of swine urine are influential sources for these drugs. Thus, not only use application but also livestock waste management significantly affect the sources of veterinary drugs.

Table 2 Correlation coefficients (R^2) between mass fluxes in rivers and human or livestock population in the catchment areas for five frequently detected veterinary drugs [a].

	Human	Cattle	Swine
Sulfamethoxazole	0.983	0.431	0.010
Trimethoprim	0.953	0.554	0.000
Sulfadimethoxine	0.964	0.534	0.001
Sulfamonomethoxine	0.006	0.525	0.982
Lincomycin	0.151	0.151	0.843

[a] **Correlation includes four rivers in this study for lincomycin, while observations in the Hirose River reported from Nakada et al. [11] were additionally included for the other drugs.**
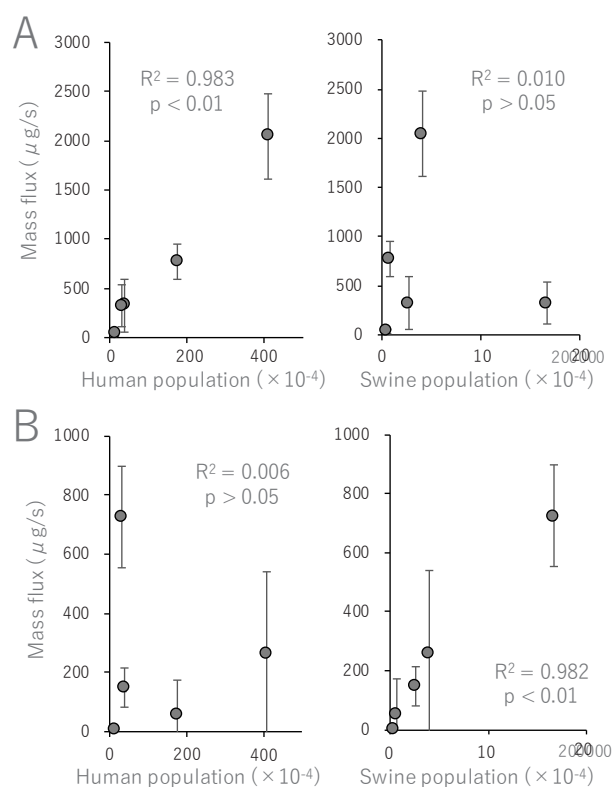
Fig. 2 Relationships between mass fluxes in rivers and human or swine population in the catchment areas for (A)

sulfamethoxazole and (B) sulfamonomethoxine. Relationships include four rivers in this study and the Hirose River observed by Nakada et al.[11]. For the mass flux, symbols denote means and error bars denote standard deviations (n = 3 for the Hirose River, and n = 17 for the other rivers).

Since human waste is treated in STPs or household septic tanks in most countries, they would be generally the major sources of drugs mostly used by humans. However, management systems of livestock waste vary among countries, resulting in different sources of veterinary drugs between countries. In the USA, most livestock waste is applied to agricultural fields as manure after storage and not directly discharged to the aquatic environment[12], also generally applicable to European countries[13]. Therefore, the major source of veterinary drugs in these regions is likely manure applied to agricultural land. On the other hand, a substantial portion of livestock waste directly enters the aquatic environment with or without treatment in Asian countries[14][15]. Although field measurements were extensively conducted there, the relationship between the spatial distribution of veterinary drugs and livestock populations in the catchment areas has not been quantified. Therefore, our findings of their correlations would provide more reliable source identification of veterinary drugs and advance our understanding on their mass loading prediction in Asian countries.

4. CONCLUSION

Mass fluxes of sulfamethoxazole, trimethoprim, and sulfadimethoxine, veterinary drugs substantially used by humans, in rivers showed a positive correlation with human population in the catchment. Their major source was considered to be STPs and household septic tanks in this area. On the other hand, mass fluxes of sulfamonomethoxine and lincomycin in rivers showed a positive correlation with swine population in the catchment area. A comprehensive analysis including their usage, livestock excrement management, and reported stability in composting process indicated that their major source is on-site treatment facilities of swine urine. To our knowledge, this is the first study linking the spatial distribution of pharmaceuticals with livestock population in the catchment.

REFERENCES

[1] Kolpin, D. W.; Furlong, E. T.; Meyer, M. T.; Thurman, E. M.; Zaugg, S. D.; Barber, L. B.; Buxton, H. T. Pharmaceuticals, hormones, and other organic wastewater contaminants in U.S. streams, 1999–2000 - A national reconnaissance. Environ. Sci. Technol. Vol. 36, pp. 1202–1211, 2002.

[2] Ministry of the Environment, Information on waste treatment technology. 2010, Tokyo

[3] Ministry of Agriculture, Forestry and Fisheries. Statistics of animal husbandry. 2007, Tokyo

[4] Okuda, T.; Yamashita, N.; Tanaka, H.; Matsukawa H.; Tanabe K. Development of extraction method of pharmaceuticals and their occurrences found in Japanese wastewater treatment plants, Environ. Int. Vol. 35, pp. 815–820, 2009.

[5] Ministry of Land, Infrastructure and Transport, Water information system Website; http://www1.river.go.jp/ (accessed April 8, 2018)

[6] Hanamoto, S.; Nakada, N.; Yamashita, N.; Tanaka, H. Modeling the photochemical attenuation of down-the-drain chemicals during river transport by stochastic methods and field measurements of pharmaceuticals and personal care products. Environ. Sci. Technol. Vol. 47, pp. 13571–13577, 2013.

[7] Ministry of Health, Labour and Welfare. Statistics Section EAD, Health Policy Bureau. Annual Reports on Statistics of Production by Pharmaceutical Industry, Tokyo; 2010.

[8] Ministry of Agriculture, Forestry and Fisheries. National Veterinary Assay Laboratory. Sales Amounts and Sales Volumes of Antibiotics, Synthetic Antibacterials, Antihelmintics and Antiprotozoals. 2010, Tokyo

[9] Ministry of Agriculture, Forestry and Fisheries. Survey on Livestock Waste Treatment. 2009, Tokyo

[10] Research Institute for Animal Science in Biochemistry and Toxicology, Public information, Academic research, How to use veterinary drugs properly (in Japanese), Available from: http://riasbt.or.jp/rias/wp-content/uploads/2014/08/kankyoueikyou-3-6.pdf (accessed June 13, 2017)

[11] Nakada, N., Komori, K., Suzuki, Y., Konishi, C., Houwa, I., Tanaka, H. Occurrence of 70 pharmaceutical and personal care products in Tone River basin in Japan. Water Sci. Technol. Vol. 56, pp. 133-140, 2007.

[12] Sarmah, A.K.; Meyer, M.T.; Boxall, A.B. A global perspective on the use, sales, exposure pathways, occurrence, fate and effects of veterinary antibiotics (VAs) in the environment. Chemosphere Vol. 65, pp. 725-759, 2006.

[13] de la Torre, A.; Iglesias, I.; Carballo, M.; Ramírez, P.; Muñoz, M.J. An approach for mapping the vulnerability of European Union soils to antibiotic contamination. Sci. Total Environ. Vol. 414, pp. 672–679, 2012.

[14] Shimizu, A.; Takada, H.; Koike, T.; Takeshita, A.; Saha, M.; Rinawati; Nakada, N.; Murata, A.; Suzuki, T.; Suzuki, S.; Chiem, N. H.; Tuyen, B. C.; Viet, P. H.; Siringan, M. A.; Kwan, C.; Zakaria, M. P.; Reungsang, A. Ubiquitous occurrence of sulfonamides in tropical Asian waters. Sci. Total Environ. Vol. 452–453, pp. 108–115, 2013.

[15] Lin A.Y.; Yu, T.H.; Lin, C.F. Pharmaceutical contamination in residential, industrial, and agricultural waste streams: risk to aqueous environments in Taiwan. Chemosphere Vol. 74, pp. 131-141, 2008.

O6-20

Impacts of Sediment Supply from a Dam Reservoir on Heavy Metals Concentrations in Downstream River Water

Yuji Suzuki[1], Hiroyuki Mano[2], Satomi Mizukami-Murata[1], Fumiaki Ogawa[1]

[1]Public Works Research Institute (PWRI), [2]National Institute of Advanced Industrial Science and Technology (Previous Position: PWRI)

Keywords: Water quality, Chemical substances, Sediment supply, Heavy metals, *Oryzias latipes*

ABSTRACT

Sedimentation in a dam reservoir is one of the important issues to overcome for utilizing the reservoir over a long term. In order to solve this, in Japan, sediment supply from reservoirs to their downstream rivers has been attempted. However, there is limited knowledge on the impacts on the water quality just after the sediment supply. In this study, leaching tests of heavy metals from reservoir sediments were conducted to evaluate the occurrences of heavy metals at the downstream after sediment supply. As a result, manganese (Mn) was considered as the dominant and concerned heavy metal in the assumed case. In addition, short-term toxicity test was conducted to determine the toxicity of Mn to Japanese medaka (*Oryzias latipes*) and the No Observed Effect Concentration (NOEC) was derived as 5 mg-Mn/L. The Predicted Environmental Concentration (PEC) / the Predicted No Effect Concentration (PNEC) ratio regarding to Mn was obtained from the result of leaching tests as 0.015 which was much lower than the value (4.67) obtained from the data of Mn contents in the sediment. It was indicated that leaching from sediment is an important factor to evaluate the environmental risk of Mn to fishes just after an event of sediment supply.

1. INTRODUCTION

Sedimentation in a dam reservoir is one of the important issues to overcome for utilizing the reservoir over a long term[1]. In addition, interrupting continuity of sediment transport by dams may cause downstream river flows to be sediment-starved (so-called hungry water), resulting in incision of river channels and/or coarsening of the bed materials[2]. In order to solve these situations, in Japan, sediment supply from reservoirs to their downstream rivers has been attempted using approaches such as sediment augmentation, sediment flushing and sediment bypass. However, there is limited knowledge on the impacts on the water quality just after the sediment supply operation despite the assumption that chemicals such as heavy metals are accumulated on the deposited sediment at the bottom of dam reservoirs.

In this study, leaching tests of heavy metals from dam reservoir sediments were conducted to evaluate the occurrences of heavy metals in river water just after sediment supply. In addition, a short-term toxicity test was conducted to determine the toxicity of manganese (Mn) to Japanese medaka (*Oryzias latipes*).

2. METHOD

(1) Leaching test of dam reservoir sediment

On November, 2016, sediment and water samples were collected from Yahagi Dam reservoir and they were used to evaluate leaching of heavy metals from reservoir sediments. Leaching test was conducted by following the standard leaching test method defined in Notification No.46 of the Environment Agency (JLT 46), Japan. Sediment was passed through 2 mm mesh sieve before tests. In addition to the condition defined in JLT 46, different liquid to solid ratios (L/S (%): 3, 5, 10, 20, 25) were examined to evaluate the relationship between leached concentration and L/S. For leaching solvents, ultrapure water (*Milli-Q*) and reservoir water were used. Test was operated by horizontal shaking for 6 hours.

The collected reservoir sediment, reservoir water and supernatants from leaching tests (filter by 0.45 μm membrane filter) were subjected to heavy metals analysis. Water samples were treated by nitric acid digestion and sediment samples were treated by microwave-assisted digestion. Pre-treated samples were analyzed by ICP-MS (X7CCT, Thermo Fisher Scientific). Target elements were Lead (Pb), Arsenic (As), Copper (Cu), Zinc (Zn) and Mn. Water content of sediment sample was also analyzed.

(2) Short-term toxicity test of Mn to *Oryzias latipes*

Oryzias latipes (*O. latipes*) was obtained from the National Institute for Environmental Studies in Japan (NIES). Mn was targeted based on the result from (1). Manganese chloride was used to prepare five different Mn solutions (Control, 0.5, 5.0, 50, 500 mg-Mn/L) and they were used for batch tests with eggs of *O. latipes*. In each beaker, 10 eggs and 50 ml test solution were added, and incubated at 24 ± 1 ℃ for 14 days. (Until 5 days after

hatching). Solution was replaced every other day. Four replicates were performed for each solution. Hatch of eggs and viability rate of larval fish were documented every day. Statistical analysis was performed using the statistical package R. The homoscedasticity of viability and hatching rate was examined by Bartlett test ($p<0.05$). Statistical significances were evaluated using Dunnett test ($p<0.05$), in the case that homoscedasticity was rejected in all the tests. The highest concentration with no differences among all treatment including control was determined as the No Observed Effect Concentration (NOEC).

RESULTS & DISCUSSION
(1) Leaching test

Results of leaching test were shown in **Figure 1**. In case of the test with *Milli-Q*, heavy metals were leached at the range of 0.02 to 0.04 µg/g-dry for Pb, 0.02 to 0.05 µg/g-dry for As, 0.02 to 0.05 µg/g-dry for Cu, 0.02 to 0.11 µg/g-dry for Zn and 1.8 to 2.2 µg/g-dry for Mn. Leached amounts tended to be more at lower L/S (For example, As was leached at 0.05 µg/L at 3%, 0.04 µg/L at 5%, 0.02 µg/L at 10-25%). In case of the test with dam reservoir water, heavy metals were leached at the range of 0.01 to 0.02 µg/g-dry for Pb, 0.01 to 0.0 2 µg/g-dry for As and Cu, 0.03 to 0.05 µg/g-dry for Zn and 0.06 to 1.27 µg/g-dry for Mn. For Pb, As, Cu and Zn, there were no significant differences among leached amounts under different L/S. In contrasts, Mn was more leached at the lower L/S (1.3 µg/g-dry at 3%, 1.1 µg/g-dry at 5%, 0.88 µg/g-dry at 10%, 0.24 µg/g-dry at 20%, 0.06 µg/g-dry at 25%).

In *Milli-Q* itself, Pb, Cu, Zn and Mn were found at 0.03, 0.18, 3.4, 0.07 µg/L, respectively. As was not detected. In contrast, in dam reservoir water itself, Pb, As, Cu, Zn and Mn were found at 0.06, 0.25, 0.45, 3.2, 0.30 µg/L, respectively. It was indicated that not only heavy metals but also other water qualities in reservoir water affected the leaching behavior of the reservoir sediment. The relationship between leaching solvent and leached amount of heavy metals were plotted as shown in **Figure 2**. Heavy metals were tended to be more leached in *Milli-Q* than reservoir water. In consideration of the both tests with *Milli-Q* and reservoir water, Mn was significantly more leached, especially at the lower L/S, among all the targeted heavy metals. **Table 1** describes the parameters of the tested reservoir sediment. The tested sediment contained Mn at 659 µg/g-dry which was the highest among all targeted heavy metals. Thus, Mn was considered as the most concerned heavy metal in this study.

Mn concentration at the downstream river water during an event of sediment supply from the upstream reservoir
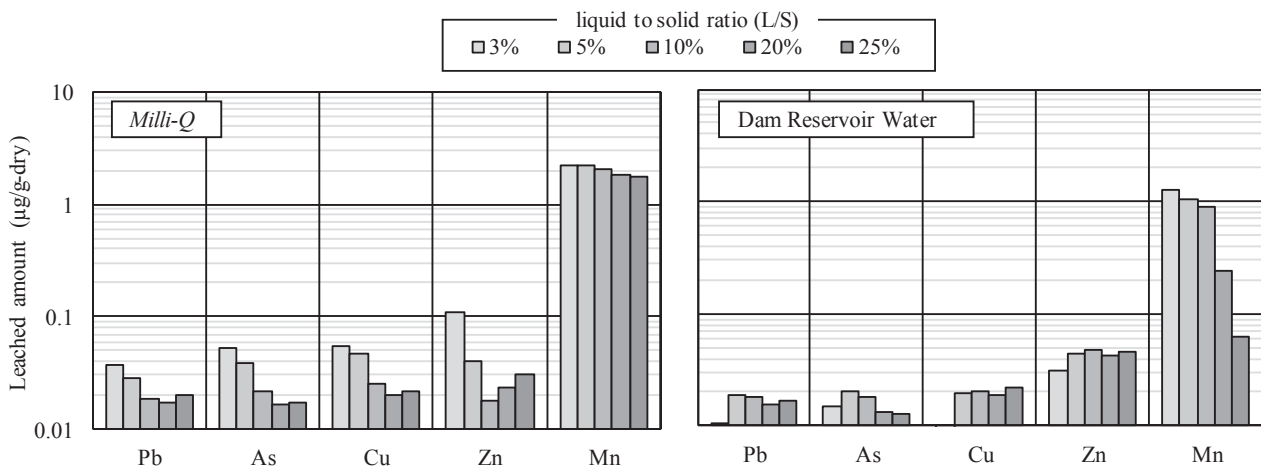
Fig. 1 Leached amounts of Pb, As, Cu, Zn, Mn after leaching tests of the reservoir sediment
(Left: dissolution solvent was *Milli-Q*, Right: dissolution solvent was dam reservoir water)
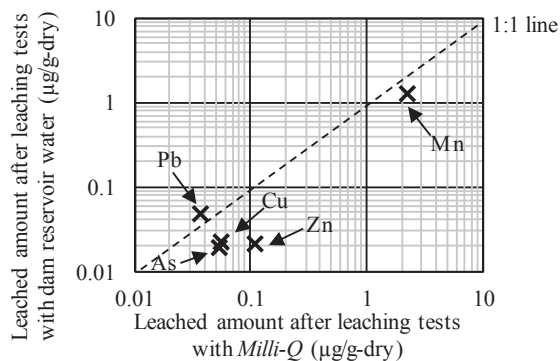
Fig. 2 Relationship between leaching solvent and leached amount of heavy metals

Table. 1 Parameters of the tested dam reservoir sediment

Particle size distribution	(%)	Heavy metals contents	(µg/g-dry)
Sand (0.075 - 2 mm)	14.6	Pb	17
Silt (0.005 - 0.075 mm)	56.9	As	10
		Cu	20
Clay (< 0.005 mm)	28.5	Zn	115
		Mn	659

was calculated using the information obtained from previous report[4]. Firstly, sediment concentration was calculated as 1.259 g/L (which was significantly lower than the L/S tested above) by the equation below.

Sediment concentration (g/L)
= Flux of input sediment (m^3/s)・Unit weight (t/m^3)・10^6
/ River water flow (m^3/s)・10^3　　　**Equation 1**

where flux of input sediment was provided as 0.14 m^3/s (from the data gained in a sediment supply experiment [4]). Unit weight was set as 1.6 t/m^3 assuming that the sediment contained pore water to the extent of a general sediment. River water flow was provided as 177.9 m^3/s.

Secondly, dry sediment concentration (g-dry/L) was calculated by using the water content of the reservoir sediment (71.9%), resulted in 0.354 g-dry/L. This value and the result obtained from the leaching test with the reservoir water (In this case, maximum leached amount (1.27 μg/g-dry) was used) were used for calculating dissolved Mn concentration at the downstream as 0.30+ 0.45 = 0.75 μg/L (Defined as Predicted Environmental Concentration (PEC)1). When all the Mn contained in reservoir sediment was assumed to be suspended in the river water, total Mn concentration was calculated as 0.30+233.37 = 233.7 μg/L (Defined as PEC2).

(2) Short-term toxicity test of Mn to *Oryzias latipes*

Japanese medaka (*O. latipes*) is one of the species recommended by OECD test guideline to evaluate the quality of river water where the temperature is relative warm. This condition is also found at the Yahagi River located at the downstream of Yahagi Dam reservoir, which was focused in this study. The result of short-term toxicity test of Mn to *O. latipes* was shown in **Figure 3**. There were no significant differences in hatching rate among all treatments. In contrasts, survival rate was significantly lower at the treatment with 50 and 500 mg-Mn/L. Thus, the NOEC of Mn to *O. latipes* (survival rate) was
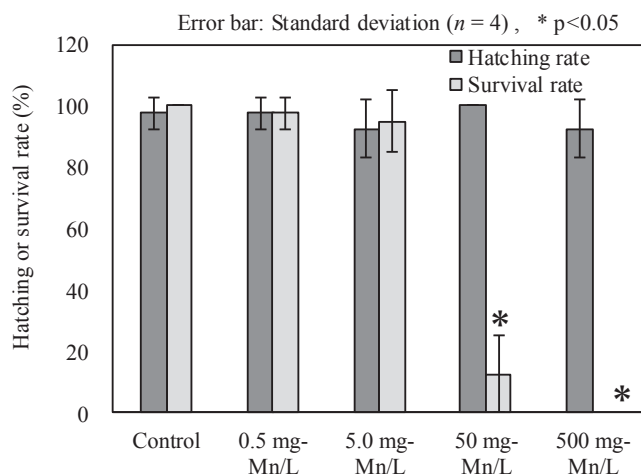
Fig. 3 Evaluation of solutions at different Mn concentration using *O. latipes* (Short-term toxicity test)

calculated as 5 mg-Mn/L in this study. Interestingly, *O. latipes* was more vulnerable to Mn at the stage of larval fish after hatching than the stage of embryo protected by egg. This result was similar to a previous study in which NOEC was calculated as 2.84 mg-Mn/L using eggs of brown trout (*Salmo trutta*) exposed to manganese chloride under an early-life-stage test condition for 62 days[5].

Environmental risk of Mn to fishes in a downstream river of a dam reservoir just after an event of sediment supply was evaluated using the test results. The Predicted No Effect Concentration (PNEC) of Mn was calculated as follows. The value of NOEC (5mg-Mn/L) was divided by the acute-chronic ratio of 10 because the obtained NOEC was considered as a subchronic toxicity index while the situation needed to be evaluated just after sediment supply seemed to be acute. In addition, another assessment factor of 10 was applied to consider the differences in sensitivities between *O. latipes* and other species. Therefore, PNEC in this study was derived as 50 μg-Mn/L. From the result of (1), PEC1/PNEC ratio was calculated as 0.015 while PEC2/PNEC ratio was calculated as 4.67.

3. CONCLUSION

In this study, leaching tests of heavy metals were conducted using dam reservoir sediments. As a result, Mn was considered as the dominant and concerned heavy metal in the downstream river water just after sediment supply. In addition, a short-term toxicity test was conducted to determine the toxicity of manganese (Mn) to Japanese medaka (*Oryzias latipes*). NOEC was derived as 5 mg-Mn/L. Consequently, PEC/PNEC ratio regarding to Mn was obtained from the result of leaching tests as 0.015 which was much lower than the value (4.67) obtained from the data of Mn contents in the sediment. It was indicated that leaching from sediment is an important factor to evaluate the environmental risk of Mn to fishes just after an event of sediment supply.

REFERENCES

[1] Fukuoka, S., *et al*. (Eds.). Advances in river sediment research. CRC Press, pp1193-1199, 2013

[2] Kondolf, G. M. Hungry water: effects of dams and gravel mining on river channels, *Environmental management*, **21**(4), 533-551, 1997.

[3] Test No. 210: Fish, Early-life Stage Toxicity Test, OECD Guidelines for the Testing of Chemicals, Section 2, 2013

[4] the Chubu Regional Development Bureau, Reports on the review committee meeting of comprehensive sediment management for Yahagi River system, 2016 (Japanese)

[5] Stubblefield, W. A., *et al*. Effects of water hardness on the toxicity of manganese to developing brown trout (Salmo trutta). *Environ. Toxicol. Chem.*, **16**(10), 2082-2089, 1997

O6-21

Recent Progress of an Advanced Eco-Hydrologic and Biogeochemical Coupling Model in Terrestrial-Aquatic Continuum

Tadanobu Nakayama[1]

[1]National Institute for Environmental Studies

Keywords: modeling, eco-hydrology, biogeochemical cycle, coupling model, inland water

ABSTRACT

The author has developed process-based National Integrated Catchment-based Eco-hydrology (NICE) model to integrate coupled human and natural systems and to assess impact of water degradation on ecosystem change. Here, the author further developed an advanced model coupling eco-hydrology and biogeochemical cycle (NICE-BGC), which incorporates the whole process of carbon cycling including surface runoff, groundwater, weathering, CO_2 evasion and sediment storage in water, and outflow to the ocean. Because the new model included CO_2 evasion and lateral carbon transport explicitly, the result suggests most previous researches have generally overestimated the accumulation of terrestrial carbon and underestimated the potential for lateral transport. The model result also showed that there is a great variability of DOC, POC, and DIC transport to the ocean reflecting biologic and hydrologic processes, and CO_2 degassing affected by both terrestrially derived CO_2 and CO_2 production through aquatic metabolism.

1. INTRODUCTION

Recently, some studies have pointed out that inland waters including rivers, lakes, and groundwater may act as a significant transport pathway for both water and dissolved substances[2,4]. However, their contribution to continental-scale carbon cycling has remained uncertain because they are generally more difficult to measure and the available data for global aquatic ecosystems are fewer and more heterogeneous than those for terrestrial ecosystems[1,4]. In this paper, the author showed the recent progress in eco-hydrology and biogeochemical cycle model in terrestrial-aquatic continuum[26]. Because these mechanisms are closely interconnected with each other[30] and sometimes the carbon cycle may be triggered or greatly altered by extreme events[31], the coupling simulation will play a role in the integration of greenhouse gas budget of the biosphere, quantification of hot spots along a terrestrial-aquatic continuum, and bridging the gap between bottom-up and top-down approaches.

2. MODEL DEVELOPMENT

2.1. National Integrated Catchment-based Eco-hydrology (NICE) model

The author and his colleagues have developed the National Integrated Catchment-based Eco-hydrology (NICE) model (Fig. 1)[5-25]. NICE takes into account complex interactions between the forest canopy, surface water, the unsaturated zone, aquifers, lakes, and rivers. This model also simulates iteratively nonlinear interactions between hydrologic, geomorphic, and ecological processes. Using

NICE, the author has previously attempted to extract the impacts of discharge and groundwater-level change, sediment deposition, and nutrient availability on the complex pattern of vegetation succession in Kushiro Wetland[5,8,9,12,19,21,24]. The model was also applied to Lake Kasumigaura[10], Tokyo Metropolitan Area[7,13,17,18,20], Changjiang and Yellow Rivers[6,11,14-16,22,23,25], West Siberia[29], and Mekong River[26], etc.
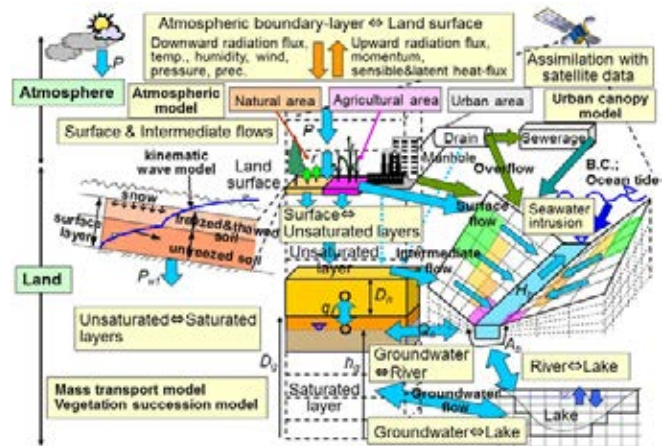
Fig. 1 NICE model

2.2. Coupling NICE with Biogeochemical Cycle Models (NICE-BGC)

In order to fill the gap in the current eco-hydrology models, the author has recently coupled the original NICE with various biogeochemical cycle models, including terrestrial ecosystems, water quality in aquatic ecosystems, and carbon weathering (Fig. 2)[26,27]. In this modified NICE

(NICE-BGC), all submodels were coupled together with the original NICE to conserve the carbon budget. Each submodel offers iterative simulation in the most efficient way by combining on-line and off-line modes. The newly coupled model incorporates the connectivity of the biogeochemical cycle and the hydrologic cycle for surface water and groundwater, hillslopes and river networks, and other intermediate regions.
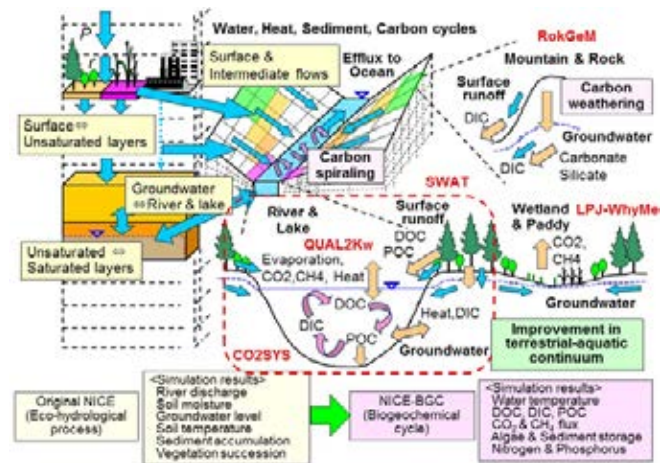
Fig. 2 New development of NICE-BGC

3. RESULTS

The author has compiled as many data as possible and calculated averaged values of CO_2 evasion to the atmosphere, and discharge, TOC, DOC, POC, DIC-flux to the ocean at global major basins. The author also showed that annual-averaged values obtained by NICE-BGC were generally in the ranges of previous studies; carbon export from land to inland water was about 2.01±1.98 PgC/yr, degassing above the water about 0.79±0.38 PgC/yr, sediment storage about 0.20±0.09 PgC/yr, and the rest transported to the ocean about 1.13±0.50 PgC/yr[27]. Fig. 3 shows the simulated seasonal variations of global carbon flux from terrestrial into aquatic ecosystems and in inland water[28]. As for terrestrial carbon flux, more DOC and POC are exported (about 458.38±474.41 TgC/season and 239.25±289.90 TgC/season) during Jan. - Mar., dominantly affected by the transport in rivers of South America and secondly by the spring snowmelt in northern boreal and subarctic peatlands[29]. In contrast, DIC flux is smallest (about 45.22±50.31 TgC/season) during Jan. - Mar. The seasonal variation of inland carbon flux is more complicated by terrestrially derived carbon inflow and carbon production through aquatic metabolism. While DOC and DIC flux are similar trend as in the terrestrial carbon flux, CO_2 degassing is higher (about 294.66±93.80 TgC/season) during Apr. - Jun. remarkable in South America, Africa, and Asia[3]. Sediment storage is larger (about 76.80±13.19 TgC/season) during Jul. - Sept. greatly

affected by the higher flow in Asia and North America.
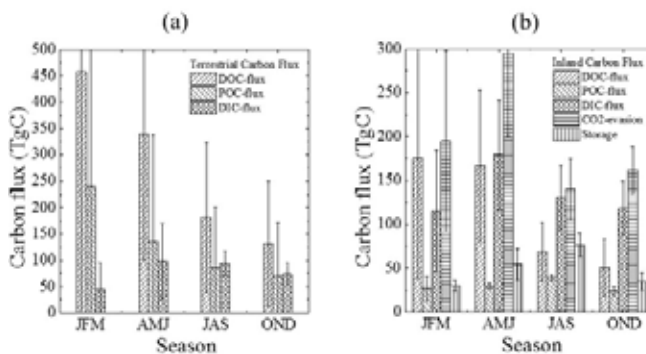
Fig. 3 Seasonal variations of global carbon flux;

(a) from terrestrial and (b) in inland water.

4. DISCUSSION

NICE-BGC calculates the whole process of carbon cycling including surface runoff, groundwater, weathering, CO_2 evasion and sediment storage, and outflow to the ocean. Yet it is necessary to improve the accuracy of the simulations; carbon assimilated by plants and water availability, weathering process, and the carbon cycle in the estuary, etc. In order to separate more clearly the carbon source in inland waters from the terrestrial carbon sink, it is necessary to couple this process-oriented model with scaling up site-level observations of aquatic ecosystems, and to improve a spatial resolution of atmospheric inverse model assimilated with the bias-corrected satellite data. If this component proves to be important, it is likely that the terrestrial CO_2 sink will prove to have a smaller contribution to the global carbon cycle than considered so far.

5. CONCLUSION

The new process-based model NICE-BGC incorporates the whole process of carbon cycling in terrestrial-aquatic continuum. The model result showed that there is a great variability of DOC, POC, and DIC transport to the ocean reflecting biologic and hydrologic processes, and CO_2 degassing affected by both terrestrially derived CO_2 and CO_2 production through aquatic metabolism. Because these were usually evaluated separately in the previous researches, there is a great improvement from them.

REFERENCES

[1] Aufdenkampe, A.K., et al.: Riverine coupling of biogeochemical cycles between land, oceans, and atmosphere. Front. Ecol. Environ., 9(1), 53-60, doi:10.1890/100014, 2011.

[2] Battin, T.J., et al.: The boundless carbon cycle. Nat. Geosci., 2, 598-600, 2009.

[3] Borges, A.V., et al.: Globally significant greenhuose-gas

emissions from African inland waters. Nat. Geosci., 8, 637-644, doi:10.1038/ngeo2486, 2015.

[4] Cole, J.J., et al.: Plumbing the global carbon cycle: integrating inland waters into the terrestrial carbon budget. Ecosystems, 10, 171-184, doi:10.1007/s10021-006-9013-8, 2007.

[5] Nakayama, T., Watanabe, M.: Simulation of drying phenomena associated with vegetation change caused by invasion of alder (Alnus japonica) in Kushiro Mire. Water Resour. Res., 40(8), W08402, doi:10.1029/2004WR003174, 2004.

[6] Nakayama, T., et al.: Simulation of groundwater dynamics in North China Plain by coupled hydrology and agricultural models. Hydrolol. Process., 20(16), 3441-3466, doi:10.1002/hyp.6142, 2006.

[7] Nakayama, T., et al.: Effect of underground urban structures on eutrophic coastal environment. Sci. Total Environ., 373(1), 270-288, doi:10.1016/j.scitotenv.2006.11.033, 2007.

[8] Nakayama, T.: Factors controlling vegetation succession in Kushiro Mire. Ecol. Model., 215, 225-236, doi:10.1016/j.ecolmodel.2008.02.017, 2008a.

[9] Nakayama, T.: Shrinkage of shrub forest and recovery of mire ecosystem by river restoration in northern Japan. Forest Ecol. Manag., 256, 1927-1938, doi:10.1016/j.foreco.2008.07.017, 2008b.

[10] Nakayama, T., Watanabe, M.: Missing role of groundwater in water and nutrient cycles in the shallow eutrophic Lake Kasumigaura, Japan. Hydrol. Process., 22, 1150-1172, doi:10.1002/hyp.6684, 2008a.

[11] Nakayama, T., Watanabe, M.: Role of flood storage ability of lakes in the Changjiang River catchment. Global Planet. Change, 63, 9-22, doi:10.1016/j.gloplacha.2008.04.002, 2008b.

[12] Nakayama, T.: Simulation of hydrologic and geomorphic changes affecting a shrinking mire. River Res. Applic., 26(3), 305-321, doi:10.1002/rra.1253, 2010.

[13] Nakayama, T., Fujita, T.: Cooling effect of symbiotic urban pavements made of new materials on water and heat budgets. Landscape Urban Plan., 96, 57-67, doi:10.1016/j.landurbplan.2010.02.003, 2010.

[14] Nakayama, T., et al.: Simulation of water resource and its relation to urban activity in Dalian City, Northern China. Global Planet. Change, 73, 172-185, doi:10.1016/j.gloplacha.2010.06.001, 2010.

[15] Nakayama, T.: Simulation of the effect of irrigation on the hydrologic cycle in the highly cultivated Yellow River Basin. Agr. Forest Meteorol., 151, 314-327, doi:10.1016/j.agrformet.2010.11.006, 2011a.

[16] Nakayama, T.: Simulation of complicated and diverse water system accompanied by human intervention in the North China Plain. Hydrol. Process., 25, 2679-2693, doi:10.1002/hyp.8009, 2011b.

[17] Nakayama, T., Hashimoto, S.: Analysis of the ability of water resources to reduce the urban heat island in the Tokyo megalopolis. Environ. Pollut., 159, 2164-2173, doi:10.1016/j.envpol.2010.11.016, 2011.

[18] Nakayama, T.: Visualization of missing role of hydrothermal interactions in Japanese megalopolis for win-win solution. Water Sci. Technol., 66(2), 409-414, doi:10.2166/wst.2012.205, 2012a.

[19] Nakayama, T.: Feedback and regime shift of mire ecosystem in northern Japan. Hydrol. Process., 26(16), 2455-2469, doi:10.1002/hyp.9347, 2012b.

[20] Nakayama, T., et al.: Multi-scaled analysis of hydrothermal dynamics in Japanese megalopolis by using integrated approach. Hydrol. Process., 26(16), 2431-2444, doi:10.1002/hyp.9290, 2012.

[21] Nakayama, T.: For improvement in understanding eco-hydrological processes in mire. Ecohydrol. Hydrobiol., 13, 62-72, doi:10.1016/j.ecohyd.2013.03.004, 2013.

[22] Nakayama, T., Shankman, D.: Impact of the Three-Gorges Dam and water transfer project on Changjiang floods. Global Planet. Change, 100, 38-50, doi:10.1016/j.gloplacha.2012.10.004, 2013a.

[23] Nakayama, T., Shankman, D.: Evaluation of uneven water resource and relation between anthropogenic water withdrawal and ecosystem degradation in Changjiang and Yellow River basins. Hydrol. Process., 27(23), 3350-3362, doi:10.1002/hyp.9835, 2013b.

[24] Nakayama, T.: Hydrology–ecology interactions. In: Eslamian, S. [Ed] Handbook of Engineering Hydrology - Vol. 1: Fundamentals and Applications. CRC Press, Florida, 329-344, 2014.

[25] Nakayama, T.: Integrated assessment system using process-based eco-hydrology model for adaptation strategy and effective water resources management. In: Lakshmi, V. [Ed] Remote Sensing of the Terrestrial Water Cycle. Geophysical Monograph Series 206, American Geophysical Union and John Wiley & Sons, Inc., 521-535, 2015.

[26] Nakayama, T.: New perspective for eco-hydrology model to constrain missing role of inland waters on boundless biogeochemical cycle in terrestrial-aquatic continuum. Ecohydrol. Hydrobiol., 16, 138-148, doi: 10.1016/j.ecohyd.2016.07.002, 2016.

[27] Nakayama, T.: Development of an advanced eco-hydrologic and biogeochemical coupling model aimed at clarifying the missing role of inland water in the global biogeochemical cycle. J. Geophys. Res. Biogeosci., 122, 966-988, doi: 10.1002/2016JG003743, 2017a.

[28] Nakayama, T.: Scaled-dependence and seasonal variations of carbon cycle through development of an advanced eco-hydrologic and biogeochemical coupling model. Ecol. Model., 356, 151-161, doi: 10.1016/j.ecolmodel.2017.04.014, 2017b.

[29] Nakayama, T., Maksyutov, S.: Application of process-based eco-hydrological model to broader northern Eurasia wetlands through coordinate transformation. Ecohydrol. Hydrobiol., doi: 10.1016/j.ecohyd.2017.11.002, 2018.

[30] Regnier, P., et al.: Anthropogenic perturbation of the carbon fluxes from land to ocean. Nat. Geosci., 6, 597–607, doi:10.1038/ngeo1830, 2013.

[31] Reichstein, M., et al.: Climate extremes and the carbon cycle. Nature, 500, 287-295, doi:10.1038/nature12350, 2013.

O6-22

Impact of climate change on changes in river water temperature simulated with SIPHER model in Takasaki River basin, Chiba, Japan

Rajendra KHANAL[1,2], Yuichi NAGANO [3], Kenji TANIGUCHI [4] and Hiroaki FURUMAI [1]

1 Research Center for Water Environment Technology, the University of Tokyo, 7-3-1 Hongo, Bunkyo-ku, Tokyo 113-8656, Japan (rajendra.khanal@gmail.com)

2 Department of Civil and Environmental Engineering, Tokyo Institute of Technology, Japan

3 Department of Urban Engineering, the University of Tokyo, Japan

4 Faculty of Environmental Design, Kanazawa University, Kanazawa, Japan

Keywords: land use, meteorological, SIPHER model, Takasaki basin, long term monitoring

ABSTRACT

In this research, uncertainty of the future climate change was investigated by continuous long term monitoring and validation of the simulated temperature obtained with SIPHER[TM] model. Model was calibrated and validated for 2012 – 2016 from water temperature collected across 8 stations in Takasaki river, Chiba, Japan. Water quality parameters namely, water temperature, water depth, and electrical conductivity were measured at every 10 minute interval with sensors. Monthly average of the observed and simulated water temperature for stations with higher pervious areas was found to be close to each other (R^2 > 0.90). In general, it was observed that the simulated temperature obtained with SIPHER model was less reproducible for small basin (R^2 < 0.90). Future metrological parameters were predicted with CNRM-CM5 general circulation model. Impact of climate change in river water was then done for the present (2000 – 2010) and future (2060 – 2070) decade. Monthly average future temperature decreased by at least - 0.2 ^{O}C in Dec-Jan-Feb-Mar, and increased by 1.2 ^{O}C in October, and at least 0.2 ^{O}C in Apr-May-Jun-July-Aug-Sep. It is confirmed that due to climate change, temperature in winter decreases whereas it increases in summer.

1. INTRODUCTION

In order to understand long term effect of the climate change, it is necessary to do continuous long term monitoring of the river water temperatures. The temperatures simulated with various models needs to be validated with the observed water temperature. Uncertainty of the future climate change must be investigated with the available data, which can be done by continuous long term monitoring and validation of the monitored data with the simulated data.

Most of the model for the simulation of water temperature

is based on the net heat balance across water bodies. The heat load comes from shortwave and long wave radiation, latent and sensible heat, wastewater and groundwater. The radiations are in-turn dependent on metrological condition, mainly the air temperature absorbance or reflectance of the water bodies and upper basin area. Depending on the nature of the basin area, it might be pervious or impervious. In pervious area, the heat from radiation is absorbed and transmitted into the ground surface, whereas in impervious area, mainly consisting of concrete drainage channel, roads, and buildings, surface runoff increases and higher will be reflectance of the longwave radiation, and higher will be the absorbed heat from the shortwave solar

radiation (insolation). With urbanization, population growth, the pervious area decreases and at the same time increase in industrial activity leads to increase in wastewater discharge, which might also act as a source of heat to the receiving water bodies.

The temperature across the Takasaki basin is simulated with deterministic model employing the physics of heat exchange between the river and the surrounding environment. Model calibration and validation was carried out using water temperature data collected at several monitoring sites during 2012 - 2016. The data are composed of the monitoring of the temperature in 8 stations across Takasaki river basin, and 1 each in Taguri and Kashima river.

The main objective of this paper is to analyze an impact of climate change in variation of present (2000 – 2010) and future (2060 – 2070) decade river water temperature in Takasaki River, Chiba, Japan simulated with SIPHER™ model across wide range of catchments.

2. METHOD

The study is Takasaki river Basin in Chiba prefecture, Japan. This Taksaski river is one of the major tributary river flowing into the lake Inba-Numa. Map of observation site and landuse pattern is shown in **Fig. 1**.
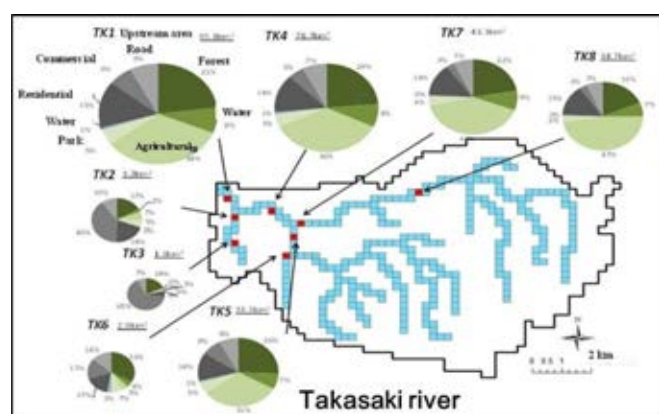
Fig. 1. Map of the sampling point in Takasaki river

The routine water quality parameters, water temperature, water depth, electrical conductivity were measured at every 10 minute interval with sensors TidbiT v2 Temp Logger, water depth HOBO Water Level Loggers respectively from April 2012 to Dec 2016.

River water temperature was simulated with the SIPHER™ model (Pacific Consultants, Tokyo, Japan),

which is a GIS based hydrologic model consisting of six submodels of evapotranspiration, ground water flow, surface water flow, channel routing, point and non-point source pollutants loading (Uehara et al., 2008). Future metrological parameters were predicted with CNRM-CM5 general circulation model.

3. RESULTS

Time series variation of observed and simulated temperature along with the precipitation and simulated flow rate for 2012-2016 for stations TK1 is given in **Fig. 2.** St. TK1 is characterized by greater pervious area (71%) and higher upper river basin area (85.1 km^2), whereas St. TK2 has lesser pervious area (30%) and lower upper river basin area (3.3 km^2) (**Table 1**). The weighted pervious area in St TK1 and TK2 is 60.4 and 1.0 km^2 respectively.

For St. TK1 with higher weighted pervious area, the simulated and observed temperature were close to each other (R^2=0.9525), and that for St. TK2 with lower weighted pervious area, the simulated and observed temperature (R^2=0.9010) varied a lot. It was found as the weighted pervious area decreased, the coefficient of determination decreased (**Table 1**). The exact reason for the higher simulated water temperature in lesser pervious area is not clear, however it might be due to overestimation of heat load from the shortwave and longwave radiation. In an area with lesser pervious area, or to say with higher impervious areas, the presence of concrete like materials, as evident by concrete water tunnel in St, TK2, the incoming shortwave radiation is overestimated than the outgoing longwave radiation and net heat load from latent and sensible heat.

Table 1. Regression coefficient for observed and simulated temperature

Weighted pervious area, km^2	Regression equation	R^2	St. code	Pervious %	Upper river basin area, km^2
60.4	y = 0.8383x + 2.934	0.9525	TK1	71	85.1
57.5	y = 0.7903x + 3.710	0.9462	TK4	73	78.7
32.9	y = 0.7652x + 4.324	0.9516	TK7	76	43.3
26.4	y = 0.6697x + 5.620	0.9163	TK8	76	34.7
23.6	y = 0.7457x + 3.981	0.9335	TK5	71	33.3
1.5	y = 0.7123x + 5.379	0.9037	TK6	53	2.9
1.0	y = 0.7214x + 0.638	0.9010	TK2	30	3.3
0.3	y = 0.5409x - 0.486	0.8123	TK3	22	1.3

Variation in present and future decade water temperature for St. TK1 varied with a minimum of -0.3 ^{O}C in February and maximum of 1.2 ^{O}C in October. In general, future water temperature during winter (Dec-Jan-Feb-Mar) decreased and in summer (Apr-May-June-Jul-Aug-Sep-Oct-Nov) increased than the present decade temperature (**Fig. 3**).

4. DISCUSSIONS

The net heat balance across water bodies is the sum of incoming shortwave radiation, outgoing longwave radiation, latent of vaporization (or condensation) and sensible heat. If heat received by water bodies is taken as positive, then shortwave is positive, longwave is negative, latent heat of vaporization is positive (or condensation is negative), and sensible heat positive or negative depending on the temperature change of water. In SIPHER^{TM} it might be that the shortwave radiation is overestimated and longwave radiation is underestimated due to higher impervious nature of the surface. In addition, heat load from groundwater is also not considered in SIPHER which makes it difficult to calibrate for the smaller basin. The upper basin land use pattern also has an influence on heat load received from surface runoff and wastewater inflow, which needs to be further streamlined to validate heat load in the smaller basin

5. CONCLUSION

- SIPHER model can accurately simulate the river water temperature in an areas with highly pervious area (> 70%), and higher upper basin area (> 30 km^2), than that in the lower pervious area (< 50%) and lower upper basin area (< 3 km^2).
- Due to climate change monthly average temperature in winter and summer will be lower and higher than the current temperature.

6. Acknowledgement

REFERENCES

[1] Uehara, H., et al., 2008. The Water Balance and Mass Balance in Lake Inba-Numa Basin by the Hydrological and Material Cycle Model. Proceedings of 11th symposium of Japan Society on Water Environment. 17-18 September, pp. 32–33 (In Japanese).

[2] Khanal, R., et al., 2016. Application of SIPHER model in analyzing present and future water temperature in Takasaki River, Chiba, Japan. The 12th International Symposium on Southeast Asian Water Environment (SEAWE2016), Hanoi, Vietnam, November 28-30, 2016
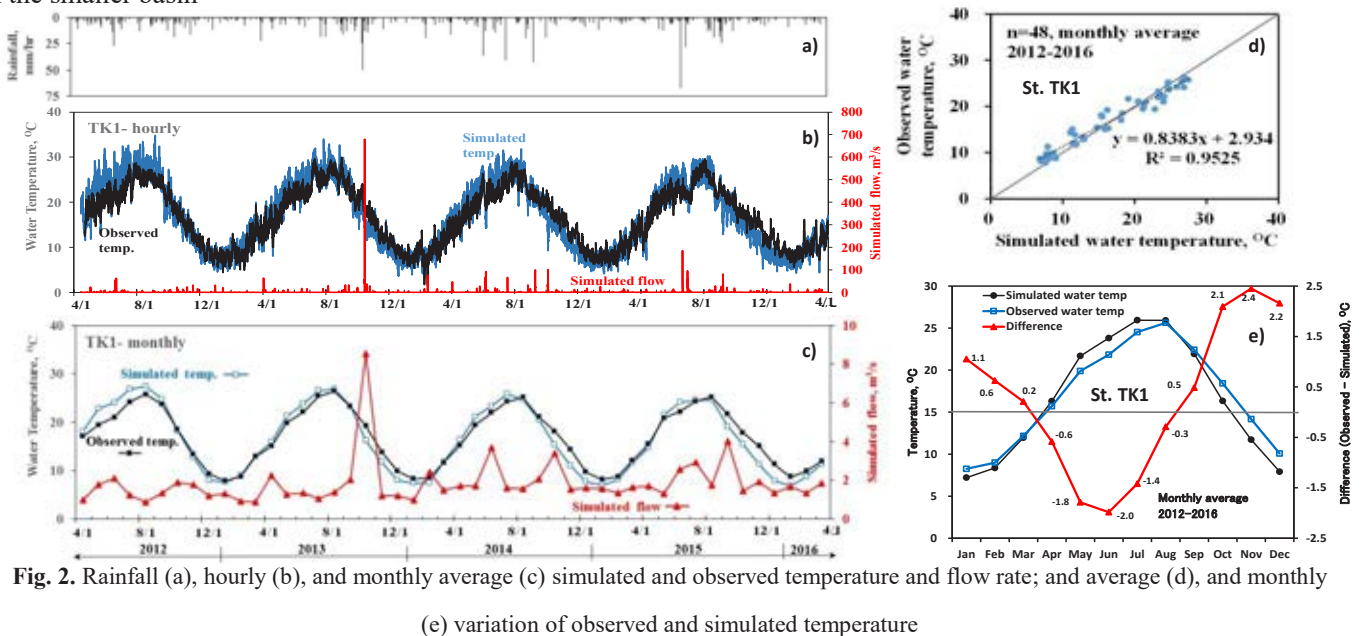
Fig. 2. Rainfall (a), hourly (b), and monthly average (c) simulated and observed temperature and flow rate; and average (d), and monthly (e) variation of observed and simulated temperature
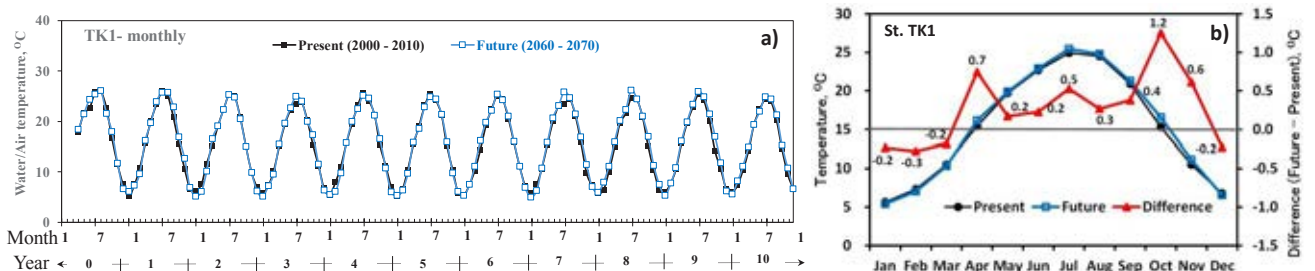
Fig. 3. a) Simulation of the present decade (2000 – 2010) and future decade (2060 – 2070) water temperature, and

O6-23

Assessment of Stream Flow Using Soil and Water Assessment Tool (SWAT) In Loktak Lake Catchment

Ritesh Sikka

Wetlands International South Asia

Keywords: Stream flow, Hydrological modelling, SWAT, Loktak, ungauged

ABSTRACT

Stream flow is very important in water cycle and a useful water resource to sustain human life. However, estimation of stream flow in an ungauged catchment still poses a challenge. Hydrological models are one of the commonly used techniques for the discharge simulation in ungauged stations. This paper focusses on the estimation of stream flow in the Loktak Lake catchment (part of the Manipur river basin) using Soil and Water Assessment Tool (SWAT). SWAT, developed by the United States Department of Agriculture which analyzes the stream flow based on Digital Elevation Model (DEM), soil map, land use map and meteorological dataset. The SWAT tool was run for the year 1999-2002 on 2 gauged sub-catchments (Nambul and Iril), which are calibrated and validated using the observed discharge. Calibration was carried out using manual iterative process and the evaluation of the model was done using Nash-Sutcliffe model efficiency (NSE) coefficient. The results between observed and modelled flow showed agreement with NSE value 0.837 for Iril River and 0.796 for Nambul River. These results were used to estimate the ungauged sub-catchment flows. The results show high variation in discharge of all the rivers with high discharge during monsoon season and low in the other month of the year. The highest flow was found in Iril followed by Thoubal. This assessment can be helpful in generating the water balance of Loktak Lake.

1. INTRODUCTION

Water resources are essential renewable resources that are the basis of existence and development of society. Proper utilization of these resources requires assessment and management of the quantity and quality of water resources. Water crises caused by shortage, floods and diminishing water supply are increasing in all parts of the world. Mismanagement and increasing pressure from human activities like water diversion, pollution and reclamation of area has added to pressure of the water resources.

Surface water being easy and direct is therefore easy to exploit as compared to other water resources. Surface water in the form of Lakes and River runoff (discharge) is predominantly obtained from rainfall after being generated from the rainfall runoff process. In order to make decision in planning of water resources long runoff data series is required. However, in most cases, this is not feasible due to a variety of reasons such as financial, logistics or purely due to lack of intent [2]. This leads to the fact that a large portion of the total number of river basins present around the globe are either poorly gauged or completely ungauged.

A rainfall-runoff model can be therefore used to estimate the streamflow. Soil and Water Assessment Tool (SWAT) is a most commonly used model for hydrological modeling which gives reliable results. SWAT is a physically based, continuous, long-term, semi distributed hydrologic model, developed by the U.S. Department of Agriculture. It is a conceptual model that works both on daily and sub daily time steps [1]. It can simulate surface and subsurface flow, soil erosion, nutrient cycling and transport, and sediment deposition, and has been applied worldwide in hydrologic and water quality modeling [9].

The objective of this study is to analyze the daily rainfall-runoff study of the basin, analyze the performance of the model with the observed data and stimulate the streamflow of the ungauged rivers in the basin.

2. METHOD

Study Area Description

Loktak wetland complex (LWC) (area 470.15 km2) is the largest freshwater wetland in North east India located in the southern part of Manipur valley along the Manipur river. Spanning between 24.400 to 24.720 latitudes and 93.760 to 93.990 longitudes, the wetland is located in the interfluvial areas as different tributaries, and hill stream connect with the main channel[9]. The complex comprises Loktak lake (the largest wetland of the complex, area 287 km2), Ikop- Kharung and Pumlen- Khoidum. The complex has a catchment area of 5203.65 km^2 which is divided into 8 sub-catchments (Figure 1)

LWC is located in the central valley of the catchment. Hills varying from 900m to 3000m amsl fringe the valley area with steep slopes[8]. The Manipur valley is made up of alluvium of fluvio-lacustrine origin, with clay being the main form of origin followed by silt and sand.

The valley is characterized by a tropical monsoon climate. During 1954-2011, the rainfall within the state varies from 956.5 to 2269.9 mm, with monsoon months (June to October) accounting for 63% of the total rainfall. With mean temperature at 4° C, January was recorded as the coldest month and July as the hottest at 29° C. [3].

Due to its rich biodiversity and its socio-economic importance, Loktak Lake was designated as a wetland of internationally importance under the Ramsar Convention in 1990. However, the Loktak Multipurpose Project for generating 105 MW of hydro-electric power, have resulted in major modifications to the lake's hydrological regime leading to raised mean water levels and reduced the magnitude of seasonal fluctuations.
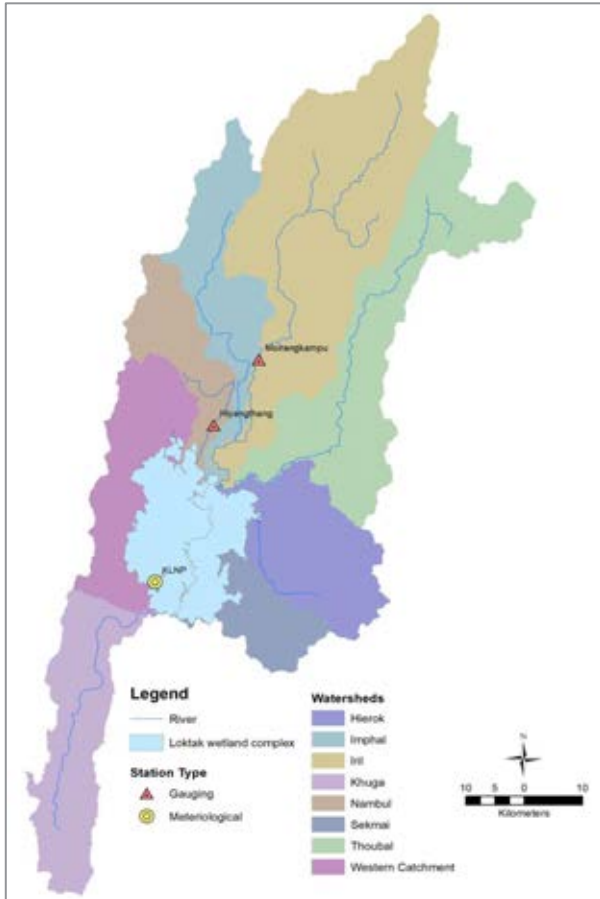
Figure 1 - Loktak Lake, its sub-watersheds and gauging stations

SWAT Model Description

To analyze the stream flow of all the rivers in the catchment Arc SWAT (version 2009) was selected. SWAT is a semi-distributed, continuous hydrological model which functions on a daily time scale to predict the impact of land management on water, sediment and water quality of large basins. This model divides a large watershed into sub-watersheds, which are further sub-divided into a series of hydrological response units (HRUs), a unique combination of land use, soil, and slope. When parameters are simulated, they are first estimated for each HRU and then accumulated for the whole watershed as a weighted average[7].

Soil water balance is the primary consideration by the model in each HRU which is represented by equation below:

$$SW_t = SW_0 + \sum_{i=1}^{t} \left(R_i + Q_{surf} + E_a + w_{seep} + Q_{gw} \right) \qquad (1)$$

Where SW_t is final soil water content; SW_0 is the initial soil water content, R_i is the amount of precipitation, Q_{surf} is the amount of surface runoff, E_a is the amount of actual Evapotranspiration, w_{seep} is the percolation from the soil profile, and Q_{gw} is the amount of return flow on day i

Dataset

SWAT requires Digital Elevation Model (DEM), Soil Map, Landuse Map and daily meteorological data as input to run the model. A brief description of the data is shown in Table 1. The location of Weather station and Gauged streams in Fig 1

Table 1-Data used for SWAT modelling

Data	Data Source	Year
DEM	SRTM DEM	Feb 2000
Soil Map	NBSS&LUP[6]	2001
Landuse Map	Landsat 8	Feb 2017
Weather Data	LDA	1999-2002
Gauged Station	LDA	1999-2002

(LDA- Loktak Development Authority, NBSS&LUP – National Bureau of Soil Survey and Land Use Planning)

Modelling Process

For the purpose of modelling the catchment of LWC has been sub-divided into eight sub-catchments namely the Thoubal, Iril, Imphal, Khuga, Hierok, Sekmai and Western sub-catchment and Nambul. Out of these sub-catchments, Iril and Nambul is gauged while the others are ungauged. The modelling of the sub-catchment was undertaken using the hydro meteorological data available for the three year (June 1999–May 2002).

Given the paucity of data, the approach to model calibration and validation was to initially calibrate the model of the Iril sub-catchment with available observed discharge data and then to apply the same calibrated parameter values to models developed for the Nambul sub-catchments as validation. The dataset set for Iril and Nambul is clipped from that of the Loktak catchment.

This form of validation exercise was considered appropriate given the similar geology, soils and vegetation cover within the sub-catchments in addition to similar flow regime with high monsoon and low dry season flows. Discharges for the ungauged sub-catchment were subsequently estimated by using the same parameters as used in validation and running the model on the whole catchment.

Model Calibration & Evaluation

The calibration needs to be taken place to identify the optimized parameter set which might have an impact on the catchment response. These parameters may or may not have any physical meaning, but they have a high level of uncertainty associated with them [4]. The calibration process takes place by adjusting the values of soil parameters, land use parameters and flow parameters like Manning's 'N' and soil saturated conductivity 'k'.

The model calibration and validation is evaluated using Nash & Sutcliffe Efficiency (NSE) method. NSE is a measure of correlation, bias and variability [5], which is one of the most widely used criteria for performance evaluation all over the world. NSE varies from -∞ to 1. A value of 1, points towards a perfect match between observed and simulated value. The expression for NSE is:

$$NSE = 1 - \sum_{t=1}^{T} \left(\frac{Q_0^t - Q_m^t}{Q_0^t - Q_0 \; mean} \right)^2 \qquad (2)$$

Where Q_0^t-Observed Discharge at time t, Q_m^t-Modelled Discharge at time t and $Q_0 \; mean$-Mean Observed Discharge

3. RESULTS AND DISCUSSION

Model Calibration

The calibration was carried out in Iril sub catchment as

described in the previous section. Calibration was carried out using manual iterative process. Manning's 'N' was the most sensitive parameter and the model was run changing the value of N and evaluating the results using NSE. The final Manning's 'N' value was calibrated to 0.014 from default value of 0.04.

Figure 3 shows the observed and projected discharge in the Iril sub-catchment for the period May 1999 to Dec 2002. The graph shows that the model is generally successful in reproducing the observed daily flows. The model is considered good with NSE value being 0.837.
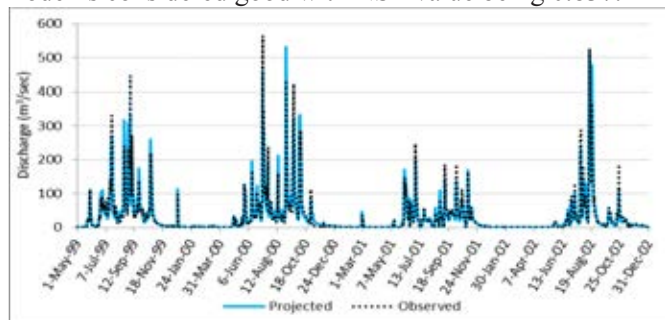
Figure 3 - Observed and Projected discharge of Iril watershed

Model Validation

The validation of the model was carried out using the calibrated parameters of the Iril model in Nambul model. The model was validated by comparing the observed and projected discharges in the Nambul sub-catchment (Figure 4). The model showed good results and was successful in reproducing the observed daily flows with NSE value being 0.796.
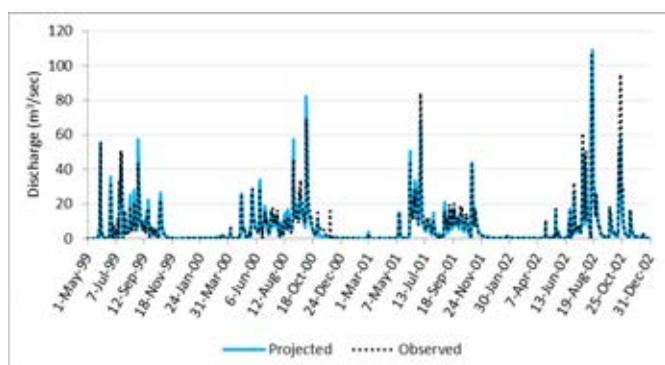
Figure 4 - Observed and Projected discharge of Nambul watershed

Runoff for Ungauged Catchment

After the validation is complete the same parameters are run the model for the whole catchment to analyze the runoff from the whole catchment as all the other sub-catchments are ungauged. The monthly stimulated discharge of all the catchments is shown in Figure 5.

4. CONCLUSION

In this study the SWAT model was applied to evaluate the streamflow in the direct catchment of the Loktak wetland Complex. The daily flow was calibrated for Iril sub-catchment and then validated in Nambul sub-catchment. Then the parameters were used to estimate the flows of the ungauged catchments.

The daily discharge in the calibration and validation
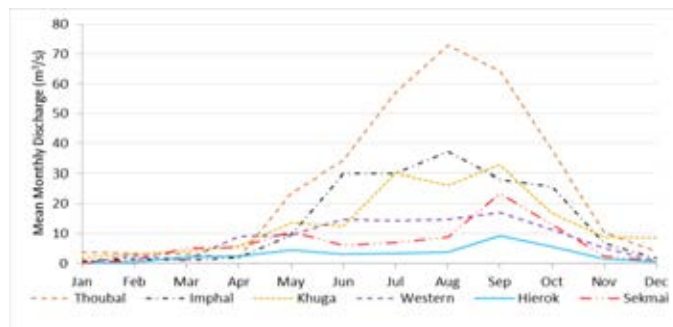
Figure 2 - Mean Monthly discharge for Ungauged watershed

models showed good performance with NSE values which is calculated from equation (2) of 0.837 in the calibration model and 0.796 in the validation model. Iril has the highest mean monthly discharge of 30.416m3/sec followed by Thoubal having 26.318 m3/sec. The minimum discharge is from Hierok and Nambul sub-catchment discharging 3.057m3/sec and 6.612m3/sec. These discharges form the ungauged catchment can be used for calculation of water balance of the lake.

Therefore, the SWAT model can be used to estimate the streamflow in the study area. But the present study is carried out using scarce data as there is no continuous metrological data management in the catchment since 2002 for the analysis of the present scenario. However detail analysis needs to be carried out to estimate the exact flow into the Lotak Lake.

REFERENCES

[1] Arnold, J.G., and N. Fohrer. 2005: Current capabilities and research opportunities in applied watershed modeling. Hydrol. Proc. 19: 563-572, 2005.

[2] Blöschl, G: Predictions in ungauged basins – where do we stand? , 7th International Water Resources Management Conference of ICWRS, 7, 2016.

[3] GoM: Manipur State Action Plan on Climate Change, Directorate of Environment, Government of Manipur, 2013

[4] Heuvelmans, G.; Muys, B. & Feyen, J.: Evaluation of hydrological model parameter transferability for simulating the impact of land use on catchment hydrology, Physics and Chemistry of the Earth, Parts A/B/C 29 (11–12), 739–747, 2004.

[5] Nash, J. E. and Sutcliffe, J. V.: River flow forecasting through conceptual models, Part 1: A discussion of principles, J. Hydrology, 10, 282–290, 1970.

[6] NBSS and LUP: Land Capability Classes of Catchment Area of Loktak Lake, Manipur, National Bureau of Soil Survey and Land Use Planning, Regional Centre, Jorhat and Kolkata, 47 pp., 2001.

[7] Neitsch, S.L.; Arnold, J.G.; Kiniry, J.R.; Williams, J.R. Soil and water assessment tool Theoretical documentation version 2009. 618p., Texas Water Resources Institute Technical Report No. 406, College Station, Texas, 2011

[8] Sing, C.R.: "Hydrological and Hydraulic Modelling for the Restoration and Management of Loktak Lake, Northeast India", PhD Thesis, University College London, United Kingdom, 2010.

[9] Trisal, C.L. and Manihar, Th.: The Atlas of Loktak Lake. Wetlands International-South Asia, New Delhi, India and Loktak Development Authority, Manipur, India, 93 pp., 2004.

O6-24

Developing A Model for Estimating Secchi Disk Depth using Landsat TM and ETM+ in Indonesian Lakes

Setiawan Fajar[1,4], Bunkei Matsushita[2], Takehiko Fukushima[3], Subehi Luki[4]

[1]Graduate School of Life and Environmental Sciences, University of Tsukuba, Tsukuba, Ibaraki, Japan
[2]Faculty of Life and Environmental Sciences, University of Tsukuba, Tsukuba, Ibaraki, Japan
[3]Ibaraki Kasumigaura Environmental Science Center, Okijyuku, Tsuchiura, Ibaraki 300-0023, Japan
[4]Research Centre for Limnology, Indonesian Institute of Sciences (LIPI), Bogor, West Java, Indonesia

ABSTRACT

A simple data pre-processing to minimize the atmospheric effects and improve data quality was proposed to build a model for estimating Secchi Depth (SD) from Landsat TM and ETM+ data. The model intended to be simply applicable without requirement of in-situ data for both atmospheric correction and model recalibration. Rayleigh scattering effects were removed using 6S software. Median filters were applied iteratively to improve the low Signal-to-Noise Ratio. Aerosol scattering effects in visible bands were reduced using the SWIR band. The reflectance extracted from pre-processed Landsat images and corresponding in-situ SD measurements from 9 lakes collected from 2011 to 2014 (ranging from 0.5 m to 18.6 m) were used for model calibration. Other in situ SD measurements from 31 Lakes collected in 1992-1993 (ranging from 0.4 m to 20 m) were used to validate the developed model. A long-term change of SD in Lake Maninjau estimated from the model was also compared with in situ data collected from 2001-2017 for another validation. Results show that the developed model provides acceptable result and robust estimates SD for both several different lakes in 1992 and long-term change SD of Lake Maninjau with determination coefficients of 0.81(with RMSE of 2.59 m, n=31) and 0.46 (with RMSE of 1.22 m, n=17) respectively. These results indicate that the developed model is simply applicable and has a potential to fill the SD data gap for further water environment studies.

1. INTRODUCTION

Lakes are habitats of great human importance as they provide water for domestic, industrial and agricultural use as well as providing food [1]. Despite their fundamental importance to humans, freshwater systems including lakes have been affected by anthropogenic disturbances. The disturbances cause the eutrophication, acidification and contamination by toxic substances. This problem is predicted to continue to increase, especially in developing countries where the developments prioritize other than environmental conservation [1]. Monitoring the environment is necessary to ensure the management practices achieve the sustainability [2]. For effective lake management, it is essential to have long-term water quality information on a broad regional and spatial scale [3].

One of important water quality parameter is secchi depth (SD). SD is the simplest and most often used for limnological measurements because its values are easily understood [4]. Assessing the SD is one of the key issues in environmental monitoring and management, because it can affect both ecosystems and water amenities [5].

Since conventional water-monitoring methods (e.g., water sampling from a boat) are very time-, labor-, and cost-consuming, the maintenance of steady monitoring is remain challenging for local and national governments with meager financial resources, especially in developing countries [6]. As the result, the number of in situ water quality data is very limited. On the other hand, the satellite remote sensing is a powerful supportive tool for assessing the spatial and temporal variation in water quality parameter such as SD [7, 8, and 9]. Combination of in situ and remote-sensing can be used to provide comprehensive data solutions to address sustainability issues because satellite technologies have the potential to provide better spatial and temporal coverage compare with traditional field sampling [2].

In general, studies on SD estimation using Landsat TM images can be classified into two major groups. The first group used the band ratio and the second group used the combination of single band plus band ratio as the SD predictor. Further, the studies can be differentiated whether they perform atmospheric correction or not. Previous models were built based on empirical relationship. Different band and band ratio combinations that were suggested from previous research may relate with the differences in image quality or limnological condition of the water body [10].

The existing models require to be recalibrated for other image from different time or other location. This is a significant challenge for the study areas which lack of in situ SD data. Kloiber et al. [11] mentioned that, ideally a

single (standard) relatively simple equation with constant coefficient values would be used to calculate SD or a phytoplankton abundance index. Their study indicated that if the atmospheric effect can be removed, then one set of coefficients can be applied for different images across time and space. However, the other challenge is the meteorological data to perform the atmospheric correction for the historical image are not always available. Therefore the objectives of this research are to develop a model for estimating SD from Landsat TM / ETM+ data, to test the model if it is simply applicable without requirement of in situ data for recalibration and to provide a showcase for long term SD estimation using the developed model.

2. METHOD

All 64 Landsat Images were downloaded from the USGS website [15] for model calibration and validation. The images were pre-processed to reduce the atmospheric effect and improve the data quality. The water bodies were extracted using the combination of Normalized Different Water Index (NDWI)[12] and Modified Normalized Different Water Index (MNDWI) [13], then area of a buffer of 150 m from the shoreline were excluded. Rayleigh scattering effects were removed using 6S with tropic atmospheric model. Median filters were applied iteratively to improve the low Signal-to-Noise Ratio. Aerosol scattering effects in visible bands were reduced using the SWIR band.

The reflectance extracted from 7 scenes pre-processed Landsat images and corresponding in-situ SD measurements from 9 lakes in Indonesia collected from 2011 to 2014 (ranging from 0.5 m to 18.6 m) were used for model calibration. Following Kloiber et al. [11] and Olmanson et al. [3] least-square multiple regressions were used to obtain the model coefficient. The model using the general form:

ln SD = a + b (single band) + c (band ratio), where a, b and c are model coefficient which can be obtained from the multiple regression analysis.

Second in-situ SD data set from 31 Lakes collected in 1992-1993 [14] (ranging from 0.4 m to 20 m) were used to validate the developed model. A long-term change of SD in Lake Maninjau estimated from Landsat using the developed model was also compared with in situ data collected from 2001-2017 for another validation.

3. RESULTS

The atmospheric correction resulted in Rayleigh and Aerosol corrected reflectance as shown in Fig. 1. It shows that over the water surface the proposed method gave better performance compare to surface

reflectance standard products [15]. The aerosol effect at the longer band (TM5 & TM7) can be mitigated pixel by pixel.
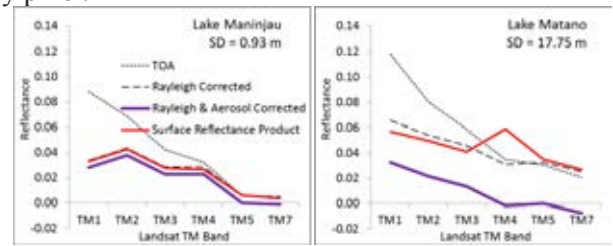
Fig. 1. Atmospherically corrected reflectance

In order to develop the model, wide ranges of in situ SD (0.5 – 18.6 m) were utilized in this research. It was limited in numbers (31 measurements from 9 Lakes), but covered a wide range of optical properties which are represent the variety of limnological conditions. The combination of filtered atmospherically corrected satellites data and the wide range in situ SD data were expected to be the optimum input for model development. All possible band combinations were tested as the result we select 6 models with best performance for further analysis, as shown in Table 1.

Table 1. Model Calibration performance

Model	Band Configuration	R^2	RMSE (m)	NMAE (%)
A1	TM1 & TM1/TM3	0.987	1.17	6.41
A2	TM2 & TM1/TM3	0.981	1.17	12.01
A3	TM3 & TM1/TM3	0.993	0.57	13.15
B1	TM1 & TM1/TM2	0.958	1.29	29.13
B2	TM2 & TM1/TM2	0.958	1.40	31.36
B3	TM3 & TM1/TM2	0.959	1.27	30.30

The accuracy of the selected models (A3 and B3) were plotted in Fig.2. The estimated SD is the average value which calculated from 90% of total water pixels (due the sampling site coordinate were not available). It was observed that the over estimation of model A3 are too large especially for clear water. Model B3 provide more acceptable result.
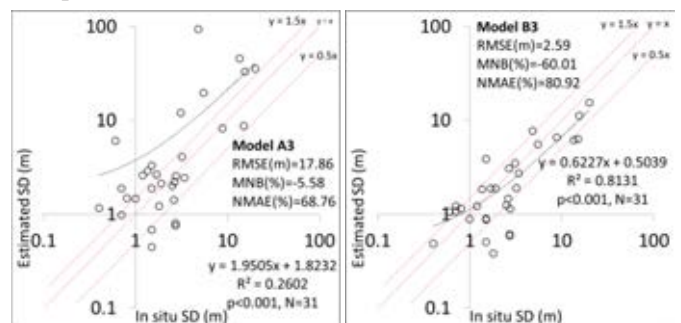
Fig. 2 Scatter plot of in situ versus Estimated SD

The water quality in lake can change over a short or long-time period. Model B3 then was used to estimate

SD of Lake Maninjau during 2001-2017 (Fig.3). The result showed that 30 years ago the average SD in Lake Maninjau was estimated around 5 m. However, starting from 2009 the SD values were steady lower than 2 m and both from measured and estimated. In-situ observation in August 2006 ranged from 2.25 m to 5.8 m, it showed that the SD in Lake Maninjau sometime was heterogeneous. From fig.3, we can also see that the estimated long-term SD from Landsat matched well with in-situ data.
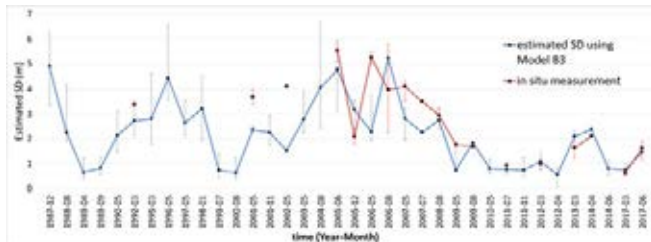
Fig 3. A showcase of long term SD estimation of Lake Maninjau using Model B3

4. DISCUSSION

The sources of estimation errors in this research are generally propagated from the time gap and the geographic location error. The validation data set 1 were collected from the field surveys conducted during 1992-1993. At those periods, the corresponding Landsat images were not always available. To make use of all in situ data we set the wider time window. Narrowing the time window into less than one month for validation data set 1, reduced the number of data which can be used into 11 data. The RMSE can be reduced to 1.21 m with the MNB = -21.23% and NMAE = 42.82%. This result indicates that a narrower time window can provide better accuracy.

The next limitation is that the sampling locations information is not available. Match-up between in situ and estimated SD from the model is not an ideal comparison. In this research, we compare the single value of in situ SD data and the average of the SD value from the whole water bodies.

5. CONCLUSION

In this study, a model for estimating SD using Landsat TM/ETM+ data has been developed. It uses TM3 and ratio of TM1/TM2 with fixed coefficient. It was proved to be consistent predictors of SD and more robust from noise.

The model can be simply applicable without requirement of recalibration on each image. Neither required atmospheric conditions information. It has been validated using two validation data set. Both estimated SD for several different lakes at the same period and time series of a lake showed reasonable result. However, the

applications for another different environment such as tempered lakes in mid or higher latitude are required to be further studied.

REFERENCES

[1] Brönmark, C., & Hansson, L: Environmental issues in lakes and ponds: Current state and perspectives. Environmental Conservation, Vol 29(3), pp. 290-307, 2002.

[2] Blake A. Schaeffer, Kelly G. Schaeffer, Darryl Keith, Ross S. Lunetta, Robyn Conmy & Richard W. Gould: Barriers to adopting satellite remote sensing for water quality management. IJRS, Vol. 34:21, pp. 7534-7544, 2013.

[3] Olmanson, L. G., Bauer, M. E., & Brezonik, P. L: A 20-year Landsat water clarity census of Minnesota's 10,000 Lakes. Remote Sensing of Environment, Vol. 112, pp. 4086–4097, 2008.

[4] Carlson, R.E: A trophic state index for lakes. Limnology and Oceanography, Vol.22, pp. 361-369, 1977.

[5] Fukushima,T., Matsushita, B., Yang, W., Jaelani, LM: Semi-analytical prediction of secchi depth transparency in Lake Kasumigaura using MERIS data. Limnology, The Japanese Society of Limnology, Vol.19(1). Pp.89-100, 2017.

[6] Matsushita, B., Yang, W., Jaelani, L., Setiawan, F. Fukushima, T : Monitoring water quality with remote sensing image data, Remote Sensing for Sustainability, Editors: Qihao Weng, pp. 163-189., CRC Press, 2016.

[7] Giardino, C., Pepe, M., Brivio, P.A., Ghezzi, P., Zilioli, E: Detecting chlorophyll, Secchi disk depth and surface temperature in a sub-alpine lake using Landsat imagery. *Science of the Total Environment, Vol.* 268 (1–3), pp. 19–29, 2001

[8] Sriwongsitanon, N., Surakit, K., Thianpopirug, S: Influence of atmospheric correction and number of sampling points on the accuracy of water clarity assessment using remote sensing application. J. Hydrol. Vol. 401 (3–4), pp. 203–220, 2011.

[9] Trivero, P., Borasi, M., Biamino, W., Cavagnero, M., Rinaudo, C., Bonansea, M., Lanfri, S: River pollution remediation monitored by optical and infrared high-resolution satellite images. *Environ. Monit.* Assess. Vol.185 (9), pp. 7647–7658, 2013.

[10] Zhao, D., Cai, Y., Jiang, H., Xu, D., Zhang, W., An, S: Estimation of water clarity in Taihu Lake and surrounding rivers using Landsat imagery. Adv. Water Resour. Vol.34 (2), pp. 165–173, 2011.

[11] Kloiber, SM., Brezonik, PL., Bauer, ME: Application of Landsat imagery to regional-scale assessment of lake clarity, Water Research Vol. 26, pp. 4330-4340, 2002.

[12] McFeeters, S. K: The use of normalized difference water index (NDWI) in the delineation of open water features. IJRS, Vol.17, pp.1425–1432, 1996.

[13] Xu, H: Modification of normalized difference water index (NDWI) to enhance open water features in remotely sensed imagery. IJRS, Vol. 27, pp. 3025–3033, 2006.

[14] Lehmusluoto, P., Machbub, B: National inventory of the major lakes and reservoirs in Indonesia. Expedition Indo danau Technical Report, pp. 1-71, 1997.

[15] https://landsat.usgs.gov/

O6-25

PEGモデルを視点とした琵琶湖水質と植物プランクトン遷移の関係解析について

池田　将平[1]，一瀬　諭[1]，古田　世子[1]

[1]滋賀県琵琶湖環境科学研究センター

キーワード：湖沼・河川モニタリング技術

抄録

　滋賀県琵琶湖環境科学研究センターでは、30 年以上にわたり琵琶湖の理化学的な調査に併せて植物プランクトンの調査を実施している。これまでの調査結果の解析において、植物プランクトンの減少や藍藻類の増加など様々な知見が明らかとなっている。しかし、これらのほとんどは群集全体の経年変化に注目したものであり、プランクトン遷移が長期的にどのように変化してきたかについては十分に議論されていない。そこで本研究では植物プランクトン分類群の生物量から Bray-Curtis 類似度指数を用いて植物プランクトン遷移の類型化を行った。その結果、植物プランクトン遷移は5パターンに分類され、そのパターンはPEGモデルに示される富栄養型のモデルから貧栄養型のモデルへと経年変化していた。この傾向は琵琶湖における栄養塩類の抑制傾向と一致し、植物プランクトン遷移が琵琶湖の栄養状態を評価する指標して有用である可能性が示唆された。

1．はじめに

　湖沼において植物プランクトンは湖内生態系の原動力であるとともに有機汚濁や湖底の低酸素化など水質形成に大きく寄与しており、異臭味やろ過障害など水利用の面でも大きな影響を与えている。このため、水質とプランクトンの動態を併せた総合的な水質評価を行う必要があり、当センターでは、30 年以上にわたり琵琶湖の理化学的な調査に併せて植物プランクトンの調査を実施している。これまでの調査結果の解析において、植物プランクトンの減少や藍藻類の増加など様々な知見が明らかとなっている。しかし、これらのほとんどは群集全体の経年変化に注目したものであり、その季節的消長が長期的にどのように変化してきたかについては十分に解明されていない。そこで本研究では植物プランクトン遷移を解析するために、季節遷移の類型化をおこない、水質の栄養状態の関係性を解析した。

2．方法

　調査は、北湖の今津沖中央（北緯35°23′41″，東経135°07′57″）（図1）における水深0.5mにおいて月2回の頻度で採取した湖水を用いて行った。植物プランクトンは湖水1mLを界線スライドグラス型式S6300（松浪硝子工業株式会社）に取り、湖水中に含まれる藻類について、光学顕微鏡下で同定および細胞数（藍藻類については群体数）の計数を行った。計数した細胞数を一瀬ら[1]の方法で容積換算を行った。

　計数した植物プランクトンを藍藻類、黄色鞭毛藻類、珪藻類、渦鞭毛藻類、褐色鞭毛藻類、緑藻類およびその他の計7分類群に分別し、各分類群の生物容量（Biovolume:mm^3/L）を調査毎に算出した。算出した生物容量は対数変換（log10(x+1)）した後にBray-Curtis指数[2]を用いて植物プランクトン遷移の類似度を求め、クラスター分析（Word法）によりデンドログラムを作成した。

図1　調査地点

3．結果

　琵琶湖における植物プランクトン遷移について、年間での類似性を Bray-Curtis 指数により算出しクラスター分析を行ったところ、遷移パターンはまず、G1 型と G2 型の大きく2つに分類され、さらに G2 型は G2A 型と G2B 型に分けられた。これら各型の遷移パターンをみると、G1 型では植物プランクトンの季節遷移に大きな変化は見られないが、G2 型では夏と秋に植物プランクトン生物量の増加が見られた。また、G2 型のうち、G2B 型は夏に大きな増加をもつパターンであり、G2A 型は秋に植物プランクトンが増加するパターンであった。G2A 型のパターンはさらに2つに分けることが出来、春に黄色鞭毛藻類の増加を持ち秋の緑藻類の増加が大きくなるG2Aα型と、春に黄色鞭毛藻類の増加を持たず、秋の緑藻類ピークをもつ G2Aβ型に分けられた。また、G2B 型も2つに分けられ、夏の緑藻類の増加に加え、晩秋に緑藻類が増加する G2Bα型と初秋に緑藻類が増加する G2Bβ型の合計5パターンに分類された（図2）。さらに植物プランクトン遷移パターンがどのような順で経年変化しているかを調べるために、クラスター分析によって各パターンに分類された年の分布状況を求めた。この結果、遷移パターンは1978 年から2014 年にかけてG2Aα型、G2Bβ型、G2Aβ型、G2Bα型、G1 型の順にパターンが変化していることが示された。

4．考察

　PEG(Plankton Ecology Group)モデル [3]の富栄養湖型のモデルでは植物プランクトンの明瞭なピークが2つあり、貧栄養湖型のモデルでは、植物プランクトンの明瞭なピークが見られないモデルとなっている。琵琶湖における植物プランクトン遷移は明瞭なピークを示すG2型と明瞭なピークを示さないG1型に分類され、これらのパターンは過去からG2型からG1型に変化していることが示された。これらは、栄養塩類の長期的な変動とも合致した。このことから、植物プランクトン遷移は湖沼の栄養塩状態を示す有用な指標であると考えられた。今後はPEGモデルに見るようにプランクトン遷移がどのような要因により生じているかを解析することで琵琶湖における植物プランクトン遷移モデルを作成していきたい。

引用文献

[1]　一瀬ら: 用水と廃水, Vol. 41 No.7, pp. 582-591, 1999.

[2]　J. Roger Bray et al: Ecological Monographs, Vol. 27 No. 4, pp. 325-349, 1957.

[3]　Ulrich Sommer et al: Arch. Hydrobiol., Vol. 106 No. 4, pp. 433-471, 1957.
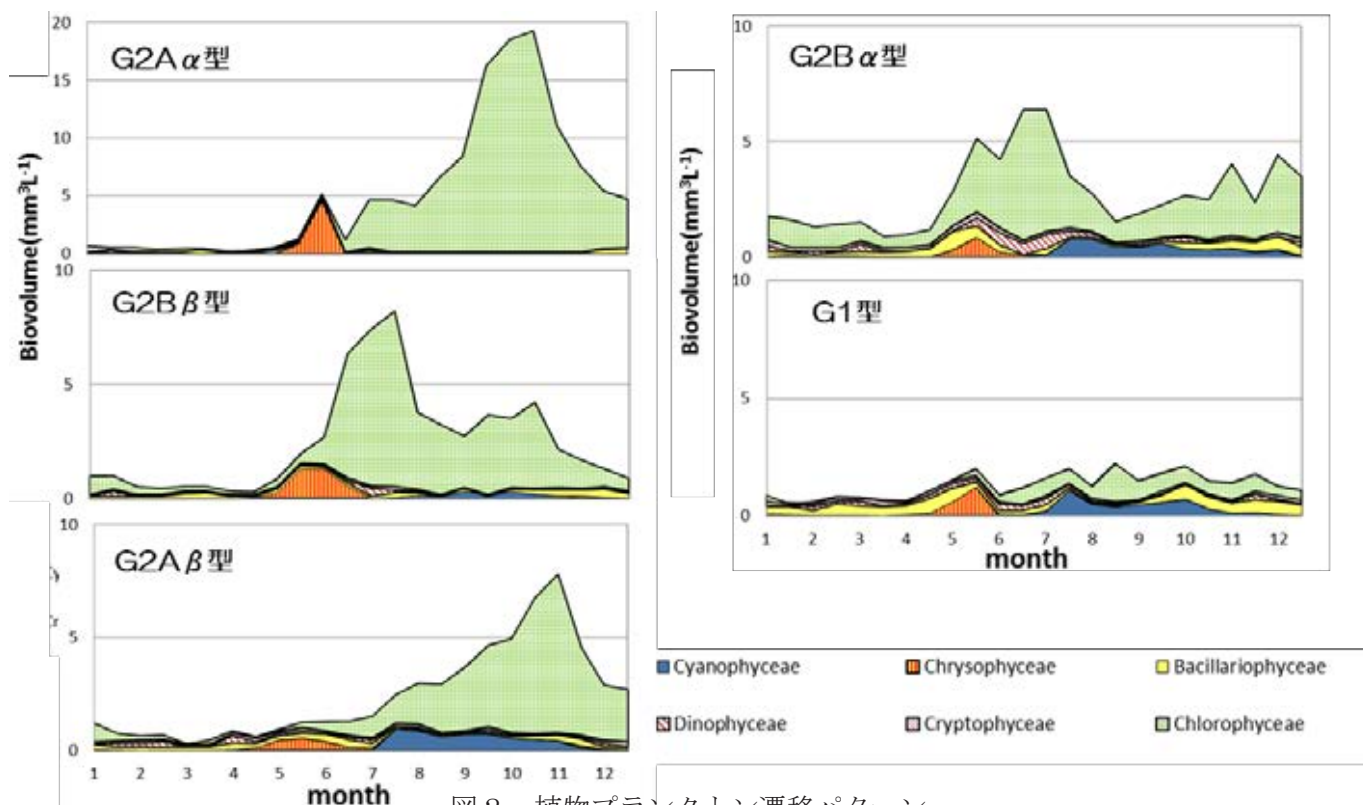
図 2　植物プランクトン遷移パターン

O6-26

琵琶湖北湖におけるウイルス・ホットスポット

沈 尚[1]，日下部 武敏[1]，清水 芳久[1]

[1]京都大学大学院工学研究科

キーワード：琵琶湖，ウイルス，空間分布、表面混合層、紫外線

抄録

本研究では、琵琶湖北湖を対象に、ウイルス数および宿主である細菌数と植物プランクトン（クロロフィル *a* 濃度）を14か月間追跡し、ウイルス数の分布が形成される要因について考察した。スピアマンの順位相関係数解析では、ウイルス数と細菌数（r = 0.47、n = 126、*p* < 0.01）およびクロロフィル *a* 濃度（r = 0.40、n = 126、*p* < 0.01）との間には正の相関がみられたが、ウイルス数の分布を説明するには不十分であった。また、ウイルス数の分布の極大点（ウイルス・ホットスポット）が宿主の分布の極大ではない水深20〜40 m 付近に出現していることを確認し、これが表面混合層のすぐ下であることを見出した。これはウイルスの分布が宿主の分布だけでなく、物理的な要因（紫外線や鉛直混合）も関わっていることを示唆するものであった。

1. はじめに

ウイルスは水中で最も多い生物学的存在であり、細菌や植物プランクトンの死亡要因としても重要な役割を担っている[1]。ウイルスによる宿主への感染と細胞破壊を通じて、微生物ループを介した高次への栄養伝達や粒子の沈降フラックスが抑制されることが理論的にも実験的にも明らかになった[2, 3]。これらのことから、物質循環におけるウイルスの役割とその重要性に関する議論は国際的に活発化している[1]。

海洋においてウイルスの宿主はほとんどが細菌および植物ピコプランクトンであると考えられている[4]。そしてウイルス数は宿主の現存量に強く依存していることが知られている[5, 6]。しかし、湖沼において季節と水深を考慮したウイルス数の分布についての研究例は乏しく、どのようにウイルスの分布が形成されるのかは不明な部分が残されている。

本研究では、琵琶湖北湖（全水深約 90 m）を対象に、9 水深で14か月間調査を実施した。そして宿主であるクロロフィル *a* 濃度と細菌数の分布に加えて、表面混合層と紫外線という物理的な要因からウイルスの分布がどのように形成されるのかについて考察を試みた。

2. 方法
2.1 採水地点

採水は琵琶湖北湖沖帯の水深（0.5、5、10、15、20、30、40、60、80 m）で 2016 年 8 月から 2017 年 9 月の間に毎月実施した。サンプルは採水してすぐに船上で化学固定（グルタルアルデヒド、最終濃度 1vol%）を行い、氷冷して実験室に持ち帰った後、観察まで冷凍保存（-30 ℃）した。

2.2 細菌数およびウイルス数の計数

化学固定した試料を、Anodisc フィルター（孔径 0.02 μm、GE Whatman）上に捕集し、SYBR Gold（核酸染色試薬）で染色した[7]。その後、フィルターを褪色防止試薬（0.1% 1,4-phenylenediamine dihydrochloride）とともにスライドガラスとカバーガラスの間にマウントした。ウイルスと細菌の数は落射蛍光顕微鏡を用いて測定した。

2.3 その他の水質項目

水温およびクロロフィル *a*（Chl. *a*）濃度については、平成 29 年度公共用水域・地下水水質測定計画（滋賀県）およびそれに準じて、滋賀県琵琶湖環境科学研究センターにより測定されたものであり、本論文執筆時点では速報値である。また、表面混合層の厚さは、表層（0.5 m）の水温から 1 ℃ 低い水深までとした[8]。

3. 結果と考察

細菌数は観測期間を通して、0.3〜4.5 × 10^6 cells/mL を推移し、表水層（水深 0〜20 m）で高く、水深とともに低下する傾向がみられた（Fig. 1C）。また、ウイルスは1.0〜12.3 × 10^7 VLPs/mL を推移し、表水層で高く、水深とともに減少する傾向がみられた（Fig. 1D）。またウイルス数と細菌数またはクロロフィル *a* 濃度との相関係数（スピアマン順位相関係数、n=126）はそれぞれ 0.47 と 0.40 と正の相関はみられたが、強い相関ではなかった。さらに、VBR（virus-to-bacteria ratio、ウイルス数を細菌
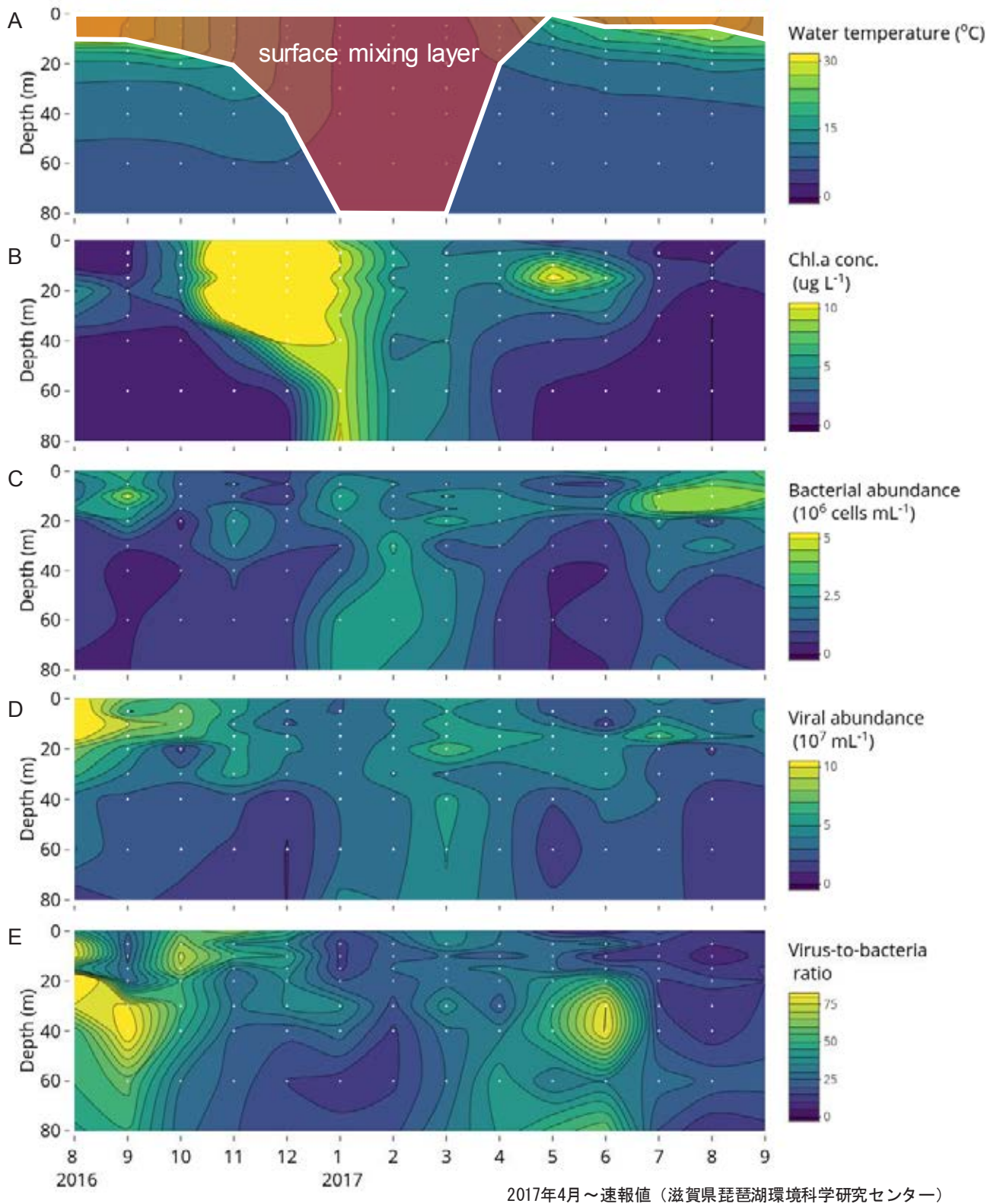
Fig. 1 Distribution of (A) water temperature, (B) Chl. *a* concentration, (C) bacterial abundance, (D) viral abundance, and (E) virus-to-bacteria ratio at Northern Lake Biwa

数除した値）は 7.8～124 を推移し、その極大点は表水層だけでなく水深 40 m 付近にもみられた（Fig. 1E）。この VBR の極大点は細菌やクロロフィル *a* 濃度（Fig. 1B）の分布と一致しなかった。

　表面混合層は成層が形成される 4 月から夏季の 9 月頃まで 5～10 m を推移した。その後、循環期直前の 12 月には 40 m に達し、全循環期である 1 月から 3 月は全水深と同じ厚さ（約 90 m）となった。表面混合層とともに図示した水温プロットから（Fig. 1A）、いくつかの VBR の極大点が表面混合層の下に現れることが明らかとなっ

た。表面混合層中に存在するウイルスは、鉛直混合により表層付近で紫外線照射を受けるが、逆に表面混合層より以深に存在するウイルスは表面混合層と隔離されているため、紫外線照射により不活化・消失するリスクが低いと考えられる。また、宿主である細菌や植物プランクトンの現存量は水深とともに減少する傾向がみられることから、VBR の極大点より以深では十分な宿主が存在せず、ウイルス数が高濃度で維持されることが難しい可能性が考えられる。したがって、季節とともに形成される表面混合層の直下がウイルスにとって「住みやすい」水深(ウイルス・ホットスポット)であることが示唆された。

4. 結論
　ウイルスは宿主である細菌や植物プランクトンと異なる分布を持つことが明らかとなった。今後は、ウイルスの現存量を決定する要因である一次生産速度や細菌の生産速度に加えて、紫外線照射への耐性や粒子への吸着速度なども同時に観測し、どのパラメータがウイルスの分布を規定するのかを明らかにしていく必要がある。

参考文献
[1] Motegi C, Nagata T, Miki T, Weinbauer MG, Legendre L and Rassoulzadegan F (2009) Viral control of bacterial growth efficiency in marine pelagic environments, *Limnol, Oceanogr.*, **54**, 1901-1910.
[2] Miki T, Nakazawa T, Yokokawa T and Nagata T (2008) Functional consequences of viral impacts on bacterial communities: a food-web model analysis, *Freshwater Biology*, **53**, 1142-1153.
[3] Suttle CA (2007) Marine viruses-major players in the global ecosystem. *Nat. Rev. Microbiol.*, **5**, 801-812.
[4] Fuhrman JA (1999) Marine viruses and their biogeochemical and ecological effects, *Nature*, **399**, 541-548.
[5] Culley AI and Welschmeyer NA (2002) The abundance, distribution, and correlation of viruses, phytoplankton, and prokaryotes along a Pacific Ocean transect. *Limnol. Oceanogr.*, **47**, 1508–1513.
[6] DeLong EF, Preston CM, Mincer T, Rich V and others (2006) Community genomics among stratified microbial assemblages in the ocean's interior, *Science*, **311**, 496–503.
[7] Patel A., Noble R.T., Steele J.A., Schwalbach M.S., Hewson I. and Fuhrman J.A. (2007): Virus and Prokaryote Enumeration from Planktonic Aquatic Environments by Epifluorescence Microscopy with SYBR Green I, Nature Protocols, 2 (2), 269-276.
[8] Sprintall J and Cronin MF (2009) Upper ocean vertical structure, Encyclopedia of ocean sciences. 6 (Steele JH, Thorpe SA, Turekian KK, Eds.).:3120-3129., San Diego: Academic Press.

O6-27

Comparisons between the Characteristics of Natural Organic Matters in Upstream Inflowing Rivers and Discharging Sources of a Drinking Water Reservoir with or without the Transbasin Diversion

Chih-Hua Chang[1], Jia-Wei Wang[1], Ching-Gung Wen[1], Chun-Hsi Lai[1], Wen-Chieh Huang[2] and Wen-Yi Wei[2]

[1]Department of Environmental Engineering, National Cheng Kung University, Tainan, R.O.C. (Taiwan); [2]Environmental Protection Administration, Executive Yuan, Taipei, R.O.C. (Taiwan)

ABSTRACT

The characteristics of natural organic matter (NOM) in the Agongdian Reservoir (AGD) and its inflowing rivers and discharging sources during the periods with or without transbasin diversion are compared using dissolved organic carbon (DOC) measurements and fluorescence spectroscopy methods. The fluorescence excitation-emission matrices (FEEM) method was applied to characterize the NOM into five organic groups, including type I simple aromatic protein (API), type II simple aromatic protein (APII), fulvic acid-like substances (FA), soluble microbial by-product-like material (SMP) and humic acid-like substances (HA). Although the main fractions of NOM are FA and HA during both periods, the average fluorescence intensity (AFI) of each group as well as the levels of DOC obtained during transbasin diversion are lower, indicating that the transbasin diversion water may not be a significant source of NOM. The total AFI of API, APII and SMP links well with the levels of human activities, and shows that discharging sources in the Wanglai tributary are the hotspots of NOM. Comparing to the non-transbasin-diversion period, the levels of total AFI are easier to be explained by the levels of DOC during transbasin diversion. Characterizing the distribution patterns of NOMs in a catchment area of source water provides useful information for identifying potential NOM sources.

1. INTRODUCTION

NOMs such as humic/fuvic substances from wetlands and farmlands, proteins from organic wastes, and microbial byproducts from metabolism of algae, are commonly found in reservoirs providing raw water to water treatment plants (WTPs)[1]. Carcinogenic or mutagenic DBPs are formed when NOMs in raw water react with oxidants or chlorine disinfectants[2]. NOM found in natural waters often has various properties and is composed of complex mixture of compounds[3] which can be linked to important information of potential sources of contamination. However, very indicators are shown by water quality parameters that are commonly used to assess the level of NOM, e.g., DOC, 5-day biological oxygen demand (BOD_5) or chemical oxygen demand (COD).

Fluorescence spectroscopy and indexes have been applied to characterize NOM based on the measurement of absorption and emission of energy by organic matter molecules. The FEEM method is sensitive with the possibility of single-molecule detection and provides discrimination between chromophoric organic matter absorbing at similar wavelengths. Characterizing NOM from samples in a water treatment train provides information for reducing the risk of the formation of DBPs[4]. Consequently, understanding the distribution patterns of NOMs in a catchment area of source water or tracking changes of NOM in a river network[5] may further help identifying and controlling potential sources through management practices.

Therefore, this work uses the FEEM method that combines both quantitative and qualitative approaches to obtain main NOM characteristics in water samples from organic matter sources of a drinking water reservoir, including inflowing rivers, discharging and transbasin diversion sources. Resolving the spatio-temporal patterns of NOM in source waters could help to remove such material at the source or evaluate purification methods during water treatment.

2. METHOD

Figure 1 shows the locations of seven NOM sampling stations in the catchment of AGD. Five stations coded from upstream to downstream as W1 to W5 are located in the northern tributary basin (Wanglai Creek) of the AGD, and two stations coded as Z1 and Z2 are located in the

southern tributary basin (Zhuoshui Creek). Both tributary basins have similar land use, which consists of mainly forest (40%), fruit plantations (35%), built-up areas (10%) and farmland (10%). The W2, W4 and Z1 stations are positioned in the drainage outlets of main sub-catchments which collect wastewater and polluted runoff. The AGD provides 30,000 m^3 of raw water per day to the Luzhu WTP that supplies drinking water for Luzhu District and Luzhu Science Park in Kaohsiung City, Taiwan. The AGD activates the empty flushing operation annually during the rainy season (June to early September) to remove the deposited sediments in the reservoir. After the empty flushing, the reservoir is refilled by the catchment runoff during the late rainy season, and discharges from transbasin diversion (path of transbasin diversion shown on Fig. 1). Notably, the Luzhu WTP experienced serious DBPs and odor problems in the produced tap water during the empty flushing period in 2013, due to high levels of DOC (2.6±0.26 mg/L) and 2-MIB (>> 10 ng/L) of the raw water.

Fluorescence spectroscopy of water samples was analyzed by the Perkin Elmer LS-55 fluorescence spectrometer. The spectrometer uses a xenon excitation source, and slits were set to 10 nm for both excitation and emission. To obtain fluorescence EEMs, excitation wavelengths are incremented from 200 to 400 nm at 10-nm steps; for each excitation wavelength, the emission is detected from 280 to 600 nm at 0.5-nm steps. Instrumental parameters are controlled by Perkin Elmer FL WinLabTM software and the fluorescence intensity and the excitation/emission wavelengths can be displayed in real-time.

First, the intensity measurement of excitation at 370 nm (Ex370) and emission at 450 nm and 500 nm (Em450 and Em500) were applied to calculate the fluorescence index (FI):

$$FI = \frac{Ex370/Em450}{Ex370/Em500} \qquad (1)$$

McKnight et al.[6] suggested that NOM is mainly contributed by terrestrial sources (autochthonous source) when FI approximates 1.4, and by microbial sources (allochthonous source) when FI approximates 1.9. Second, from the FEEM spectroscopy (Fig. 2), five organic fractions were divided according to the research of Chen *et al*.[7]. Region I is known as API such as tyrosine. Region II is related to APII such as tryptophan and BOD_5. Region III is identified as FA. SMP material is classified as Region IV. Region V is represented by HA. Additionally, the EEM contour plot was analyzed using fluorescence regional integration method to perform quantitative information. The intensity of each group of organic matters are

quantified using the AFI method on each region of the FEEM spectroscopy. Samples for DOC (or NPDOC) quantification were measured by NIEA W530.51C method with Shimadzu TOC-5000.
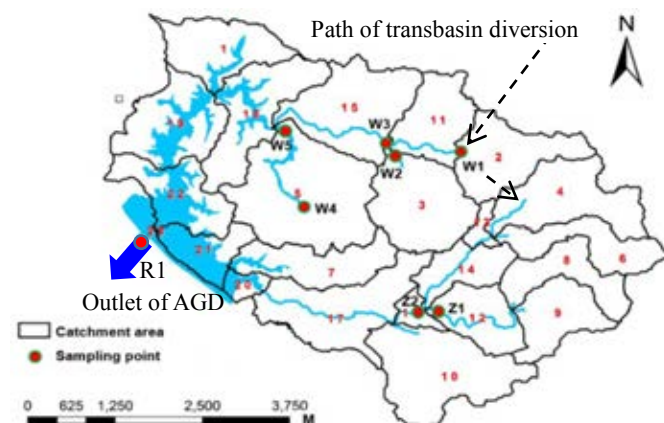
Fig. 1 The NOM sampling locations in study area
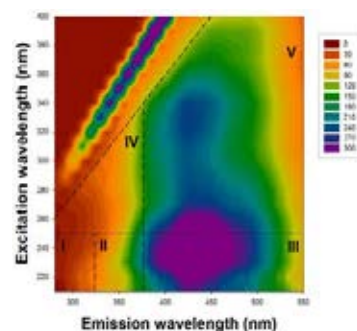
Fig. 2 A typical 2D FEEM spectroscopy showing the fluorescence emission intensities (colored contours), and emission-excitation wavelengths of a water sample.

3. RESULTS AND DISCUSSIONS

The comparisons between results of FEEM collected during the periods with and without transbasin diversion show that the main fractions of NOM are both FA and HA (Fig. 3), however, the AFIs as well as the levels of NPDOC obtained at the period of transbasin diversion are much lower. It indicates that the level of five NOM components in transbasin diversion water are lower (Fig. 4), although its NOM characteristics are similar to that of the inflowing waters (Fig. 3). Additionally, the spatial distribution of NOM intensities reflect a typical water pollution path during the period without transbasin diversion: NOMs were accumulated from up- to down-stream in both Wanglai Creek (W3>W1) and one of its main drainage (W5>W4), and diluted from drainages to receiving creeks (W3<W2 and Z2<Z1).

Figure 5 shows that the NOM in inflowing rivers and discharging sources of AGD are mainly contributed by terrestrial sources for both the periods with and without transbasin diversion. The relationships between human activities and the resulting NOM levels are obtained by comparing the fruit plantation (agriculture) and residential (human) areas in the catchments of each sampling points

(W1 is excluded) to the NOM measured by different approaches. Comparing to commonly used water quality parameters (Fig. 6b), the NOM intensity in terms of FEEM-AFI has a higher correlation with the human pollution strengths (Fig. 6a), especially the correlations between human and AP (API and APII) + SMP, and that between agriculture and HA + FA.

As shown on Fig. 7, because the NOM characteristics are simpler and the levels of DOC are lower during transbasin diversion (dilution effects), the levels of total AFI at different sites are well to be explained by the levels of DOC. In the other hand, DOC concentration may not be a good indicator of NOM characteristic during the non-transbasin-diversion period.
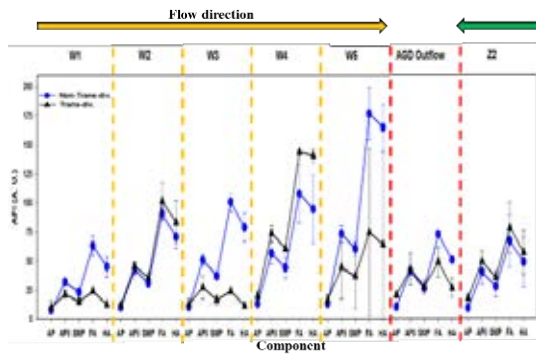
Fig. 3 Comparisons between 5 component AFIs for 7 sampling sites during the periods with and without transbasin diversion
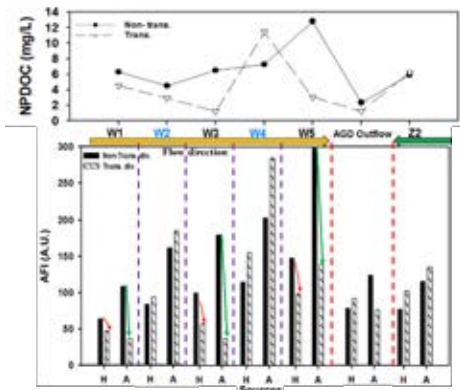
Fig. 4 Comparisons between total AFIs for 7 sampling sites during the periods with and without transbasin diversion
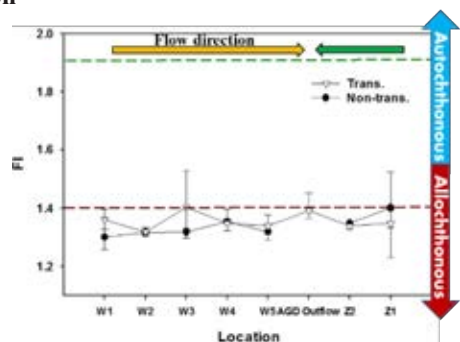
Fig. 5 Comparisons between average FI for 8 sampling sites during the periods with and without transbasin diversion
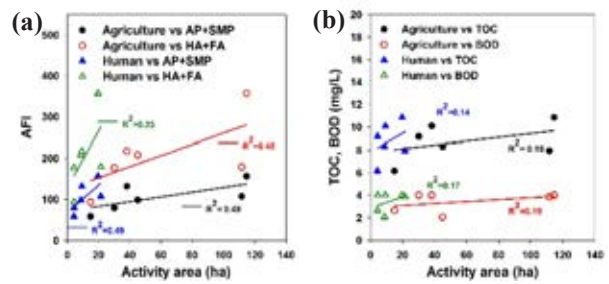
Fig. 6 The relationships between human activity strengths and the resulting NOM intensities obtained by (a) FEEM-AFI, and (b) DOC and BOD concentrations.
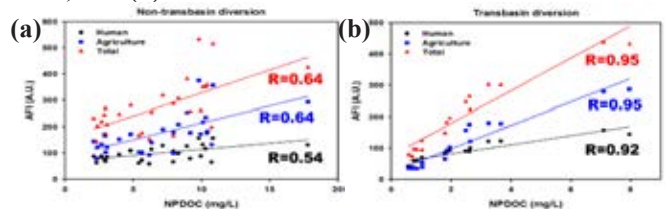
Fig. 7 Comparisons between the correlation relationships between total AFI and NPDOC during the periods (a) without transbasin diversion, and (b) with transbasin diversion.

4. CONCLUSION

Results indicated that the NOM fractions of simple aromatic proteins and soluble microbial byproducts in AGD may source from municipal wastewaters. Additionally, the high level of humic/fulvic acid-like substances shown by FEEM and AFI, as well as the high DOC concentrations, may be the result of high density planting of fruit trees in the catchment of AGD.

REFERENCES

[1] Chang C-N, Ma Y-S, Fang G-C, Zing F-F: Characterization and isolation of natural organic matter from a eutrophic reservoir, Journal of Water Supply: Research and Technology-AQUA, Vol. 49, pp. 269-280, 2000.

[2] Hebert A, Forestier D, Lenes D, Benanou D, Jacob S, Arfi C, et al.: Innovative method for prioritizing emerging disinfection by-products (DBPs) in drinking water on the basis of their potential impact on public health, Water research, Vol. 44, pp. 3147-3165, 2010.

[3] Filella M: Understanding what we are measuring: standards and quantification of natural organic matter, Water research, Vol. 50, pp. 287-293, 2014.

[4] Baghoth S, Sharma S, Amy G: Tracking natural organic matter (NOM) in a drinking water treatment plant using fluorescence excitation–emission matrices and PARAFAC, Water research, Vol. 45, pp. 797-809, 2011.

[5] Bhattacharya R, Osburn CL: Multivariate analyses of phytoplankton pigment fluorescence from a freshwater river network, Environmental science & technology, Vol. 51, pp. 6683-6690, 2017.

[6] McKnight DM, Boyer EW, Westerhoff PK, Doran PT, Kulbe T, Andersen DT: Spectrofluorometric characterization of dissolved organic matter for indication of precursor organic material and aromaticity, Limnology and Oceanography, Vol. 46, pp. 38-48, 2001.

[7] Chen W, Westerhoff P, Leenheer JA, Booksh K: Fluorescence excitation− emission matrix regional integration to quantify spectra for dissolved organic matter, Environmental science & technology, Vol. 37, pp. 5701-5710, 2003.

琵琶湖・淀川流域における難分解性有機物に関する
調査研究のための流域連携

和田 桂子[1], 津野 洋[1]

[1](公財)琵琶湖・淀川水質保全機構 水質浄化研究所

キーワード：難分解性有機物, モニタリング体制, 流域連携, GIS

抄録

琵琶湖・淀川水質保全機構水質浄化研究所は, 琵琶湖の BOD と COD の乖離について 1997 年から難分解性有機物の問題および削減対策の研究に取り組んできた。一方, 各研究機関もそれぞれの研究目的で進められているが, 測定方法が確立されていないこと, また測定に時間を要するため, 既往知見や測定データが少ないことが課題であった。そこで, 琵琶湖・淀川流域の関係研究機関(滋賀県, 京都府, 大阪府, 兵庫県)の協力を得て2年間にわたるワーキングを実施した。そして, 各流域の水質状況や影響, 自治体の取り組みなどを整理し, 難分解性有機物に関する手引書となるよう, 対象水ごとの知見を体系的にとりまとめた。とくに, 今後データを活用する際には, 統一した生分解性試験の方法が重要と考え,「標準的な生分解性試験方法」を検討し提案した。この分析手法により多くのデータの蓄積が進み, 流域全体での難分解性有機物の状況把握等が可能になると期待できる。

1. はじめに

琵琶湖を含む淀川水系の有機汚濁問題は, 近年では改善傾向にある。これらはおもに下水道整備によるものであり, 河川の BOD 濃度の減少に大きく寄与した[1]。一方, 湖沼や閉鎖性海域は, COD 濃度が漸増傾向にあり, その要因の一つとして難分解性有機物の関与が指摘されている[2]。この難分解性有機物の問題は, これまでも種々の知見が得られてはいるものの全容は解明されていない。しかし, 環境基準であるこれら有機物を水域で管理する場合, 対象水域およびその流域における濃度や負荷量の実態, 時空間分布などの特性, 水質保全対策との応答等を調査・検討することが必要である。今後,「環境の時代」にふさわしい水質管理が求められる中で, 難分解性有機物の取り扱いは重要となっている。さらに, 難分解性有機物は微生物によって容易に分解しないことから, 生態系への影響や流域全体に蓄積していくことが懸念される。

このような背景から, COD に関する今後の効果的な行政対応に資するために, 琵琶湖・淀川流域および大阪湾への影響が顕在化してきた「難分解性有機物」について, 流域研究者の協力を得て連携した取り組みを実施することを目的に検討会を行った。本発表では, 琵琶湖・淀川流域の難分解性有機物に関して体系的にとりまとめた手引書(案)の概要およびデータ蓄積や流域内でのデータ解析の比較を推進するために「標準的な生分解性試験方法」を提案したのでこれらを紹介する。

2. 方法

2.1 難分解性有機物

琵琶湖・淀川流域を構成する当研究所や自治体の研究機関等では, これまでに様々な研究目的で「難分解性有機物」の調査を行ってきた。それらの既往調査・研究成果をもとに, 琵琶湖, 淀川流域, 大阪湾, その他の水域の有機物指標の動向とCODとBODの乖離現象などについて整理した。また, 難分解性と易分解性有機物を定義し, 各水域(河川, 湖水, 海域)や各排水中での難分解性有機物の指標等について示した。

2.2 難分解性有機物の分析方法

難分解性有機物の捉え方には様々な方法があり, 各分析方法による有機物に関する指標の考え方を取りまとめた。さらに, 各水域における難分解性有機物の生分解試験方法はそれぞれ条件が異なることから, 今後, 水質管理や実態把握等を行う際の難分解性有機物のデータ取得では, 統一した方法が重要であり, 生分解性試験の条件を明示することが必要と考えた。そのため, まず先行して実施されている琵琶湖や大阪湾などの淡水や海水の環境水, 路面排水などの各種排水等で行われた方法を整理した。それらの条件を踏まえて, 対象水別に基本となる生分解性試験の条件をとりまとめ, 前処理や培養条件などを示した「標準的な生分解性試験方法」を手引書(案)として策定した。

3. 結果および考察

3.1 難分解性有機物の動向と定義

　本研究での難分解性と易分解性有機物の定義を図1に示す。
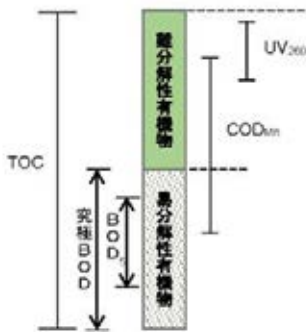
図1 難分解性と易分解性有機物の定義

　水中の有機物総量を炭素量で表したものが TOC (Total Organic Carbon)であるが，難分解性有機物自体は直接的に表す指標がないため，これまでも様々な方法で定性的・定量的に把握する研究がなされてきた。例えば，DOM (Dissolved organic matter) を指標としてその分画分布による特性評価[3]や三次元励起蛍光スペクトル測定による難分解性有機物起源の把握[4]などがある。ここでは，流域全体の湖沼や河川の 20 年間の変化を COD/BOD 比で検討した。図2に示すように，琵琶湖北湖で明確に現れており，BOD と COD の乖離現象が進行していることがわかる。また，琵琶湖のみならず下流の淀川等においても問題が顕在化していることが明らかであった。

3.2 難分解性有機物の分析方法

　これまで当研究所や各研究機関が測定に供した方法を踏まえ，種々の方法や条件を整理し，流域での難分解性有機物の測定を推進するために重要である生分解性試験について検討した。おもな内容は，①試料採取量，②前処理，③培養容器容量・材質や洗浄作業，④培養機材の準備，⑤培養条件の設定（培養期間、分析頻度，水温、光条件、曝気や振とうの有無，植種添加の有無，栄養塩および緩衝液添加の有無，ブランク試験の実施），⑥水質分析方法　の条件である。培養時のイメージを図3に示した。詳細は手引書(案)[5] に記す。
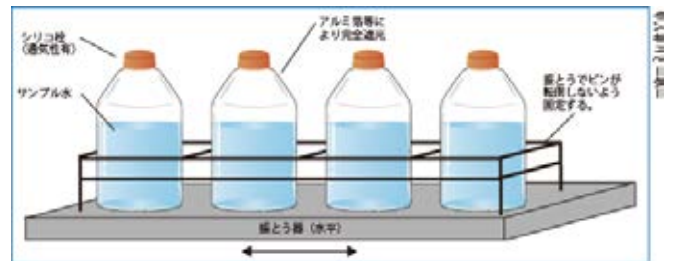
図 3-1 曝気を考慮しない場合の培養機器構成例の概要
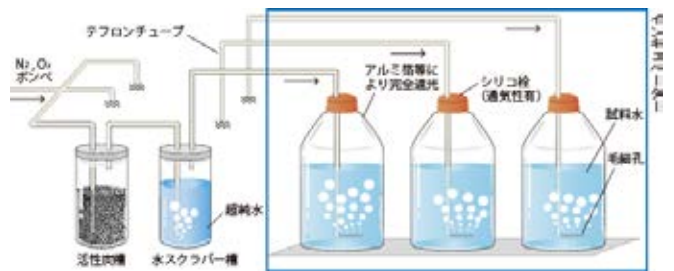
図 3-2 曝気を考慮する場合の培養機器構成例の概要
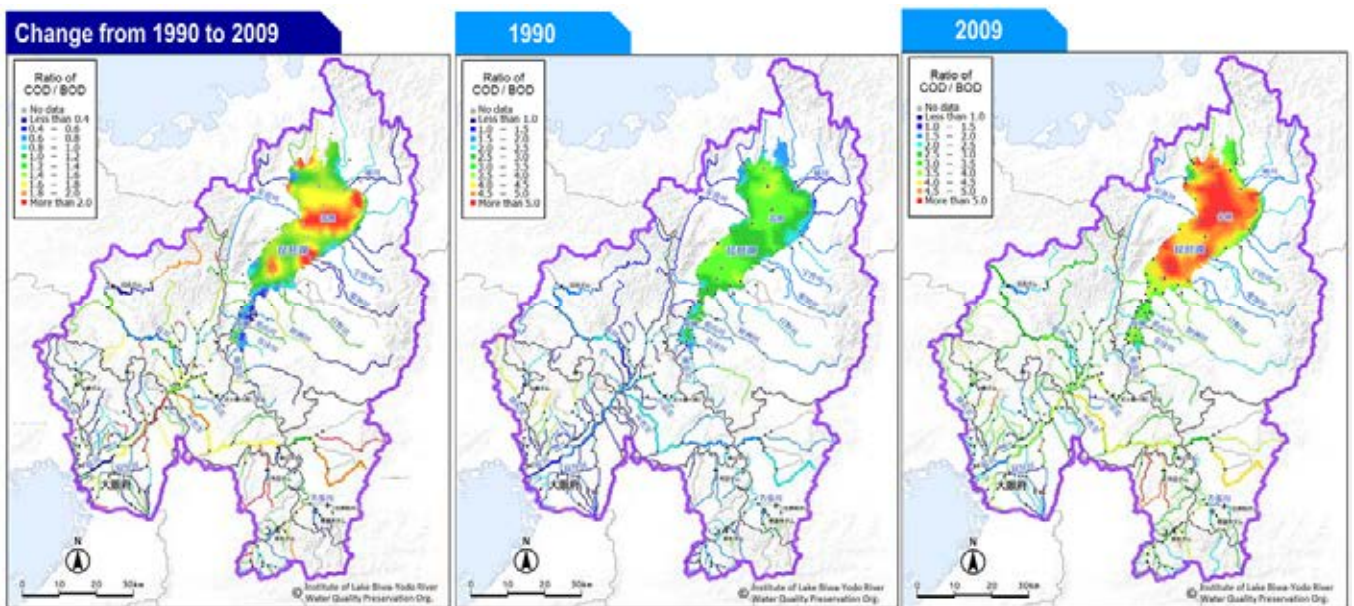
図 2 琵琶湖・淀川流域の COD/BOD 比の 1990 年から 2009 年までの 20 年間の変化

4. 結論

　環境基準である「有機物 (BOD・COD)」を対象に，「難分解性有機物」に焦点をあて，琵琶湖・淀川流域や他の湖沼にて得られた知見や文献情報を収集整理し，流域全体の現在の実態把握や事例を体系化してとりまとめた。さらに，流域の研究機関のメンバーとともに生分解性試験の方法等について検討し，各水域や培養条件などを考慮した「標準的な生分解性試験方法」を立案した。この方法を参考にすることで，難分解性有機物のさらなる調査・測定データの蓄積や流域内の他の結果との比較解析などが進み，より一層の難分解性有機物に関する知見の充実が期待できると思われる。

謝辞

引用文献

[1]　K. Fijio, K. Wada, S. Fukujyu, H. Tsuno and K. Ueno: Development od Distribution Analysis Tool Using Water Quality Information and GIS Data in Lake Biwa and Yodo River Basin: Examination Case on Effects of Sewage Improvement, Journal of Water and Waste, Vol. 57 No. 2, pp. 132-138, 2015. (in Japanese)

[2]　K. Wada, S. Yamanaka, M. Yamamoto and K. Toyooka: The characteristics and measuring technique of refractory dissolved organic substances in urban runoff, Water Science and Technology, Vol. 53 No. 2, pp. 193-201, 2006.

[3]　A. Imai, T. Fukushima, K. Matsushige, T. Inoue and T Ishibashi: Fractionation of Dissolved Organic Carbon from the Waters of Lake Biwa and its Inflowing Rivers, Jpn. J. Limnol, Vol. 59, pp. 53-68, 1998. (in Japanese)

[4]　小松一弘: 三次元励起蛍光スペクトル法を用いた霞ヶ浦湖水の解析, 国立環境研究所ニュース25巻5号, 2006. http://www.nies.go.jp/kanko/news/25/25-5/25-5-04.html (accessed 16 Apr. 2018).

[5]　公益財団法人琵琶湖・淀川水質保全機構 琵琶湖・淀川水質浄化研究所: 琵琶湖・淀川流域の難分解性有機物に関する調査検討会, 琵琶湖・淀川流域の難分解性有機物に関する調査・分析の手引書(案), 2016.